Learning to Perform Actions from Demonstrations with Sequential Modeling

A Dissertation

Presented to

The Faculty of the Graduate School of Arts and Sciences

Brandeis University

Michtom School of Computer Science

James Pustejovsky, Advisor

In Partial Fulfillment

of the Requirements for the Degree

Doctor of Philosophy

by

Tuan Do

June, 2018

This dissertation, directed and approved by Tuan Do's committee, has been accepted and approved by the Graduate Faculty of Brandeis University in partial fulfillment of the requirements for the degree of:

DOCTOR OF PHILOSOPHY

Susan J. Birren, Dean of Arts and Sciences

Dissertation Committee:

James Pustejovsky, Chair

Anthony G. Cohn

Pengyu Hong

Timothy J. Hickey

Acknowledgments

Abstract

Learning to Perform Actions from Demonstrations with Sequential Modeling

A dissertation presented to the Faculty of
the Graduate School of Arts and Sciences of
Brandeis University, Waltham, Massachusetts

by Tuan Do

Learning from Demonstration (or imitation learning) studies how computational and robotic agents can learn to perform complex tasks by observing humans. This closely resembles the way humans learn. For example, children can imitate adults in a variety of domestic tasks, such as pouring milk from a carton to a cup or cleaning a table, and after one or a few observations, they can replicate the action with relative accuracy. This research tests the feasibility of a virtual agent that can process multimodal (linguistic and visual) captures of actions and learn to reenact them in a simulated environment.

In particular, this thesis looks into the problem from two perspectives. The first perspective is taken in a realistic setup, in which we will teach learning agents skills by showing real demonstrations of the skills. We will only focus on a small set of actions involving spatial primitives. The objective is for agents to learn to perform complex action skills from a limited amount of training samples. We will also try to teach agents in an interactive environment, in which immediate feedback is provided to agents to correct them in due time.

The second perspective is taken in a synthetic setup. In this setup, a parallel corpus mapping natural language instructions to demonstrations is generated by soliciting human descriptions for complex action demonstrations in a two-dimensional simulator. The problem is framed in a sequence to sequence translation framework. We will discuss the difference between two

perspectives, as well as advantages and disadvantages of corresponding learning frameworks.

The system is composed of the following components: a. an event capture annotation tool (ECAT) that captures human interaction with objects using Kinect sensor; b. an event representation learning method using recurrent neural networks with QSR feature extraction; c. action reenacting algorithms using reinforcement learning and sequence to sequence methods; d. evaluation methods using 2-D and 3-D simulators.

Contents

List of Tables

List of Figures

List of Algorithms

Chapter 1

Introduction

The community surrounding "learning from demonstration" (LfD) studies how computational and robotic agents can learn to perform complex tasks by observing humans (Young and Hawes, 2015). Work in this area can be traced back to reinforcement learning studies by Smart and Kaelbling (2002) or Asada et al. (1999), and closely resembles the way humans learn. Infants can imitate adults in a variety of household tasks, such as *pouring milk from a carton to a cup* or *cleaning a table*, by replicating actions after one or a few observations. LfD is, in part, an AI movement that aims to achieve *stronger* AI, which is AI systems that can adapt to new environment, to learn new skills and can cooperate with humans to perform tasks.

So far the development toward more adaptable AI has faced with many obstacles, leading to the fact that most robots developed in the previous decades have shipped with pre-installed programs, limited to a set of predefined functionalities. Learning approaches in the robotics community seek to move toward smarter and more adaptable robots, for, among others, the following reasons:

- Consumer desire for mobile or household assistant robots that can perform multiple tasks with flexible apparatus, such as multiple grasping arms (Bogue, 2017). Robots with behavioral robustness can learn from a broader range of experiences by operating in a dynamic human environment (Hawes et al., 2017).
- Advances in deep learning have afforded robotic agents a high-level understanding of embedded semantics in multiple modalities, including spoken language, gesture, visual perception, and navigation.

- Robots that can communicate and cooperate with humans to perform tasks are desirable, as fully automated robots are far from able to perform complex tasks in novel environments or circumstances. Understanding the nuances in human languages requires communicative robotic agents to learn various human concepts, such as the predicates "put" or "closer to", in the form of action programs that are compositional with arguments. Humans can only communicate using qualitative semantics, such as "put A closer to B", while robots function in a lower quantitative level of semantics, such as "put(A, coordination_XYZ)".

For robots to achieve this level of autonomy and understanding, a scaffold of robot learning can be summarized as follows:

- Robots learn object forms (shape, color, size, etc.) and their mappings to human languages (round, square; red, green; big, small) (Alomari et al., 2017). Moreover, robots also need to learn relative relations among objects (such as whether one object could contain another object (Liang et al., 2015)) and between agents and objects (what is generally called object affordances, a.k.a what a human or robotic agent can do with the object (grasping, pouring) (Koppula et al., 2013)).

- Robots learn to perform simple actions by learning compositional programs, such as to learn the programmatic form of action verbs (put, slide, push, roll, etc.), in addition to the programmatic form of motion adjuncts specifying trajectories of motion (on, in, next to, etc.).

- Robots learn to perform more complex actions (actions that are generally represented by structured programs, such as procedural or repetitive programs), such as "make a row from given objects".

- Robots learn to communicate with humans in a feedback loop to make necessary correction, or to improve learned models. While human experts can give instructions or demonstrations, robots might not be able to recognize immediately very abstract concepts that are intended by experts. For example, with the same learned action as before, a smart robotic learner can recognize that the intended action is a repetitive program of "move A next to B", but it would be hard to recognize "direction of extension need to follow the longest axis".

While the listed items seem to reach beyond the state-of-the-art in robotics at the time being, it might happen just after a decade or two, given the current advances in AI and Machine Learning. We should not forget how fast technology has changed "impossible" things to not only possible but universal. In the 1980s, chess was considered exclusively human prowess, and people believed that we would never be able to create machines to beat chess-masters. That belief became obsolete when IBM's Deep Blue gained the upper hand over chess champion Garry Kasparov. In the 90s, facial recognition and identification were considered a challenging task, and even just locating locations of faces in an image was still hard (Yang and Huang, 1994), let alone identifying who are there in the image. Nowadays after twenty years of machine learning development, we see applications of facial identification everywhere. Facial detection is employed for secure authentication by Apple's iPhones, for automation of image tagging by Facebook, and now even police forces use it to track down criminals from surveillance footage.

We might soon see a similar revolution in robotics. To some extent, robotics is intertwined with advances in AI, and it is hard to believe if recent developments in AI would not transform the robotic landscape as well. That is a fundamental assumption for this dissertation, and this thesis, hopefully, will bring about new discussions on what directions we should lead in this exciting frontier of AI.

While the discussion so far has been about robots, it applies to virtual agents as well. Moreover, as most of the learning process could be simulated, this dissertation focus on the learning capacity of a communicative virtual agent that is co-situated with humans. The virtual agent can observe what the humans have done, perform actions in novel situations, and receive feedback from human partners.

The most significant part of this work investigates the capacity of virtual agents to learn to perform actions from real human demonstrations, given frame-based instructions of actions (Chapter 5). Our action set comprises a set of trajectory-based movements, manifested in action instructions as spatial descriptive adjuncts specifying a trajectory of motions. We will apply a few machine learning techniques for this purpose, examining which is more suitable for the problem at hand.

Besides, we will also address some other side problems, either serve as a preliminary study leading to the main topic of this dissertation (in Chapter 4), or provide a complementary perspective to the focus (in Chapter 6). The result of this dissertation work would be a feasibility study of a multi-step framework combining various components, including a module to learn

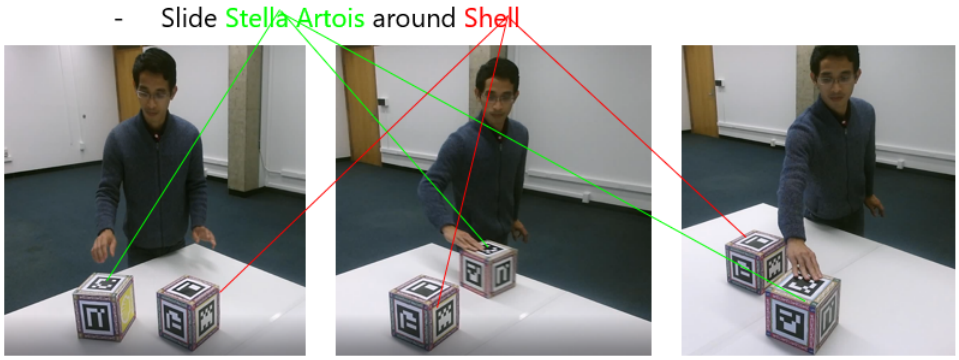

Figure 1.1: Learning from Demonstrations with visual and linguistic inputs

action representation from video captures, one to generate different simulations of the virtual agents performing the action, and one to visualize those simulations for evaluation.

1.1 Background

In this section, a number of ideas that have inspired this work is recapitulated. The arching theme is the ability of AI systems to learn in an adapting environment, to communicate with humans on different levels of abstraction and by different modalities and to learn new actions by mimicking human companions.

The most critical contributing idea is a collaborative environment for communication between humans and computers, presented in Subsection 1.1.1. For humans to teach robots new actions, we can employ LfD approach, summarized in Subsection 1.1.2. While classical LfD is typically built upon robot sensorimotor modality, to extend it for linguistic modality, we need a linguistic theory for the mapping between action represented in language and in reality, discussed in Subsection 1.1.3. Two machine learning frameworks to recognize and perform actions are sketched in Subsections 1.1.4 (Sequential Modeling) and 1.1.5 (Reinforcement Learning). System evaluation is facilitated by human feedback on visualization of performed actions, presented in Subsection 1.1.6.

Other inspirations to this thesis work come from: interpretation of spatial cognitive reasoning and its application in spatial control for robotic systems, as well as qualitative reasoning as a common knowledge interface between humans and AI systems, discussed in Subsection

1.1.8; XAI as an emerging AI sub-field that aims for machine learning models that could be interpreted by domain experts (1.1.7); usage of video captures to infer or recognize event/action structure (Subsection 1.1.9), and especially the usage of RGB-D datasets (Subsection 1.1.10); cognitive linguistic work regarding the human ability to learn new concepts or to perform novel actions (Subsection 1.1.11).

1.1.1 Communicating with Computers

As a general term, communicating with computers can be understood in the same way as human-computer interaction (HCI), in which there is an exchange of information between human and computers. Communicating with Computers (CwC) program, a DARPA project in specific, advance HCI to take into account multiple modalities, namely vision, spoken language, and gestures. Moreover, it would enable humans to share complex concepts with computers, building upon more elementary concepts. Quoting the program's statement, it *focuses on developing technology for assembling complex ideas from basic ones given language and context*.

More importantly, for computers to be able to understand complex concepts from elementary concepts, it is necessary that we include **learning from demonstration** as one modality of communication. Not only that this kind of learning allows an agent to learn new concepts through interaction, incremental learning allows humans to provide immediate feedback to the computers to change its execution programs.

In this thesis, some potential methods to incorporate feedback from human interlocutor to improve our AI's learned action model will be explored. Because in real-world collaborative environment, communication is carried out over multimodal channels, we will discuss]] potential sources of feedback. In Section 5.3.6, we will investigate the use of two simple kinds of feedback (positive-negative acknowledgment and deixis/pointing feedback), leaving more complex ones, such as linguistic instruction/correction for a possible future extension.

1.1.2 Learning from Demonstration

Learning from Demonstration (LfD) can be traced back to the 1980s, in the form of automatic robot programming. The earliest form might be called *teaching by showing* or *guiding*, in which a robot's effectors could be moved to desired positions, and the robot's controlling system records their coordinates and rotations (controlling signals) so that when the robot is asked to

execute the program, the controller will move its effectors according to the recorded controlling signals. This mechanism, though rudimentary, has proved successful with little memory or computational power in the eras before the popularity of general-purpose computers. It is, however, just *record and replay* method, which is agnostic to the environment (Lozano-Perez, 1983).

This simple *guiding* framework has developed into robot Programming from demonstration (PbD) framework, which has several developments in recent time. In primary, it still applies the same principles of using sensorimotor information of robot's joints to learn models of actions. However, it has been able to generalize from just *record and play* method, by allowing interpolation for novel configurations or new environments. Calinon et al. (2007) is exemplary, in which a teacher guides a humanoid robot's hands to move a chess piece forward through kinesthetics. Recently, the field starts to pick up newer machine learning tools such as Artificial Neural Networks (ANNs), Radial-Basis Function Networks (RBFs), etc. Moreover, the field progressively expands with other modalities of teaching-learning interface, such as vision, haptics, etc.. A representative work that shows this development is the thesis of He (2017), in which robots observe multiple object manipulation (in-hand rotation of objects) and process them into visual and haptic features, and learning action policy by applying RBFs network over these feature vectors.

Another branch of the original line of research is its interdisciplinary variance, named **imitation learning**. Evidence from biology, neuroscience, cognitive sciences and human-computer interaction (HCI), has been used to guide its research methods. For instance, neuroscientific research showed that primate imitation learning requires a conceptual model of object spatial and relative locations, resolved from visual sensory information (Maunsell and Van Essen, 1983). HCI contributes a framework for incremental learning, which makes the interaction between humans and computers an essential component in the learning process. This effectively speeds up the learning rate, corrects learning errors, or guides learning agent to focus on a specific part of learning. In particular, for action learning, deixis cues (pointing or gazing) could be used to limit the start and end of a demonstration or to define the participating objects (Calinon and Billard, 2006).

On the terminology used in this thesis, the term Learning from Demonstration (LfD) will be used, following discussions in Argall et al. (2009). Programming by Demonstration will not be used because this term applies typically to robot PbD, and in this thesis, all experiments will be

carried out in a simulated environment. Also following Argall et al's survey, this research could be categorized as an *imitation with external observation* approach, which means the **teacher execution** (motion of human body) could not make an Identity mapping to the **recorded execution** (input from 3-D sensors), and **recorded execution** could not make an Identity mapping to the **learner execution** (the agent's planning policy). However, this subcategorization is not widely adopted by other authors, such as Billard et al. (2008). In fact, Billard et. al uses *imitation* to only mean the reenacting part of the whole system, not including the *re-demonstration* part. Without adding more confusion, we will use the most accepted term that could be found in the literature, which is Learning from Demonstration.

In subsections 1.1.4 and 1.1.5, we will describe two machine learning techniques used in this thesis: temporal-sequential modeling learns models of the skills from demonstrations, and search/reinforcement learning methods to reproduce the learned skill in a new context.

1.1.3 Dynamic Event Structure

This work is a culmination of an effort to cross-pollinate different lines of research in our Brandeis's Computational Linguistic lab. Pustejovsky's rigorous framework of dynamic events and event participants (Pustejovsky (2013)) led to different lines of research: a top-down semantic framework called *Multimodal Semantic Simulations (MSS)*, which can be used to encode events as programs in a dynamic logic with an operational semantics, and in turn is used to create a conversational and grounding interface between humans and computational agents; a bottom-up approach that learning event representation through machine learning methods, using data from 3-dimensional video captures. The first approach requires programming of various predicative types, such as verbal-action types (**slide**, **roll**, **put**), and spatial adverbials (**on**, **in**, **next to**, **around**). The second approach, so far, can only make distinctions between different verbal-action types and spatial adverbial types (Do and Pustejovsky (2017a)). This work is trying to bridge the gap between two approaches, which is to learn the programmatic form of actions directly from the data.

This work is also related to traditional treatment in computational linguistics, in particular, in lexical semantics, motion verbs can be divided into *manner-* or *path-* oriented predicates. Adjuncts, then, can be used to complement meaning on the other aspect of motion (Jackendoff, 1983). This classification corresponds to answers of *how* the movement is happening and *where*

it is happening. Taking, for example, these two following sentences (Krishnaswamy, 2017):

(c) The ball rolled$_m$ across the room.

(d) The ball crossed$_p$ the room rolling.

In the first sentence, the predicative verb describes the *manner* of motion, while the adjunct refers to the motion's path and vice versa for the second sentence. While this work will focus on learning ability in regard to motion's path, the methodologies in this work can be applied to motion manners as well, with a consideration that the *manner* of motion usually refers to movement gradient of the object over time. For example, *slowly* refers to a small change of movement, while *roll* refers to an intrinsic change of its orientation over time. The difficulty of learning these *manners* of motion lies in the fact that these movements depend on object affordances. For instance, a ball can be rolled, but not a cube.

1.1.4 Temporal-sequential modeling

Essentially, temporal-sequential models are any algorithmic, machine learning or logical models that allow us to represent changing of system states over time. There are many different types of models belonging to this category, with a wide variety of application, including classification (Do and Pustejovsky, 2017a), text/dialog generation (Serban et al., 2017), etc. Some popular sequential modeling systems are: finite-state machine or finite automaton (FSM) in either deterministic or non-deterministic forms; its development with more explanatory power, Hidden Markov Model (HMM); interval temporal logic, etc. More recently, the development of neural methods has brought about several sequential neural network models, such as Recurrent neural networks (RNNs), with its flavors such as Long short term memory (LSTMs) or Gated recurrent unit (GRU).

Arguably, predictive sequential learning model is the most appropriate model for learning of trajectory level skills. What the learners observe in each action demonstration is a frame-by-frame sequence of feature vectors, and a predictive model could be used to produce different label of the sequence: which category of action it is, whether it has been terminated or not, etc. A feed-forward network such as RNN can be aptly trained to fit a high level of intricate patterns in the feature vectors.

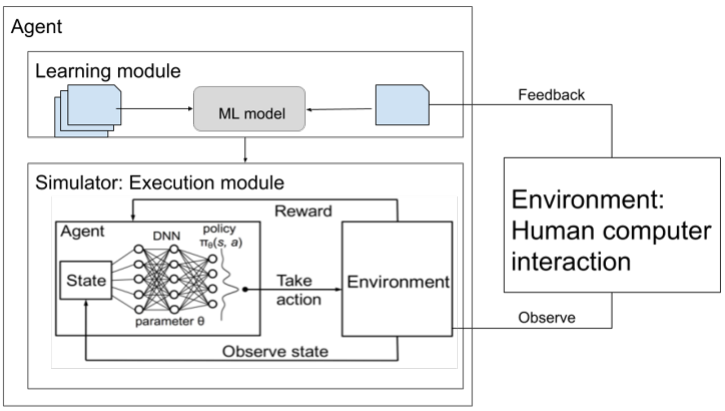

Figure 1.2: Reinforcement learning framework

In Chapter 4, we will use RNN models to learn an action recognizer that can distinguish between fine-grained actions. The RNN models we use are instances of sequence-to-one classifiers that predict a distribution of action classes for each input.

In Chapter 5, we will use RNN models to learn functions called *progress functions*, and each helps to guide the agents to complete an action. A progress function is an instance of sequence-to-one regressor that produces a value from 0 to 1, that will be used to as a reward function for reinforcement learning (briefly described in Section 1.1.5).

In Chapter 6, we will use a more advanced form of RNN models (called Attention RNN) to learn a mapping from natural language instructions to action sequences. The model is an instance of Seq2Seq models that have been successfully used in a wide spectrum of applications, such as neural machine translation (Wu et al., 2016) and image caption generation (Xu et al., 2015).

1.1.5 Reinforcement learning

Reinforcement learning (RL) is a set of methodologies used for robotic or virtual agents to learn by interacting with an environment, finding an action policy to optimize a target value function while exploring the action search space. In this work, we will explore some combination of search methods and reinforcement learning methods, especially ones belonging to Monte Carlo family.

A general formalization of reinforcement learning includes the following components: a *policy* dictates actions of agents given the current state of the environment (*state* or *observation*), a *reward signal* dictates the goal of RL problem in the form of a single reward value returned from the environment after each action is performed, and a *value function* is the accumulated reward over a long run. In this problem, *state* refers to a feature vector that describes the current configuration of the simulated environment, which builds upon qualitative spatial features between objects, *action* refers to a movement of blocks (and which block to move), and *value function* refers to the progress function mentioned above.

A particularly appealing framework that can be applied in learning policy in continuous space is one of policy gradient methods. In a nutshell, these methods learn a *parameterized policy* by optimizing a target value using *stochastic gradient descent* methods. In this dissertation work, we will use different *policy gradient* methods, including REINFORCE (Williams (1992)) and some variances.

In this thesis, we constrain the set of actions so that all of them could be simulated in a 2-dimensional environment. This is not really a requirement for the idea to work, but it allows us to develop a 2-dimensional simulator to try different RL algorithms quickly. An extension to 3-dimensional space by employing a more sophisticated physical engine simulator that can generate, possibly in parallel, multiple simulations, without visualization expense (as seen in game engines like Unity).

1.1.6 Evaluation interface

To evaluate, we will visualize the actions being performed in 2D and 3D simulation environment, which allows evaluators to judge whether the system has successfully learned the novel concepts. The 2-D simulator could be used to evaluate the learned model quickly. The 3-D simulator aligns better with human cognitive ability, allowing more precise and intuitive judgment, but is generally slower to set up.

The 2-D simulator is written with Python's *matplotlib* library, supporting simple human-machine interactions. Users can reset new starting configuration of objects in a 2-D environment, then observe learning agents to plan actions step-by-step. Besides using it for evaluation, it can also be used as a playground for interactive learning, as discussed in Subsection 2.4.1.

The 3-D simulator is based on Krisnaswamy's Voxicon Simulator (VoxSim Pustejovsky and

Krishnaswamy (2014)) used for generating visual scenes from textual sentences. VoxSim is, in turn, developed using the popular Unity 3-D game engine. VoxSim has been explicitly configured to test action simulations in a **Block World** environment, whereas a virtual humanoid agent named Diana can be commanded to move objects around on a flat table.

VoxSim, with the connection to a real-time gesture recognition using deep convolutional neural networks (Krishnaswamy et al., 2017) allows human-computer communication with generation and interpretations of multiple modalities, including text, gesture, and visualization. In fact, that creates a robust framework for interactive and incremental machine learning. Though not discussed in this dissertation, VoxSim can also be used for interactive learning, i.e., users can gesture to Diana sequential locations of a block as a demonstration of an action.

1.1.7 Explainable AI

In Chapter 4, we will use a deep learning model to learn an action recognizer. As typical to deep learning models, the model has a "black box" nature, i.e., it can hardly be explainable. That creates an issue of knowing whether we have actually learned action representations, or we have learned something else that helps on classification task. For example, deep learning methods on activity recognition have a tendency to employ all channels from RGB-D input to predict action classes (Rahmani and Mian, 2016). While this method leads to a higher performance score, it is not necessary that the classifier can capture action representations. For example, when there is an action like "open a door", can we tell that the learned model really captures the semantics of that action? Or it might just recognize the door observed in the scene? Or it might actually capture just the shiny doorknob? We do not know. As long as the only target of a machine learning model is to optimize objectives on validate data, it is hard to understand and visualize the landscape of the predictions that the model produces.

In recent years, there have been several efforts to make sense of machine learning models, i.e., to demystify their black box nature. For example, uses of adversarial samples to "fool" deep learning model (Papernot et al., 2016) is one way explore the "landscape" of deep network models, to understand when they fail, how they fail and how to combat against this bad behavior of DNN.

Another, more explicit effort, is to push forward the development of more interpretable machine learning models. For example, DARPA's Explainable AI (XAI) initiative (Gunning,

2017) calls for the creation of new machine learning techniques that piggyback on current high-performing but opaque models such as deep learning or random forests, but are also trained to optimize a meta-objective of being interpretable. Models of this type include models generating high-level and interpretable features automatically from deep networks (Si and Zhu, 2013), models generating visual explanations for classification of images (Hendricks et al., 2016), etc.

Although this work is not directly related to the XAI initiative, XAI has been a recurring topic discussed in our lab. The development of our VoxSim and EpiSim (an in-house service for visualization of VoxSim epistemic model) is an effort to allow humans to peek into the machine's brain. In that spirit, we propose that for action recognition, the most interpretative model is the one that allows re-enaction of the action on a novel setup. The learned action representation is analogous to *disembodiment* of actions from the training observations, just to be incarnated in a novel situation.

1.1.8 Qualitative reasoning

Qualitative reasoning (QR) is, first and foremost, the logical reasoning strategy that humans employ to cope with an infinite amount of data. Our brain, though a very complex system with billions of neurons, can still only process and memorize a finite amount of data. We, therefore, always make decisions on partial knowledge. Moreover, we do not usually need to remember exact values. Simple binary or categorical distinctions often work as well for us in our decision-making process (probably excepts for financial matters). For example, we stop if the traffic light is red, we go if it is green. That tendency allows us to memorize and reason only on *qualitative* descriptions, which are reduced from quantitative descriptions. We, therefore, only focus on some *landmark values* ((Bobrow, 2012)) - a subset of infinite possible values, and disregard others. For instance, "freezing" and "boiling" are too natural landmark values of water temperature.

Qualitative reasoning, as applied in computer science, is a framework that applies the same qualitative principle in designing decision-making machines. Think of a smart home system that allows you to set a rule "Turn off the heater when it gets too hot". You might have pre-defined what room temperature is considered "too hot" a while ago, but with that *landmark value* already fixed, you can communicate on a more meaningful level with this system, while disregarding the mundane details of what exact temperature you have set.

Qualitative reasoning is strongly associated with natural languages. Before the invention of measurement devices, we can still talk about temperature. It could be freezing, cold, warm or hot. These *landmark values* are more subjective, fuzzy and personal (for example, a hot day for a Siberian person might be a freezing day for me), and language-dependent, but as long as there is some conversational convention, they allow humans to communicate and collaborate effectively.

Qualitative spatial reasoning is a sub-field of qualitative reasoning, directly applied to AI systems, such as robots. As embodied systems, they process inputs, plan actions and navigate spaces through reasoning on spatial information (Bhatt et al., 2011; Cohn and Renz, 2008). While robots can work on raw data, communication between robots and humans requires an intermediate level of representation, which spatial qualitative principles can be aptly used.

In the experiment part of this dissertation, we will see that qualitative features play an important role in facilitating learning of action model as well as to reduce planning space when we re-enact actions in a new environment.

Admittedly, qualitative reasoning applied in this work is more of a feature extraction method than to represent learned models in a way readable to human examiners. This representation is, however, better than a wholly symbolic and human-readable representation but hard to work on for machine learning methods, and also better than a raw feature-based representation that generally requires more training data to learn efficiently.

1.1.9 Action learning from videos

Human activities such as *running*, *sitting*, *eating*, and *playing sport* have been investigated in previous research, such as in Shahroudy et al. (2016). These human activities have significantly different motion signatures, therefore, classifying them is pretty simple. Recently, some studies have begun to introduce datasets with more complex activities, primarily involving human-object interactions, such as cooking (Rohrbach et al., 2012), taking medicine (Koppula and Saxena, 2016), or human-human interactions, such as handshaking (Ryoo and Aggarwal, 2010). More recently, Li and Fritz (2016) investigate the possibility of predicting partial activities using a hierarchy label space. These studies have gradually led to a more fine-grained treatment of event classification.

Actions can be learned atomically, i.e., entire actions are predicted in a classification manner

(Shahroudy et al., 2016), or as combinations of more primitive actions (Veeraraghavan et al., 2007), i.e., complex action types are learned based on recognition of combined primitive actions. For the former type of event representation, there are quantitative approaches based on low-level pixel features such as in Le et al. (2011) and qualitative approaches such as induction from relational states among event participants (Dubba et al., 2015). For the latter approach, systems such as described in Hoogs and Perera (2008), use state transition graphical models such as Dynamic Bayesian Networks (DBN).

Action classification using qualitative spatial methods has been discussed in a fair amount of work. Suchan et al. (2013) use the Regional Connected Calculus (RCC5) adjusted for depth field, with data also recorded by Kinect®Sensor. This work classifies events related to people moving, sitting, or passing each other. Dubba et al. (2015) provide a novel framework which gives a summary explanation for a sequence of observations by alternating between inductive and abductive commonsense reasoning. They apply their method for two activity types from RGB captures, aircraft and truck movements at an airport, and human-object interaction.

As a precursor for this research, we have done some preliminary work on learning action representation from a movie dataset, namely the Movie description dataset (Rohrbach et al., 2015). The idea is simple: can we learn the representation of an action, such as "slide" from a dataset that has mappings between a short video snippet and an action description? We also want to compare that to the same verb "slide" represented in our semantic framework of VoxML (Figure 1.3). It is attractive if we could use some readily available and large dataset like that to facilitate learning representation of actions. However, text descriptions from this dataset are highly stylistic, and scenes described with the same verb "slide" are highly varied that they are hardly comparable to our prototypical semantic definition. Following are some examples of text descriptions from the movie corpus. Without the visual scenes, it is still evident that the nature of actions described in these sentences is very diverse:

- He wipes out and his bike slides underneath the vehicle.
- Someone slides across a white limo's hood.
- As the car slides into a turn, he loses control and spins out completely.

$$
\begin{bmatrix}
\textbf{slide} \\
\text{LEX} = \begin{bmatrix} \text{PRED} = \textbf{slide} \\ \text{TYPE} = \textbf{process} \end{bmatrix} \\
\text{TYPE} = \begin{bmatrix}
\text{HEAD} = \textbf{process} \\
\text{ARGS} = \begin{bmatrix} \text{A}_1 = \textbf{x:agent} \\ \text{A}_2 = \textbf{y:physobj} \\ \text{A}_3 = \textbf{z:physobj} \end{bmatrix} \\
\text{BODY} = \begin{bmatrix} \text{E}_1 = grasp(x,y) \\ \text{E}_2 = [while(hold(x,y), \\ \quad while(EC(y,z), \\ \quad move(x,y)))] \end{bmatrix}
\end{bmatrix}
\end{bmatrix}
$$

Figure 1.3: Sample voxeme: [[SLIDE]]

1.1.10 RGB-D datasets

Because the central part of this work is on learning actions from RGB-D datasets, it would be a deficiency if we do not cover some previous work on RGB-D datasets and learning with depth-field data. A detailed review of RGB-D dataset is provided by (Firman, 2016). In this subsection, we will only give a brief introduction to a few relevant datasets.

Cornell 3D activity dataset: A dataset with the intention of capturing not only human activities but also to recognize object affordances for robots to interact with objects (Koppula et al., 2013). This is, we believe, the first effort to use human activity dataset to teach robots object interaction and action planning. It has 120 activity sequences of ten different high-level activities, with activity-subactivity annotation, as well as affordance labels on objects.

Robotic grasp dataset: A static RGB-D dataset that has bounding-box annotation at grasping positions of objects. This dataset and the learning methods from Lenz et al. (2015) allows real robots to operate on novel objects. Learning how to work with objects in the real world is a very complicated task. Even for a primitive kind of actions such as "grasp", the problem is not yet solved. Even if robots can pick up objects, the grasping point might not be the correct grasping position to allow further interaction with objects (e.g., where to grasp a water jug to pour to a cup; where to grasp a pen to write).

Watch-n-Patch ((Wu et al., 2015)): A dataset captures human activities, each containing a sequence of sub-actions dependent in a causal-chain manner. For example, a complex activity such as *warming milk* is a sequence of subactions such as *fetch-milk-from-fridge*, *microwaving*, *fetch-bowl-from-oven*, *put-milk-back-to-fridge*. The authors of this dataset also proposed an

unsupervised method to auto-segment extended activities into sequences of sub-actions.

Manipulation Action Dataset ((Aksoy et al., 2015)): A dataset of 8 activities *push, hide, put, stir, cut, chop, take, uncover*. The authors of the dataset also used a sequential model called semantic event chain (SECs), that learns a probabilistic graphical model with states being simple RCC relations (*touching*, *not touching* and *absence*).

As a side product of this thesis work, two datasets are generated based on RGB-D inputs: one is used for fine-grained activity recognition task in Chapter 4, and one for action reenactment task in Chapter 5. Notice that the datasets published online are tracking coordinates of objects and humans from RGB-D datasets, while original and raw RGB-D data are not available for privacy reasons.

1.1.11 Humans' action learning capability

To develop AI systems that can learn from humans, we could look into the way babies learn simple skills from adults for inspirations. Baby humans are the most potent learning agents in the world, with the ability to learn to grasp multiple types of objects, then moves on to use different kinds of tools in just the first few years of their lives.

Action and language are connected through the language of actions, mostly reflected by verbs and spatial adjuncts. There is a strong association between verbs and actions in infantile learning. For example, it has been shown that new verbs are learned more quickly when the action is named just before the infant performs it (Tomasello and Kruger, 1992). Also, new verbs are learned more effectively if they also perform the action instead of just watching it (Gampe et al., 2016). Toddlers also show sensorimotor activity (reflected by electroencephalography (EEG)) during auditory processing of action verbs (Antognini and Daum, 2017). These clues, combining together, suggest associative learning happens between visual perception, sensorimotor and linguistic faculties.

To understand how infants learn action skills, first let see how they learn simple reach and grasp actions. These are among the first object-interaction actions of infants, but quickly they would become tool manipulation skills. We know that infants start to explore the world in a random manner. While exploring the world, a child sometimes randomly makes contact with objects (under 4 months). A primitive, infantile reflex called *palmar reflex* causes his finger to reflex that creates an involuntary grasp (Kuipers, 2010). Grasping causes further actions,

such as "picking it up", "sliding it away", etc. Between 7 and 12 months, after mastering picking up objects, the child could start to explore them in details, by passing them between his hands, rotating them to check from different angles, or selecting the best grasp. As early as 12 months, he starts learning complex object compositional relation, such as *container-containee* relation (Garner and Bergen, 2006). After that, more oriented activities such as playing toys help children to explore more diverse and complex compositional characteristics of objects, such as learning of the distinction between functional parts of objects (e.g., parts corresponding to objects' *Gibsonian* versus *telic* affordances (Pustejovsky et al., 2017)).

Mapping that to our learning discussion, we can see the analogy between infantile learning and reinforcement learning, or in a broader sense, an *exploration-exploitation* learning mechanism. Exploration allows learning of new knowledge without direct teaching by incorporating perceptive inputs while exploring searching space. Exploitation allows applying learned models to perform actions efficiently.

Infantile action learning is usually through pretending plays, for example, using a brush on their hair or drinking from a cup. These are the effect of both mirroring from adults (whether or not adults intentionally teach children to use tools), and mastering of tool functionality. As pointed out by Gergely et al. (2002) and Schwier et al. (2006), pre-verbal toddlers, as young as 14 months (in the first work) and 12 months (in the second work), interact with tools by imitating adults performing actions, but with complex inferential process, rather than just emulation. They found that toddlers imitate adults switching a light bulb by using forehead if the adult performers have their hands free, but they would not imitate the forehead action if the adult hands are tied. It suggests that children at this age start to have a distinction between the goal and the mean of an action.

In Chapter 5, we can see a reflection of that distinction in the form of actions we teach AI agents. Actions, as well as events, extend a duration of time, and without further instructional input, AI agents might not be able to reason whether the whole action is important to learn (the mean), or only the final result (the goal) is needed. We will see that in the experimental setup, we will include both types of actions to find out if AI agents can learn them using the same framework.

1.2 Outline

This dissertation is structured as follows: Chapter 2 describes the scaffolding learning framework, with a brief introduction to the capture and annotation guidelines, feature extraction methods, and machine learning models that are common for the remaining chapters; Chapter 3 is dedicated to introducing a tool named ECAT, used for capturing and annotating actions captured from RGB-D inputs; Chapter 4 describes an action recognizer, that we have developed to study appropriate representation for action learning; Chapter 5 is the primiary focus of this dissertation, describing a methodology for learning agents to learn to perform a set of primitive actions from observing real human demonstrations, using sequential modeling and reinforcement learning; Chapter 6 flips the problem setup in Chapter 5 on its head, teaching learning agents to perform chain of actions directly by "neural" translating from textual instructions, using Sequence to Sequence models. We will close this thesis with conclusions and future directions in Chapter 7.

Chapter 2

Learning Framework

The learning framework for this research rests on the mapping among linguistic, visual and programmatic representations of actions. Inputs that robots could take in include text or spoken instructions from humans, visual features (including RGB, depth-field and infra-red, etc.). The mapping between linguistic and visual representation allows robots to recognize and describe actions, whereas an additional step of mapping from linguistic and visual representation to programmatic representation (or program form of action) allows robots to perform the action given human linguistic commands.

Linguistic action representation in this work is modeled as verbal subcategorization in a frame theory, a la Framenet (Baker et al., 1998), with thematic role arguments. In addition, we also account for *extra-verbal factors*, i.e., the aforementioned adjuncts describing paths of motions. Therefore, we consider *A moves B toward C* and *A moves B around C* as different action types and aim to learn each action type as a separate *atomic* action. A future work that includes learning the *manner* of an action would allow further distinction such as between *A rolls B toward C* versus *A slides B toward C* and combination of path and manner aspects of actions.

Our visual action representation comprises visual features extracted from tracked objects in captured videos or virtual object positions saved from a simulation environment. Both types of feature represent information visible to humans and observable by a machine in object state information. The machine, thereby, can observe humans performing actions through processing captured and annotated videos, while humans can observe machines performing actions through

watching simulated scenes.

Programmatic action representation is any representation that can direct robotic agents to perform an action with an object of known properties. This can be based on either formal action semantics or on feature-based machine planning. It is stressed that this representation is not the same as the representation for recognition tasks. From the machine learning perspective, these two tasks require different learning methods as well.

This chapter could be considered an extension of Chapter 1, but we will focus on various machine learning techniques and environmental setups used in this work. In particular, we will first discuss environment for capturing of learning actions in Section 2.1. We will then move on to discuss feature extraction framework used to process the captured data in Section 2.2. We will briefly discuss a general framework of sequential modeling using Long Short Term Memory method in Subsection 2.3.1, discussing its architecture, practices, and advantages over other sequential models. We will also cover two simulation/visualization modules, a Python 2-D simulator implemented to run multiple reinforcement learning episodes quickly (Subsection 2.4.1) and a 3-D visualizer extended from VoxSim (Krishnaswamy and Pustejovsky, 2016) for more realistic demonstrations (Section 2.5).

2.1 Capture environment and annotation guidelines

In this work, we use Event capture and annotation tool (ECAT) for capturing and annotating actions. We will separately discuss ECAT in chapter 3. In this section, we will only focus on the experimental setup for action capturing:

1. ECAT is installed on DARPA CwC Apparatus (Tamrakar, 2015). It includes the following components: a square table about 5' x 5', one flat screen mounted on one side of the table, and two Microsoft's Kinect® devices mounted on two sides next to the side mounted the screen (Figure 2.1).

2. Blocks are 6" cube blocks marked with ARUCO markers. The blocks belong to the original CwC setup, each printed with a brand name, such as *Pepsi*, *Stella Artois*). The ARUCO markers are stuck on different sides of the blocks (Figure 2.2).

3. The apparatus is so located that performers can move freely around the performing table,

and can observe the captured scenes on the flat screen, to ensure that they do not move out of the field of view (FoV).

Figure 2.1: DARPA CwC Apparatus

Data capture guidelines are as follows:

1. Create a separate project for an action type. Under each project, for each performer, capture a long session of the performer doing multiple instances of an action.

2. The performers are given the textual description of an action, such as *slide A around B* or *make a row from three blocks*, and are asked to perform according to their understanding of the action.

3. After each demonstration, the performers move the blocks to some initial configuration for the next demonstration. The performers are asked to vary the initial locations of blocks in each demonstration as much as they can, to vary their position with regard to the table, and change their performing hands. These strategies are mainly to add variation into training data.

4. Data capture is carried out with one person being the action performer, and one person helping with starting/stopping capturing sessions. The helper also watches the live capture to make sure that the performer is still tracked and objects are not pushed outside of the capturing FoV.

Figure 2.2: Block with ARUCO markers

Annotation guidelines are as follows:

1. Annotators first mark the surface of the table throughout multiple frames of a session, by drawing a polygon boundary. Then the annotators click on *Generate 3D* to generate the 3-D planar equation for the table.

2. Annotators create or load ARUCO markers prototype file. This file maps a block name to its ARUCO markers. In turn, each ARUCO marker is represented by a 5x5 bitmap.

3. Annotators click on *Detect objects* for the ARUCO marker detection algorithm to run. The algorithm first maps the marker it sees on a face of a block to an Id (e.g., ARUCO 129). The ARUCO marker is, in turn, mapped to a block name.

4. Annotators click on *Map to 3D* to map objects into 3-D coordinates using the captured depth-field.

5. Annotators annotate actions by marking action spans (beginning and end frames) as well as adding a description of the action (e.g., The performer slides Pepsi around Stella Artois) while watching the replay of a session. Annotators are asked to mark the beginning of an event when the object starts to move, and the end when the performers stop moving object and release their grasp.

2.2 Feature extraction module

To facilitate action classification and reenactment, it is necessary to present them in a learnable format. This introduces the question of how to represent actions, namely the difficulty in defining their temporal and spatial extensions, as well as the difficulty in selecting an observational perspective.

Moreover, the feature representation for actions needs to be shared between the real captured-data used for training and the artificial data generated from the simulator. The feature space in these two types of data are largely different: the real captured data is fuzzy and sometimes includes noisy outliers (shown as flickers when a captured session is visualized); the simulated data is smooth and interpolated frame-by-frame from planned actions.

This leads to the difficulty in finding an appropriate feature set as a common abstraction to bridge these two kinds of data. Some feature types will be presented in this section. They can generally be divided into two sets: quantitative and qualitative, whereas qualitative features are calculated based on quantitative features.

Both quantitative and qualitative features of the captured data are calculated based on projecting the blocks' coordinates on the 2-d surface of the apparatus's table. The details of the projecting algorithm are presented in Algorithm 1.

Input: 3-D coordinates of markers for each block (one block might have multiple visible markers)
Size of the block **Purpose**: Estimate a 2-d square for each block on projecting surface
Result: Centroid and angle of projected 2D square
Estimate plane equation P of the table;
for *Each block* **do**
  Select the marker that has the most number of corners, and the largest size (most clearly observed marker) ;
  Estimate plane equation Q of the marker face;
  if *the cosine product of P and Q norm vectors* < 0.5 **then**
    Calculate the square T that perpendicular to Q, have the correct size, and have the edge on the middle line of marker P;
    Project T on P (T_P);
  else
    Rescale and project the marker on P (T_P);
  end
  Use a single point on P as the (0,0) origin, estimating the transform of the 2-d square from (T_P);
end

Algorithm 1: Algorithm to project blocks on 2-D simulator

2.2.1 Quantitative features

Firstly, in each demonstration of an action, objects are ranked by their salience, i.e., the object that moves the most is the most salient. Quantitative features include the followings:

1. Location of the centroid of a block, and the block's angle made with regard to the Ox axis (the transform as estimated from Algorithm 1).

2. The difference between transforms of the most salient object to the second salient object.

3. The gradient of the transforms of the objects, i.e., the difference between two frames.

While quantitative features are not the focus of our discussion, we will include them to provide a more comprehensive picture, and to give a comparison to the qualitative methods.

2.2.2 Qualitative features

Qualitative spatial reasoning (QSR), a sub-field of qualitative reasoning, is considered to be akin to the way humans understand geometry and space, due to the cognitive advantages of conceptual neighborhood relations and its ability to draw coarse inferences under uncertainty, and also analogous to the way humans map from continuous space of spatial perception to discrete space of linguistic description (Freksa, 1992, 1991).

It is also considered a promising framework for robotic planning (Cohn and Renz, 2008). QSR allows formalization of many qualitative concepts, such as *near*, *toward*, *in*, *around*, and facilitates learning distinction between them (Do and Pustejovsky, 2017b). The use of qualitative predicates ensures that scenes which are semantically close have very similar feature descriptions.

Moreover, from a machine learning perspective, as pointed out by Yang and Webb (2009) and Jiang et al. (2017), qualitative representation is a method of discretization, which makes data sparser, therefore easier to learn. Especially when taking the difference between features of two adjacent frames, as a qualitative feature strongly distinguishes between 0 and 1, the effect of a feature change is more pronounced.

There is extensive literature supporting the use of discretization for feature embedding. Yang and Webb (2009) show that discretization is equivalent to using the true probability density function. More recently, Jiang et al. (2017) have used this method for classification of GPS trajectories. They studied three different approaches for discretization, including *equal-width binning*, Recursive Minimal Entropy Partitioning (RMEP) (Dougherty et al., 1995) and fuzzy discretization (Roy and Pal, 2003). Their finding is that the *equal-width binning* approach is both simple and effective, so we use this approach for quantization of both distance and orientation.

QSRLib (Gatsoulis et al., 2016), a library that allows computation of Qualitative Spatial Relations and Calculi is employed to generate qualitative features. In particular, the following feature types from QSRLib are used:

- CARDINAL DIRECTION (Andrew et al., 1991) a.k.a QSRLIb *cardir*, transforms compass

relations between two objects into canonical directions such as North, North East, etc. In total, this qualitative relation gives 9 different values, including one where two locations are identical.

- MOVING or STATIC (QSRLIb *mos*) measures whether a point is moving or not.
- QUALITATIVE DISTANCE CALCULUS (QSRLib *argd*) discretizes the distance between two moving points, i.e., the distance between two centers of two squares.
- QUALITATIVE TRAJECTORY CALCULUS (Double Cross) a.k.a QSRLib *qtccs*: QTC_C is a representation of motions between two objects by considering them as two moving point objects (MPOs) (Delafontaine et al., 2011). The type C21 of QTC_C (implemented in QSRLib) considers whether two points are moving toward each other or whether they are moving to the left or to the right of each other. The following diagram explains this:

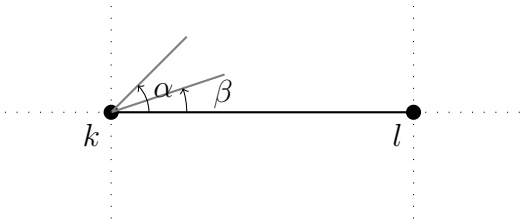

QTC_C produces a tuple of 4 slots (A, B, C, D), where each could be given either -, + or 0, depending on the angle α. In particular, A and C explains the movement of k toward l, and vice versa for B and D. A is $+$ if $\alpha > -90 \wedge \alpha < 90$, $-$ if $\alpha > 90 \wedge \alpha < 270$, and 0 otherwise, i.e., whether k moves toward l or away from l. C is $+$ if $\alpha > 0 \wedge \alpha < 180$, $-$ if $\alpha > 180 \wedge \alpha < 360$, and 0 otherwise, i.e., whether k moves to the left or right of l. QSRLib also allows specification of a *quantization factor* θ, which dictates whether the movement of a point is significant in comparison to the distance between k and l.

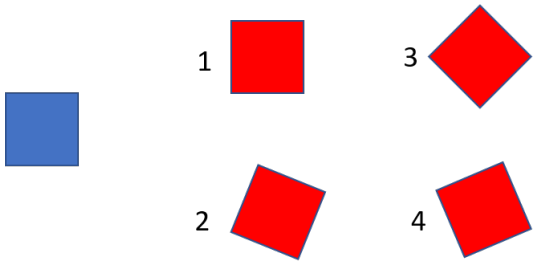

Figure 2.3: Quantizing object rotations

The followings are the qualitative features used in this research:

- F1: cardinal direction between two centers
- F2: qualitative distance between two centers
- F3, F4: $\Delta(F1), \Delta(F2)$
- F5, F6, F7, F8: 4 QTC_C slots
- F9, F10: quantized orientations of the first and second objects, as described in Figure 2.3.
- F11: F9 - F10
- F12, F13: $\Delta(F9), \Delta(F10)$

There is some correlation between these features. In addition to the features that are derived from other (like the Δ features), some features have similar meaning but different implementation. For example, F4, F5 and F6 are very similar. The difference is that F4 is only sensitive to the change of quantized distance, while F5 and F6 are usually much more sensitive. F5 and F6 distinguish which object is moving, while F4 does not.

2.3 Supervised machine learning module

The main supervised learning method used in this dissertation is Recurrent Neural Network, with a specific version of Long-short term memory (LSTM) (Hochreiter and Schmidhuber,

1997) as the processing cell. LSTM has found utility in a range of problems involving sequential learning, such as speech and gesture recognition, human activity recognition and movie description generation. While we have given a short introduction to sequential modeling methods in Section 1.1.4, in this section, we will address the architecture of LSTM used in this research and common practices needed to learn a successful LSTM model.

Even though LSTM has existed for a long time (more than 20 years!) and has somewhat become an industrial standard for sequential modeling, its working principle is arcane, and its model is hard to interpret, as shared by most, if not all, deep learning models. While it is hard to explain why LSTM, as a specific flavor of Recurrent Neural Network, has been so successful over the years, there are a few crucial points worth recapitulating in respect of the motivation for the specific form of LSTM architecture (Section 2.3.1). Over the time, use of LSTM models has created some common practices, which we will summarize in Section 2.3.1.

Moreover, we will also provide a brief review of a few other popular sequential models, including their advantages and disadvantages (in comparison with neural network based models like LSTM), as well as their appropriateness for the problem at hand. Two popular families of models will be addressed in Section 2.3.1, discrete hidden state models such as Hidden Markov Model (HMM) and Chained Conditional Random Field (Chained CRF), and continuous state models such as Linear Dynamical System (LDS). Note that another sub-type of CRF (Tree-CRF) will be discussed later for constraining classification outputs, but not for sequential modeling.

2.3.1 LSTM

Architecture

LSTM, first and foremost, is a flavor of Recurrent Neural Network. Recurrent Neural Network is just a neural network that retains a **state** or **memory** during learning, while a simple Feed Forward Neural Network (FFNN) does not keep any memory, just a set of **parameters**. RNN is, therefore, more powerful and generative than FFNN, which can be considered as RNN in one step. Following is an example to illustrate this difference. Let's say you want to learn a Part-of-speech tagger using neural network methods. The FFNN method would use some features of the current context window (word forms, suffixes of the current words and some words before it) as a feature vector to feed into a neuron network that predicts the output POS. In contrast,

RNN would keep another memory vector, accumulating information from the beginning of the sentence (and also from the end if you use Bidirectional RNN); as a result, you can capture long-distance dependency, such as if you have a left quote somewhere in a sentence, there should be a right quote as well. For POS tagging task, it might not be straightforward what is the benefit of using sequential modeling, but the Bi-LSTM model is among state-of-the-art models, outperform FFNN method by a small margin (Huang et al., 2015). A state update of classical RNN is represented by Equation 2.1. State from the previous time step is concatenated with input X_t and then passed through a neuron with $sigmoid$ activation function. W is the weight and B the bias matrices.

$$H_t = \sigma(W * (H_{t-1} : X_t) + B) \tag{2.1}$$

LSTM is an RNN that has a special calculating unit called LSTM cell, depicted in Figure 2.4. In a nutshell, an LSTM cell has two states, one is the *memory state*, denoted by C_t, and one is the actual output vector denoted as H_t. Outputs from 4 neurons are called gates: I is input gate, G is new input gate, F is forget gate and O is output gate. Updating the memory state C and the output cell H is given by the following equations (From (Zaremba et al., 2014)):

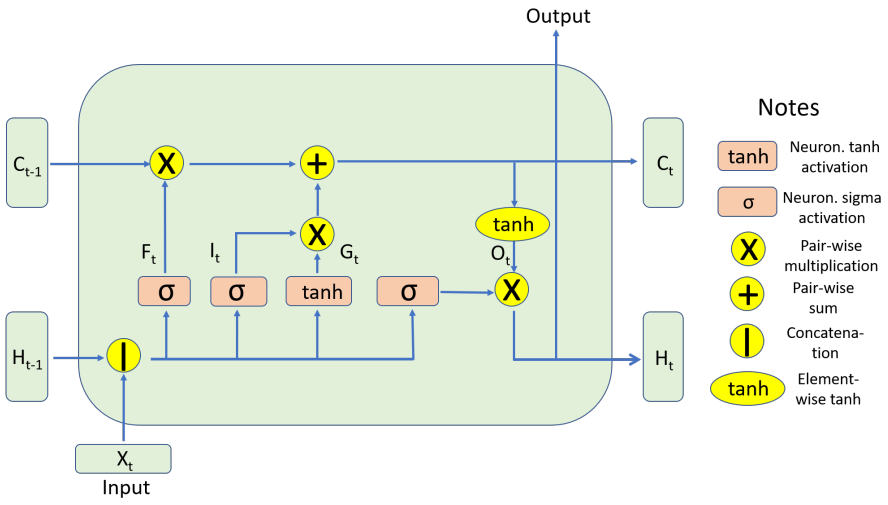

Figure 2.4: Architecture of an LSTM node. Note the color code for simple (pairwise, or elementwise) operations is yellow, color code for neural operation is light orange.

$$C_t = \underbrace{F_t \odot C_{t-1}}_{\text{Long}} + \underbrace{I_t \odot G_t}_{\text{Short}} \tag{2.2}$$

$$H_t = O_t \odot tanh(C_t) \tag{2.3}$$

$$\tanh(z) = \frac{e^z - e^{-z}}{e^z + e^{-z}} \tag{2.4}$$

The intuition for the equation 2.2 is that at each time step, we want to keep a part of the memory at the previous step, scaled by a scaling factor at **F gate**, plus a new value for the memory, calculated at **G gate**, also scaled by another scaling factor at **I gate**. Because F and I are two scaling factors, their component values are between 0 and 1. Therefore, they are given by two neurons with $sigmoid$ activation function. **G gate** calculates a new candidate value for the *memory state*; therefore it is given by a neuron with $tanh$ activation function (value ranged from -1 to 1). The advantage of LSTM model over vanilla RNN is the use of the *memory state* C. Without it, the model outputs values from **O** (from 2.3) directly, and become vanilla RNN model.

You might ask why we need a product of two gates I and G as the candidate value for new *memory state*, or why we multiply output gate value O with $tanh$ activation of *memory state*. Fortunately, the arcane architecture of the LSTM cell has been demystified by the work of (Jozefowicz et al., 2015). They proved that not all the gates in LSTM are strictly necessary. Except for forget gate, you can drop any other single gate without sacrificing too much of performance.

In short, technically, the most important characteristic of LSTM model is the use of *memory state* separated from the output as two states of LSTM cells. Intuitively, cell output is *predictive*, i.e., trained to predict some labels, whereas *memory state* is *explanatory*, i.e., explain why you predict such label. Also fundamental is its breakdown into an update to *long-term* memory and a new capture of *short-term* memory (Equa. 2.2).

Common practices

Over the years, the development of LSTM has picked up a few standard practices. The followings are some good practices for various purposes, including practice to process inputs, to combat over-fitting, to tune hyper-parameters, etc.:

1. Use of a dense layer as the last layer of the network: An output vector H_T from an LSTM cell has the same dimension as the *memory state*, so a common practice is to pass it through a dense linear layer. For classifiers, the output is a logarit probability vector; its dimension is the number of classes. For regressors, it is just one real value.

2. Chunking of input sequence: A common practice when generating inputs for LSTM network is to pad input sequences so that all feeding sequences have the same length. For tasks such as categorizing text inputs, each sentence will be truncated or padded to a fixed length (e.g., 50 words) before being fed to the model. For the problem at hand, because we have a long continuous sequence of visual inputs, the most appropriate method is to chunk the long input sequence into multiple shorter sequences, each sequence will be considered as one input sample. Notice that we could not achieve independent and identically distributed (i.i.d) property for this dataset because all input sequences are captured in a small set of long videos. However, by randomly permuting them before training, the issue of temporal correlation among samples is minimized.

3. Multi-layer LSTM: As typical in deep learning methods, when we go deeper, the model performs better, with a trade-off of longer training time, and a larger model to keep. For LSTMs, go deeper means stacking multiple layers of LSTM cells on top of each other. The output from H_t is fed as the input to the LSTM cell on the next layer, while we are keeping multiple *memory states*, each for a layer of the LSTM model.

4. Retaining of *memory state* between training (or testing) mini-batch: While we call the state vector C_t as long-term *memory state*, whether it can capture long-term dependency between input sequences or it just capture context from the beginning of each sentence depends on another property of the model, called *statefulness*. A stateful model retains the memory states between consecutive mini-batch updates, whereas a stateless model resets the memory states after each mini-batch. In practice, the matter of using stateful LSTM models is coupled with the matter of shuffling training samples. As training samples are shuffled before training, a stateless model is used.

5. Dropout: Dropout is a standard method in deep neural network training to address the problem of overfitting(Srivastava et al., 2014). In training, in each mini-batch, a percentage $1-p$ of network nodes are chosen randomly to be skipped so that only the parameters

of p remaining nodes are updated. In testing, all nodes are present, but the activation output is scaled with p. For deep feed-forward neural networks, one can choose to thin out different layers with different dropout rates. For LSTM model, as pointed out by (Jozefowicz et al., 2015), only two vertical edges in Figure 2.4 can be applied dropout: Input edge from X_t to concatenation operator, and output edge from H_t. In total, information flow from the input to the output of the LSTM can be corrupted $L + 1$ times where L is the number of stacked LSTM layers, independent of the number of steps in the sequence. Also, as theoretically proven by (Gal and Ghahramani, 2016), we need to use the same dropout operator (exact same set of dropout nodes) for all learning steps.

6. Training method: LSTM, similar to other deep learning models, typically use an online-learning method, such as Stochastic gradient descent or Adam (Kingma and Ba, 2014), to minimize an objective by continuously calculating the objective and updating the parameters on a portion of the training data.

7. Hyper-parameter grid searching: In training a neural network model, there are a number of hyper-parameters that are difficult to set right from the beginning. By grid searching over some different values for these hyper-parameters, we can select the best combination. They include $keep\,prob$ (the percentage of nodes remained in dropout layer), $hidden\ size$ (the size of a feature vector in the *memory state* C_t), $num\ layers$ (the depth of the LSTM stack), $learning\ rate$ (the speed of updating model's parameters), $training\ algorithm$.

LSTM versus other sequential models

In this section, we will pit LSTM against two classical sequential models: discrete State Markov Models and Linear Gaussian State Space Models (LG-SSM) (RNN and LSTM are, by no mean, recent, as we have discussed previously, but enter mainstream focus only after the advance of deep learning methods).

Firstly, discrete state Markov Models, such as Hidden Markov Model (HMM), its discriminative sibling Maximum Entropy Markov Model (MEMM), and their cousin Chained CRF, are very similar to RNN in their nature. MEMM is analogous to a classical RNN which has a hidden state represented by a one-hot encoding vector (vector that is zero, except for the position corresponding to an active state), and the neuron has a **hardmax** activation function (the

hardmax function turn a probability distribution to a one-hot vector by setting the value at max category to 1, and other to 0). There are two disadvantages of this set of methods. The first problem is that while they can be aptly used for label tagging (sequence to sequence), it is not trivial to turn them into a classifier or a regressor (sequence to one model). Using HMM method as a classifier for multiple categories requires training K different HMM models, one for each category, then selects one that maximizes the posterior. It also seems quite hard to create a regressor (like the progress function) from HMM. To the best of our knowledge, there is no popular way to implement a regressor using HMM method. The second problem lies in the fact that we typically want to choose HMM because of its explanatory power. It is always nice to be able to name the hidden states and has the HMM model keeping track of which state you are in. However, when we need more complex models, which means we have to increase the number of hidden states v, the number of parameters is also dominated by a squared term of v (transition probability table), which is the same as RNN models (we will see their number of parameters soon). With the same number of parameters, the use of the *hardmax* function in these discrete state models limits their learning ability, in exchange for obscure interpretability.

Another family of popular sequential models is linear-Gaussian state space models (LG-SSM). Equations from 2.5 to 2.8 represent an LG-SSM. In this model, we have z_t is the hidden state, u_t is an input or control signal, and y_t is the observation. Notice the similarity between equations of LG-SSM and the classical form of RNN (Equa. 2.1). The difference is the explicit reification of error terms in LG-SSM, in particular, as two Gaussian distributions.

$$z_t = A_t z_{t-1} + B_t u_t + \epsilon_t \tag{2.5}$$

$$y_t = C_t z_t + D_t u_t + \delta_t \tag{2.6}$$

$$\epsilon_t \sim \mathcal{N}(0, Q_t) \tag{2.7}$$

$$\delta_t \sim \mathcal{N}(0, R_t) \tag{2.8}$$

The method to filter on LG-SSM (i.e., to predict the hidden state z_t given the history of $u_{1:t}$ and $y_{1:t}$) is to use the famous Kalman filter (Bishop et al., 2001). To train the parameters of A, B, C, D, Q, R of LG-SSM for the problem at hand, where we have training samples of the input signals u_t and observed outputs y_t, without knowing the hidden states z_t, the well-known method is to use Expectation Maximization (analogous to the Baum-Welch algorithm

for HMM). The limitation of linear-Gaussian SSM is that it can only capture linear relationships between u_t, y_t, z_t. For example, in its application on object tracking problem (e.g., tracking a controlled drone), u_t is the signal sent to drone (left, right, up, down), y_t is observed location and velocity of the drone (with some noise of recorded device) and z_t is the real location and velocity of the drone. y_t is, therefore, just $z_t + \delta_t$ whereas $z_t = z_{t-1} + u_t + \epsilon_t$, When we could not make this assumption, LG-SSM would not perform well.

The number of parameters for LSTM model: A single-layer LSTM model with input dimension i, cell size (which is also memory size and output size) is o (notice that dimensions of C_t and H_t are the same), has $4*(i+o+1)*o$ of parameters. A two-layer model with the same hidden size has $4*(i+o+1)*o+4*(2*o+1)*o$ parameters (outputs of the first layer become inputs for the second layer). For example, the final configuration used for all action classes has $i = 8, o = 200$, and 2 layers, so the number of parameters is 488000, dominated by a squared term of cell size. That even does not include a dense layer connecting the output of LSTM cell to the target output, such as the progress value (1 output) or action classes (5 outputs). Superficially it might sound like a disadvantage of LSTM model, as the number of parameters might even be larger than the number of training samples, but it has become a standard in deep learning community that you can use an over-complete model, that can easily overfit your data and regularize it, e.g., by minimizing validation error rates. The reason for this phenomenon is not well understood, but it has been observed in other classical machine learning algorithms as well (Belkin et al., 2018).

2.3.2 Progress learner

"Learning from Demonstration" framework is one of the *frontier* reinforcement learning topics, as discussed in (Sutton and Barto, 2018, Chapter 17). The RL community are actively working on finding reliable methods to learn them. The problem presented in this thesis, in particular, actually goes beyond the scope of Markov decision process (MDP) formalization. A default assumption in classical MDP is that at each time step, the subsequent action is defined only by the immediately preceding state and action. In this problem, there is no defined way to summarize the "shape" of the progressing action into the state. Therefore, MDP is not satisfied.

There are typically two approaches to learning behaviors from experts' demonstrations. One is exclusively supervised learning (for example, Zhang et al. (2018) on learning to draw Chinese

character), sometimes called *Behavioral cloning* (Bain and Sommut, 1999), or *BC*. *BC* is quite simple and straightforward but strictly requires MDP assumption. In *BC* we usually train a classifier to predict actions given states. When applied for execution, the classifier provides the necessary action strategy.

Even though for most of the time, MDP requirement can be relaxed, there still remains an issue with Behavioral Cloning. For an action like "Slide Around", there is no straightforward way to define its termination condition. Indeed, in BC, termination is usually handled by an external signal.

Another approach is extracting a reward signal from experts' behavior for reinforcement learning. That is the approach we use in this research. We will use a reward signal produced by training a regression model, as described in this section.

Inputs are sequences of feature vectors taken from capture-data or from the simplified simulator and outputs are a value that corresponds to the progress of an event. In particular, it is a function that takes a sequence S of feature vectors, current frame i and action e: $f(S, i, e) = 0 \leq q_i \leq 1$

The training set of sequential captured data is passed through an LSTM network, which is fitted to predict a linear progressing function. At the start or outside of an event span, the network produces 0, whereas, at the end, it produces 1.

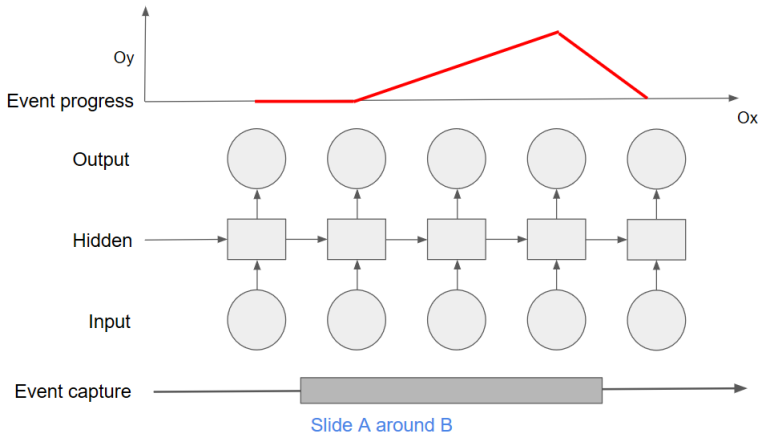

Figure 2.5: LSTM network producing event progress function

2.4 Simulation module

This module encompasses both a 2-D simulator that can quickly generate multiple demonstrations of actions, as well as multiple algorithms to learn the best policy to generating an action. In the implementation, it is also a wrapper around the predictors of the aforementioned supervised machine learning module (Section 2.3), and also around the feature extractors (Section 2.2).

Therefore, this module simulates the whole mechanism of a virtual agent's faculty of action learning. Section 2.4.1 gives a summary of the 2-D simulator, including its components and functionalities. Section 2.4.2 describes search algorithms that search over the space of trajectories in a heuristic manner. Section 2.4.2 sketches out some reinforcement learning algorithms that can generate a strategy for a new situation without searching over the entire space.

2.4.1 2-D Simulator

For the updating loops in the reinforcement learning algorithms, we want to simulate observational data faster than real-time simulation for efficient computation. As a real-time, graphic-heavy simulator, Unity engine is not feasible for this task. While being aware of a few other physical simulation environments such as Gazebo[1], but as the focus is not physical constraints in this study, we implemented our own simplified simulator in Python.

The set of learnable actions is limited to ones that can be readily approximated in 2D space. 3D captured data is transformed into simplified simulator space by projecting it onto a 2D plane defined by the surface of the table used for performing the captured interaction. The 2D simulator has the following features:

- It is equipped with aforementioned feature extractors. These extractors are used to generate features on a frame-by-frame basis from the simulator.
- It includes the aforementioned progress learner (Section 2.3.2) for each action type. This allows us to calculate an accumulated reward function after a move has been carried out.
- Each object is represented by a polygon (or square) and attached with a $transform$ object that stores its position, rotation, and scale.

[1] http://gazebosim.org/

- The searching space is so constrained that objects do not overlap, and objects could not locate outside of a square rectangle (table boundary).
- Objects can be moved to a new location (change of the attached *transform* object), by receiving an action command in the simulator. If the action is an illegal move (moving to the outside of the playground, or to a taken location), it is recorded, but not executed.
- Recording speed can be so specified that object movement can be recorded as a sequence of interpolated feature vectors on a frame-to-frame basis.
- It supports step-by-step visualization of a sequence of moves, or locations of objects can be interpolated, and the movement can be recorded into videos. Therefore, it provides a simple visualization and debugging environment.

In details, the 2-D simulator is implemented with the following components:

- An environment simulator component that supports adding of objects at specified locations. A movement command can be sent to the environment to change the location of one object, as far as: a. the destination location is not blocked, b. assuming that the object is moved with the original orientation, and only changes its orientation at the end of the movement, the moving corridor needs to be clear for the movement to happen.
- An action environment component that inherits *gym.Env*, a class from OpenAI Gym (Brockman et al., 2016) Python package. It is an adapter for reinforcement learning methods to the aforementioned simulator, providing functionality for initiating environment with random configurations, and support recording and traversing through the history of each episode.
- 2-D Visualizer/debugger that can show an episode to an interactive python notebook, or save it down as a video. It can also be used to visualize the captured data as they are projected onto the 2-D space.

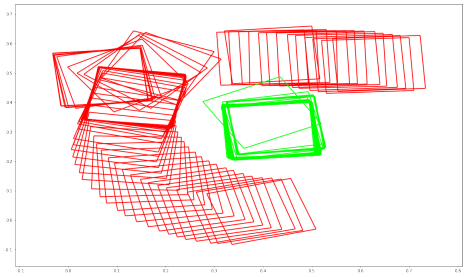

Figure 2.6: An recorded demonstration of "Move A around B" projected onto the 2-D simulator. A is projected as a red square, B as a green square. In this image, the simulator is in offline mode, and only used to show the trajectory of a recorded demonstration.

Interactive mode: The visualizer can be switched to an *interactive* mode, in which the visualizer shows the demonstration step by step, and users can click on a Next button to move to the next state, or Prev to back to the previous state. At each time step, the simulator uses the greedy algorithm presented in Section 2.4.2 to plan the next action.

At any point, users can decide that the next action is a bad decision, and choose another location on the interactive interface as the location of next action. The interactive mode will be used for incorporating feedback into the learned model.

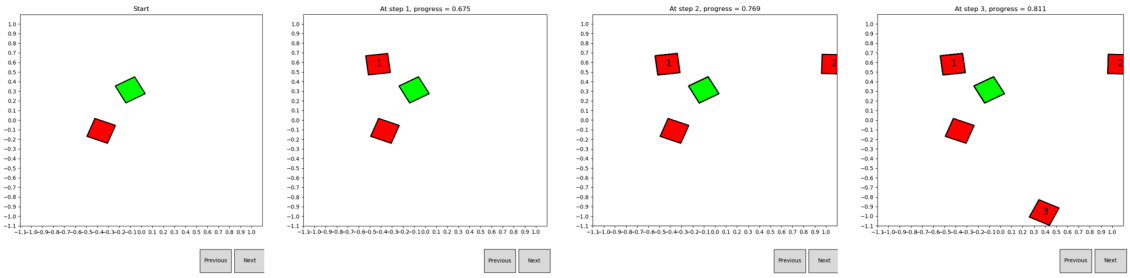

Figure 2.7: A demonstration in interactive mode using continuous learned progress function. At each step, the simulator looks for the best action that can increase the progress value. The progress values at the top improve from 0 to 0.675 to 0.769 to 0.811

2.4.2 Reinforcement learning algorithms

In the following sections, we will introduce two algorithm families used in Reinforcement learning framework. The first one is heuristic search algorithms [2]; the second one is policy gradient algorithms. We use search algorithms as a quick way to evaluate the correctness of the progress learner (Section 2.3.2) in producing correct demonstrations. Algorithms of this type are, however, agnostic to past demonstrations. Therefore, for each novel setup, they would have to search through the entire space to find a good solution.

True reinforcement learning algorithms usually have overhead, as we train them through generating a number of trial episodes. They have an advantage that after training time, you can just use the learned policy to generate higher valued episodes (corresponding to better demonstrations of actions in this discussion). The learned policy, however, depends on the progress learner and therefore, has to be retrained if the progress function changes.

Search algorithms

In this section, we will address two heuristic search algorithms. One algorithm is a *greedy* algorithm, in which from any current state, we pick the action that leads to the next state that has the highest possible reward. This algorithm can be used in the *interactive mode* of the 2-D visualizer.

The second search algorithm is one-step *beam search* algorithm. The general idea of *beam search* algorithms is that at each step, we keep a list of "good" explorations. For each exploration, we randomly generate a number of sequences of actions, to create some candidate explorations. For example, at each time step, we have b explorations $L_l, l \in \overline{1..b}$. From each of them, with a two-step *beam search* algorithm, we generate 3 sequences of actions S_{li}, each sequence has two actions a_{lij}. We then apply each sequence of actions on L_l, to generate exploration L_{li}, each with a different progress p_{li}. By sorting all resulted explorations according to their progress values, we select the next batch of explorations of size b. The one-step beam-search algorithm is shown in Algo. 3. This algorithm could not be used in *interactive mode*, because at any time step, we keep a list of candidate explorations, and the best exploration of the next step is usually not the continuation of the best exploration from the previous step.

[2] Technically speaking, heuristic search algorithms are not *reinforcement* learning, because they do not remember what the past experience, but they usually share the same learning setup as true RL algorithms

input : state of the 2-D simulator (locations of blocks, which block will be moved), desired progress threshold (e.g., 0.80), search breadth n
output: A chain of actions
init : Randomize initial state in simulator space X_0, progress value = 0
for *Step* $k \leftarrow 1$ **to** max_step **do**
    Random n actions u_{ki} on the searching space;
    for *action* u_{ki} **do**
        Do action u_{ki} ;
        Calculate progress p_{ki} and reward r_{ki};
        Back to the previous state;
    end
    Select $u_{k\ best}$ according to best progress value $r_{k\ best}$;
    if $r_{k\ best} > 0$ **then**
        Do action $u_{k\ best}$;
    end
end

Algorithm 2: Greedy search for a trajectory of action

input : Same as Algo. 2 + A beam search width b (e.g., $b = 20$)
output: Same as Algo. 2
init : A list of explorations L and their progress values P (stored in a map). At the beginning it has only one exploration $[(X_0)]$ which is the blocks are at their original positions, no movement has made yet (progress value = 0)
for step $k \leftarrow 1$ **to** max_step **do**
  $L_{candidate} = L.clone()$;
  for $l \leftarrow 1$ **to** b **do**
    Exploration $e = L_l = [X_{l0}, u_{l1}, X_{l1}..]$, progress $P[e]$;
    Random n actions u_{lki} on the searching space;
    for *action* u_{lki} **do**
      Do action u_{lki}, lead to state X_{lki}, reward r_{lki} ;
      Create candidate exploration $e' = e + [u_{lki}, X_{lki}]$, progress $P[e'] = P[e] + r_{lki}$;
      $L_{candidate}.add(e')$;
      Back to previous state;
    end
  end
  Sort $L_{candidate}$ so that the highest progressed explorations are at the top;
  Set $L = L_{candidate}[: b]$;
end
Return the best exploration L_0

Algorithm 3: One-step beam search for a trajectory of action

Policy gradient algorithms

In this work, we will experiment with both running RL on continuous space and discretized space, and we can evaluate the effectiveness of both methods in solving this problem. The selected algorithms for both cases are policy gradient algorithms, including REINFORCE (Williams, 1992) and ACTOR-CRITIC. These algorithms could be used for both continuous and discretized RL problems.

While digging deep into several RL concepts is not the focus of this dissertation, it is sensible for us to include a very brief introduction of policy gradient algorithms, and the reason of selecting them in this research. Concerned readers can find more details in other seminal RL work, such as (Sutton and Barto, 2018, Chapter 13).

The first important point to note about policy gradient methods is that they typically have

two learning functions (or *estimators*). One is called *policy estimator*, i.e., a function that takes in a state, and outputs a probability distribution over a set of actions that could be taken from this state. Another estimator is called *state estimator*; technically an optional baseline used to reduce learning variance, formalized as a function from a state to the expected reward that one can achieve when starting from that state. For each estimator, we have a set of parameters that we would like to learn.

Now the reason these methods are called *policy gradient* is that we will apply online gradient learning methods, such as Stochastic gradient descent, to learn the optimal policy estimator. Optimality is defined by the accumulated reward (or episode *value*) that one can get for every possible starting condition.

input : Initial policy parameters θ, learning rate α^{θ};
Initial state parameters ω, learning rate α^{ω}
Learned progress function f, Termination condition q, No. of episodes M
output: Learned policy parameters θ_{final}, ω_{final}

Algorithm 4: Inputs and outputs of REINFORCE and ACTOR-CRITIC algorithms

In particular, REINFORCE algorithm depends on the intuition that if one does not know which policy leads to the best reward, one should try exploring the environment by following some random policy until termination, each exploration we will call an *episode*. After each episode, we observe the reward collected from the episode and improve upon the random strategy, *rewarding* actions that lead to better accumulated rewards, and *punishing* ones that do not. For example, if we have seen a common state s in two previous *episode* e_1 and e_2, at time step t_1 and t_2, but the strategy chose two different actions a_1 and a_2. Starting from this common state s, at the end of each episode, we accumulated two different values $v_1 > v_2$. Intuitively, we should reward a_1 and punish a_2, and update our action policy at state s. In practice, we add an additional term called *baseline*, which estimates the expected value of state s, and instead of comparing between two values v_1 and v_2, you can compare them with the baseline, rewarding the action corresponding to value higher than the baseline and punishing one that is not. Details of the REINFORCE algorithm is presented in Algorithm 5. Notice that it is presented here in a generalized form, in which we replace the selection of an action according to the action policy with a beam search step. The generalized form is called Hybrid REINFORCE + n-action beam search.

for *Episode* $j \leftarrow 0$ **to** M **do**
  init: policy estimator $\pi_\theta \leftarrow \theta$, state estimator $\hat{v}_\omega \leftarrow \omega$, randomize initial state in simulator space X_0, progress r = 0
  for *Step* $k \leftarrow 1$ **to** ∞ **do**
    Draw a set of n actions from policy distribution $u_{ki} \leftarrow \pi_\theta(X_{k-1}), i = \overline{1..n}$;
    for *action* u_{ki} **do**
      Do candidate action u_{ki} in the simulator, get candidate next state X_{ki}, record frame-to-frame sequential features, feed them into LSTM network to get progress output;
      Calculate immediate reward as $r = \delta_f = f(X_{ki}) - f(X_{k-1})$;
      Back to previous state;
    end
    Select action u_k that leads to highest reward r_{max};
    Do action u_k in simulator;
    Get next state X_k;
    if $q(X_k) = True$ **then**
      break ;
    end
  end
  After episode terminates, obtain $X_{0:H}$, $u_{1:H}$, $r_{1:H}$;
  for *step k from H to* 1 **do**
    Calculate R_k, state value of X_{k-1} as the accumulated reward from step k to the end of episode;
    Estimate baseline by state estimator $baseline = \hat{v}_\omega(X_{k-1})$;
    Calculate $advantage = R_k - baseline$;
    Estimate gradient and update parameters for value estimator
    $g_\omega = \bigtriangledown_\omega \hat{v}_\omega(X_{k-1}) * advantage$;
    $\omega = \omega + \alpha^\omega * g_\omega$;
    Estimate gradient and update parameters for policy estimator
    $g_\theta = \bigtriangledown_\theta log\ \pi_\theta(u_k|X_{k-1}) * advantage$;
    $\theta = \theta + \alpha^\theta * g_\theta$;
  end
end

Algorithm 5: Hybrid REINFORCE + n-action beam search in the simulator. Notice that if the number $n = 1$, the algorithm becomes true REINFORCE with baseline

ACTOR-CRITIC is different from REINFORCE in an important aspect. While in REINFORCE, we have to run the episode until termination to decide the episode *value* of each state and only update the model at the end of each episode (in what is called *Monte Carlo* approach), ACTOR-CRITIC models are updated much more eagerly, i.e., after each action step. Because we do not have real state value R_k when we have not terminated the episode, we estimate this value by a term called *temporal difference target* or td_target, basically the sum of the current reward and the *expected* accumulated reward from the next state. ACTOR-CRITIC algorithm is presented in Algorithm 6. Because these two algorithms are similar in formalization and in inputs/outputs, and only different in details of parameter update, we will show ACTOR-CRITIC in an abridged form.

for *Episode* $j \leftarrow 0$ **to** M **do**
  init **:** Same as REINFORCE
  for *Step* $k \leftarrow 1$ **to** ∞ **do**
    Select the best action u_k from a set of n actions drawn from policy distribution $u_{ki} \leftarrow \pi_\theta(X_{k-1}), i = \overline{1..n}$, the corresponding reward is r_k, next state X_k ;
    $td\_target = r_k + \hat{v}_\omega(X_k)$;
    Using td_target instead of the real state value R_k
    Estimate gradient and update parameters for value estimator
    Estimate gradient and update parameters for policy estimator
    if $q(X_k) = True$ **then**
      break ;
    end
  end
end

Algorithm 6: Hybrid ACTOR-CRITIC + n-action beam search in the simulator. Abridged form, same inputs and outputs as REINFORCE, same gradient estimation and update steps as REINFORCE

Because REINFORCE[3] and ACTOR-CRITIC are similar in their setup, they are generally considered to be variances of the same algorithm in RL implementation.

Some common practices that we should note in training policy gradient algorithms are listed

[3]REINFORCE actually stands for *REward INcrement = Nonnegative Factor times Offset Reinforcement times Characteristic Eligibility*

as follows:

- Optimizer: Because of the form of gradient update in policy estimator, only the simple Stochastic Gradient Descent optimizer can be used for policy update, other optimizers (such as Adam) would be not appropriate. For the value estimator, because the model is very simple, with just one neuron, SGD is used for simplicity.

- Termination condition q: Because in this problem, we do not have an inherent termination condition (cf. Gridworld problem (Tizhoosh, 2005), where we terminate when the agent hit a target, or fall out of the grid boundary), we have to craft a termination condition. Two termination conditions are considered: one is a limit of the number of steps, and the other being *early-stopping* when progress surpasses a certain a threshold.

- Updating order: In two algorithms, we show the classical order of predicting (get $\hat{v}_\omega(X_k)$) and updating ($\omega = \omega + \alpha^\omega * g_\omega$) value estimator in which the predicting step is taken before the updating step. However, it is observed that if the value estimator is updated *before* being used for prediction, the algorithm has less variance and generally converges toward better result (intuitively, if we know that the *updated* model is better, than use it for prediction would lead to better results). This detail is considered a preferable implementation variance, rather than an algorithmic difference.

- Use of learned algorithms: a learned policy estimator has a stochastic nature because you choose an action based on the produced probability. However, when we use the learned policy for downstream applications, we should use a greedy method to pick the most probable action for each state.

- Use of hyperparameters: Similar to when we train sequential models, we usually make the learning rate decay over time, i.e., we keep a high learning rate at the beginning so that learners can pick up some learning pattern quickly, but lower the learning rate later to avoid learners jumping out of the good parameter region.

- Performance of reinforcement learning algorithms is shown by the episode value, in this case, the progress value, averaged over a sliding window of a specific size. We can tell whether an RL run is effectively by examining this value; it needs to increase over time.

We can also analytically evaluate the learned policy by printing out the predicted action probabilities for each state.

2.5 Visualization module

The visualizer is modified from our lab's internally developed environment for generating animated scenes in real time using the real-world semantics of objects and events (Krishnaswamy and Pustejovsky, 2016). The whole framework is a robust system that can work with a large set of actions and objects, and backed by a solid theoretical foundation (Pustejovsky and Krishnaswamy, 2016). In this dissertation work, we will only describe the particular scene (5.14) used to generate visualization data for testing the learning methodology:

1. In the original setup, the scene has an embodied agent, named Diana, playing the role of a communicative agent; she can move blocks around using her hands. In the production of visual scenes, however, her movement is quite shaky, especially in the transition phase between two actions in a row. Therefore, we remove her out of the scene.

2. The scene has a Loading button that can be used to load an existing demonstration. After loading a demonstration, the users can click play and record the visualized scene.

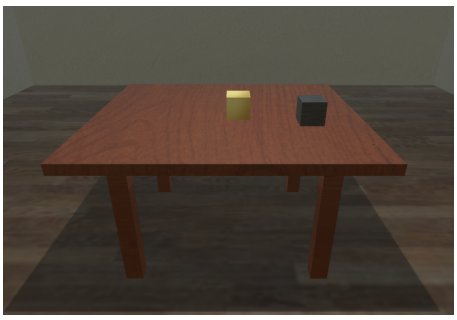

Figure 2.8: Visualizer is implemented as a Unity scene

Chapter 3

Event capture and annotation tool (ECAT)

3.1 Motivations

ECAT is an open-source interface tool for annotating events and their participants in videos, capable of extracting the 3D positions and orientations of objects in video captured by Microsoft's Kinect® hardware. ECAT is created to address the lack of an annotation tool that can handle multimodal motion captures and allow multiple layers of semantic annotation on top of captures. ECAT can also be used as a general-purpose toolkit for the development of multimodal resources for machine learning tasks.

Mainly, ECAT addresses the deficiency of two other Kinect's capturing software packages. The first one is the official tool provided by Microsoft's Kinect SDK that writes the captured data in a proprietary format. It is also not open source, and it is impossible to add semantic annotation extension on top of it. The second tool is the CwC apparatus API that can coordinate between two Kinect sensors, but the output depth stream data are also raw, and again, it is proprietary. In order to make ECAT independent of those tools, and to remedy their shortcomings, ECAT provides its own capturing, tracking and annotating functionalities. ECAT is initially designed to be interoperable with Communication with Computer (CwC) capturing and tracking apparatus API. However, following the progress of CwC project, the API was deprecated, and ECAT became a standalone and general-purpose application. The toolkit has been presented at the International Workshop on Interoperable Semantic Annotation ((Do et al., 2016)).

We also look for other possible applications of ECAT, besides its original purpose. ECAT

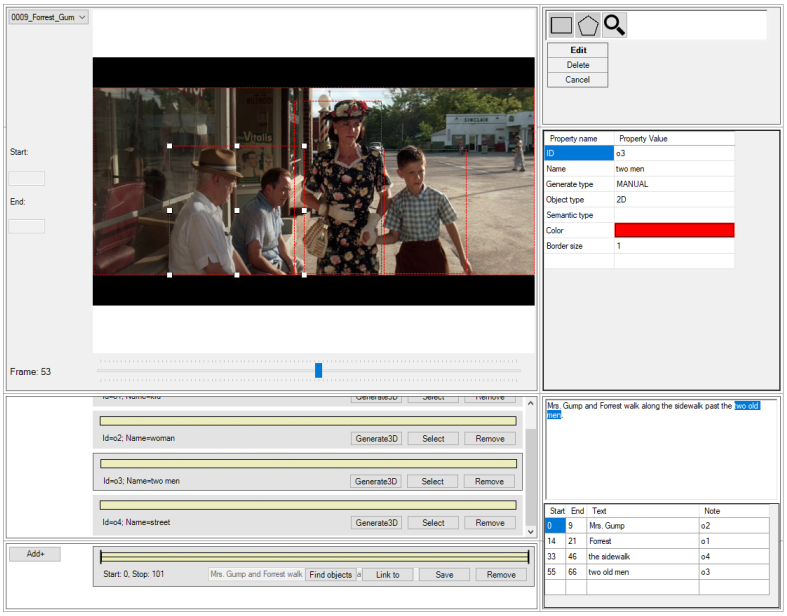

Figure 3.1: An example of ECAT-based annotation of the Movie dataset

has been used to capture and annotate data for fine-grained event classification of human-object interaction (Do and Pustejovsky, 2017a) and for action annotation in movie snippets (Do, 2016). In the next section, the details of these applications are presented.

3.2 Applications

In this section, we will list some applications of ECAT that we have explored, and some others that might be of interest for future consideration:

- To generate corpora for events and human activities captures: together with an RGB-D motion captures, ECAT supports tracking and marking of positions and orientations of objects and human body-rigs. These objects can be annotated as participants in the recorded motion event, and these labeled data can then be used to build a corpus of *multimodal semantic simulations* of these events that can model object-object, object-agent, and agent-agent interactions. A library of simulated motion events can serve as a novel resource of direct linkages from natural language to event visualization. For example, Do and Pustejovsky (2017a) have used ECAT to capture actions for event classification. This

project has shown that ECAT-based capture and annotation are convenient for multimodal captured data.

- To create an annotated resource for video understanding. ECAT has been used to collect dynamic event semantic annotation for movie dataset (Do, 2016). By annotating complex human activities and human-human as well as human-object interactions, we can extract adequate features to detect salient events in movie snippets. For example, we can use ECAT to annotate binary predicates (over humans and objects), such as HOLD, LOOK AT, POINT AT, etc. These can be used to mark locations of salient events in movie snippets (See Figure 3.1 for an example annotation).

- To create an annotated resource for learning of object Gibsonian affordances (Pustejovsky et al., 2017). For example, ECAT can be used to capture video of an object from multiple viewpoints, and one can annotate the part of the object that corresponds to its Gibsonian affordance region (i.e., the part of a tool that supports grasping for manipulation). As we have discussed in the Introduction, object affordances are an important concept in action learning. While there is some annotated static image corpus for locations of grasping (Lenz et al., 2015), a similar corpus but with captured videos could be of interest for the robotic community.

3.3 Graphical user interface

Figure 3.2 shows the ECAT GUI. Its components are listed below:

1. Project management panel. Each project can hold multiple captured sessions.

2. Video display. For displaying either the color video or grayscale depth field video, and locating objects of interest in the scene—e.g., the table outlined in green in Figure 3.2.

3. Object annotation controller. Yellow time scrub bars show when each tracked object appears in the video. Black ticks mark frames where an annotator has drawn a bounding polygon around the object using the object toolbox (item 5). *Link to* button links the selected object to another using a specified spatial configuration. *Generate3D* button generates the selected object's tracking data using the depth field.

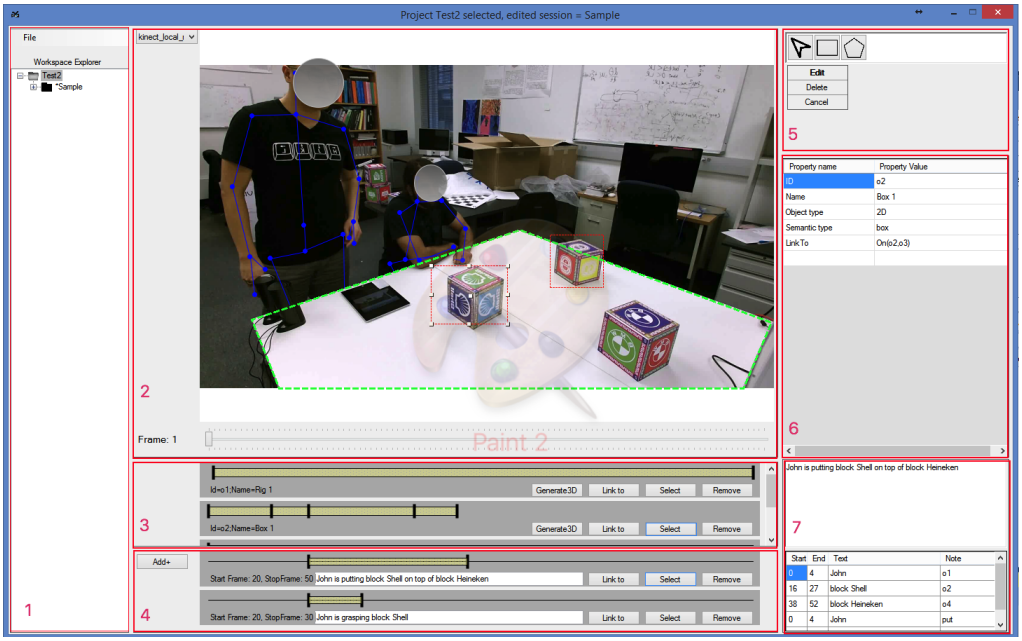

Figure 3.2: ECAT GUI. The left panel allows annotators to manage their captured and annotated sessions. Recognized human rigs are displayed as blue skeletons. Objects of interest are marked in color in the scene view. Here shows an example of collecting data for human activity corpus

4. Event annotation controller. Time scrub bars here show the duration of a marked event. Users provide a text description of the event or use *Link to* button to link the selected event to another captured event as a subevent. ECAT supports marking events that comprise multiple non-contiguous segments. Due to space constraints, not all annotated subevents are visible in this screenshot.

5. Object toolbox. Annotators can manually mark an in-video object with a bounding rectangle or arbitrary polygon. Marked bounds can be moved across frames as the object moves.

6. Object property panel. Data about a selected object shows here, such as ID and name.

7. Event property panel. The selected event's properties, including its type and participants, show here, and the event can also be linked to a VoxML event type.

3.4 Functionality

1. ECAT provides a tracking mechanism based on OpenCV implementation of a detection algorithm for ARUCO markers (Garrido-Jurado et al., 2014). Users can put different ARUCO markers on different sides of a block so that ECAT can calculate its pose/orientation change over time. In a nutshell, the algorithm looks for parallelograms (demarcated by strong contrast pattern of black and white borders) by searching through a gray image. Then it looks for the checker pattern after transforming the parallelograms to squares. Searching over the whole image is carried out every 10 frames, whereas, for remaining frames, the algorithm looks for space in the neighborhood of the previous frame.

2. ECAT provides mapping back and forth between 2-D representation and 3-D representation of objects. It can infer corner coordinates of cubes in 3-D from detected ARUCO markers. It can also infer the equation of the geometrical plane of a flat surface (such as the supporting table). The inference is based on object's `semanticType`, that can be linked to VoxML (Pustejovsky and Krishnaswamy, 2016). For example, if it is a $marked\_cube$, ECAT can infer the cube's 3-D coordinates, whereas if it is a $flat\_surface$, it can infer the equation of the surface's geometrical plane.

3. Users can mark the presence of an object using the object toolbox. Marking the boundary of an object in 2-D can be used to infer its convex hull in 3-dimensional space by using depth-field data.

4. Annotators may also mark spatial relations between objects. For example, at 3.2 two blocks are on top of the table. Users can create a link between a block object and the table object, using the *Link_to* button on the object tracking panel, and specify the relation between the objects as "on," resulting in the creation of a predicate $ON(Block\_1, Table)$ that is interpretable in a modeling language such as VoxML.

5. ECAT allows annotators to mark subevent relations between events. Thus, as in the example, the overarching event may be annotated as *put*, but it contains the subevents *grasp*, *hold*, *move*, and *ungrasp*, which may overlap partially with each other.

3.5 Future extensions

The following are a list of desirable functionalities that the next version of ECAT will support:

- Recording of audio inputs: Currently ECAT does not support recording and playback of audio inputs. We can imagine a scenario of using audio inputs to annotate actions, i.e., action spans and action descriptions automatically. Action spans can be demarcated by saying keywords such as START and END, while action descriptions can be automatically recorded by a speech recognizer.

- Multiple camera support: in robotics, there are usually multiple cameras operating at the same time, capturing a scene from multiple viewpoints. The aim is three-fold: to extend the robot's field of view (FOV), to compensate for object occlusion, and to augment object tracking. This addition will generally require users to calibrate different cameras for their coordination before capturing.

- Integration with object detection (and tracking) library: deep learning object detection library, such as (Ren et al., 2015) could be integrated with ECAT to provide an easy-to-use toolkit for researchers that are not familiar with working principle of deep learning methods. This feature also expedites the annotation process by automatically selecting annotation regions for objects.

- Support for generic cameras: one of the current deficiency of ECAT is that it only supports Microsoft's Kinect®V2 hardware. It is desirable to include a module for capturing from generic cameras (or other types of RGB-D sensors, as Microsoft Kinect®V2 project has been killed off for lack of interest from the gaming community).

Chapter 4

Action recognizer

The most intuitive approach to learn action representations is to learn an action recognizer that can classify different action types. Apparently, this does not directly lead us to a representation that allows machines to perform actions, but we would come close to an useful feature representation for the reenactment task.

This chapter describes a machine learning framework used to make distinctions between different fine-grained action types. Particularly, it could be used to classify different action types that combine *manner-* and *path-* aspects of motions.

Technically, the framework uses the LSTM models we have addressed in Section 2.3.1 as the backbone to classify frame sequences, and Conditional Random Field (CRF) as a constraint layer for output labels. In this infrastructure, *manner-* and *path-* motion aspects could be jointly classified.

4.1 Motivations

To learn action models that allow AI agents to reenact actions, current coarse-grained human activities learner are not sufficient. For example, assuming that we have a learner that can distinguish generic coarse-grained activities such as *running*, *sitting*, *eating*, and *playing tennis*, it is unclear how to turn it into an actionable model. Therefore, we have to zoom into the details of each action. For example, action model of *playing tennis* would be a loop of *hitting the ball to the other side*. This unit action, in turn, requires a model of the tennis ball's trajectory, of

robot's locomotion, of racket swing and of the opponent, etc. We focus on a much simpler type of actions, but the principles hold, we need to peruse the details of actions, i.e., we need to treat actions in a fine-grained level.

We can distinguish two different dimensions of fine-grained treatment, i.e., *temporal* granularity and *semantic* granularity.

***temporal* granularity**: Take the event *The performer rolls A past B* as an example. Zooming into different parts of the event, we see different things. At the beginning of the event, the performer reaches his hand to A, A starts to roll closer to B till some point of time at which we can claim that A moves past B. A might continue rolling, with or without force from the performer's hand. If we slice different windows throughout the capture of this action, the action description will change from time to time. It is, therefore, can start as "The performer reaches A", then "The performer rolls A", then "The performer rolls A toward B", then "The performer rolls A past B", then "A stops rolling", etc.

***semantic* granularity**: *manner-* and *path-* aspects of motions are reflected in the verb and adjunct slot in a frame-based representation of an action description. For example, a description *The performer pushes A toward B* could be mapped to the slot representation (Subject, Object, Locative, Verb, Adjunct) as (The performer, A, B, Push, Toward). An ensemble learner could learn all the slots at the same time by combing multiple sequential learners. In particular, outputs from multiple LSTM learners, one for each slot, could be constrained to produce a combined output tuple.

In this section, we will investigate a machine learning classifier between different fine-grained action types. To do so, we will use ECAT (Chapter 3) to capture demonstrations of actions and annotate them on a fine-grained scale. Feature extraction is carried out using quantitative and qualitative features (Section 2.2). The learning models are based on the LSTM model described in Section 2.3.1.

4.2 Models

4.2.1 Conditional Random Field (CRF)

Conditional Random Field (CRF) is a common undirected discriminative graphical model for machine learning of structural data. The most generic form of CRF is shown by Equation 4.1

or its log form (Equation 4.2):

$$p(y|z,w) = \frac{1}{Z(z,w)} \prod_c \psi_c(Y_c|z,w) \tag{4.1}$$

$$log(p(y|z,w)) = \sum_c \phi_c(Y_c|z,w) - log(Z(z,w)) \tag{4.2}$$

In these equations, z is input, y is output, w is model parameters (weights), Z is the **partition function** that sums over all joint configurations to normalize p into true probability. c is short for clique (a set of nodes that you want to model their co-dependency), and ψ_c (and its log version ϕ_c) is called a **clique potential**, which is a function over the values of all nodes in the clique. Notice that this function is not a true probability function, therefore, the partition function Z is always required to normalize the value on the right-hand side into true probability. In other words, if we represent our graphical model as a *hypergraph*, each clique corresponds to a *hyperedge*, and we constrain values of nodes on each *hyperedge* by the clique's potential function. In its simpler form (called pairwise CRF), where we model on a normal graph with normal edges, clique potentials are reduced to functions on nodes (node potential) and edges (edge potential). In the following equations of pairwise CRF, we do not show the dependency on w for brevity:

$$log(p(y|z)) = \overbrace{\underbrace{\sum_{s\in\mathcal{V}} \phi_s(y_s|z)}_{\text{node potential}} + \underbrace{\sum_{(s,t)\in\mathcal{E}} \phi_{s,t}(y_s,y_t|z)}_{\text{edge potential}}}^{\text{Un-normalized log prob}} - log(Z(z)) \tag{4.3}$$

$$Z(z) = \sum_{y\in\mathcal{Y}} exp(\sum_{s\in\mathcal{V}} \phi_s(y_s|z) + \sum_{(s,t)\in\mathcal{E}} \phi_{s,t}(y_s,y_t|z)) \tag{4.4}$$

where $\mathcal{V}$ is the set of nodes, $\mathcal{E}$ is the set of edges, $\mathcal{Y}$ is all combinations of labels y.

4.2.2 LSTM-CRF

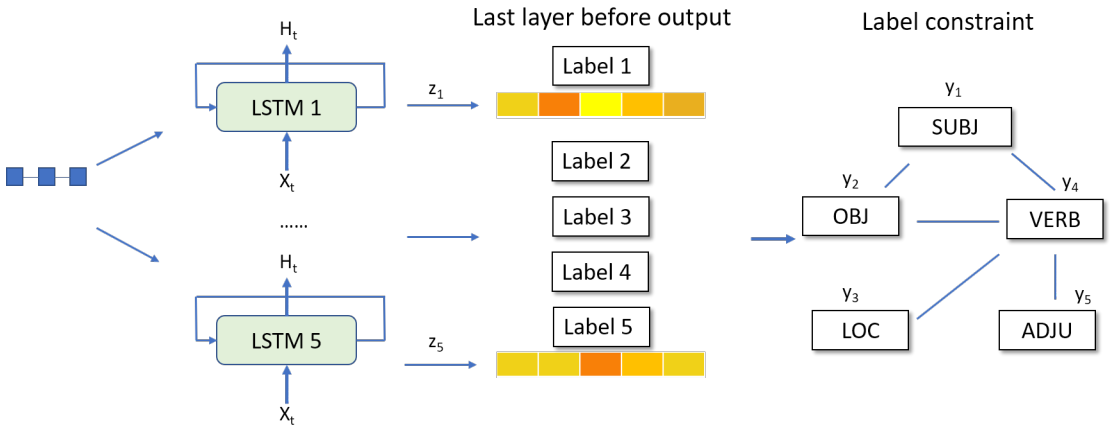

Figure 4.1: An array of LSTM models produce an array of output values, each corresponds to a sentence slot classifier. The values at the last layer of each LSTM is a probability distribution (in practices, their logarit values). These values are fed into CRF as values of x in Equation 4.3

Now let say we want to use CRF to constrain outputs from LSTM models, we can use the log probabilities calculated from the last layer of each LSTM as input z for the CRF layer (remember, for each LSTM, we produce a log probability vector, see the first common practice in Section 2.3.1, so $z = (z_1, z_2, z_3, z_4, z_5)$ where z_i is the lob-probability vector for i-th LSTM). The value of y is a tuple of thematic slots, corresponding to our predictive label of (Subject, Object, Locative, Verb, Adjunct). For the node potential, we can just use the log probability directly from the LSTM+Dense output, selected for the value of y_s (Equation 4.5). For the edge potential, we can entirely ignore the input z, and model the function on the labels of the edge's vertices. The edge potential for an edge (s, t) turns into a lookup into a 2-dimensional array that keeps a correlation value for each possible pair of (y_s, y_t) (Equation 4.6).

$$\phi_s(y_s|z) = z_s[y_s] \tag{4.5}$$

$$\phi_{s,t}(y_s, y_t|z) = \phi_{s,t}(y_s, y_t) = L_{s,t}[y_s, y_t] \tag{4.6}$$

While a standard formula could be used, i.e., to set $\phi_{s,t}(y_s, y_t|z) = L_{s,t}[y_s, y_t] * z_s[y_s] * z_t[y_t]$, we can replace the logit values $z_s[y_s]$ and $z_t[y_t]$ with a hardmax value of 1, to get the edge potential as in Equation 4.6.

4.2.3 CRF to Tree-CRF

The parameters of CRF are the lookup tables along the edges of the graph ($L_{s,t}$ in Equation 4.6), together with parameters of the individual LSTM models. Training the model with a set of training samples $(x_i, y_i), i \in \overline{1..S}$ will require calculation of the value of z_i by passing x_i through LSTM models, then calculate $log(p(y_i|z_i))$. The complexity lies in the calculation of $Z(z_i)$, as we have to sum over all possible combinations of y_i. Using the model to predict for a novel sample x_i will be equally expensive, as we still have to calculate the probabilities for all possible combinations of y_i, before finding the best combination by $y_{i\ best} = argmax_{y \in \mathcal{Y}} \quad log(p(y|z_i))$.

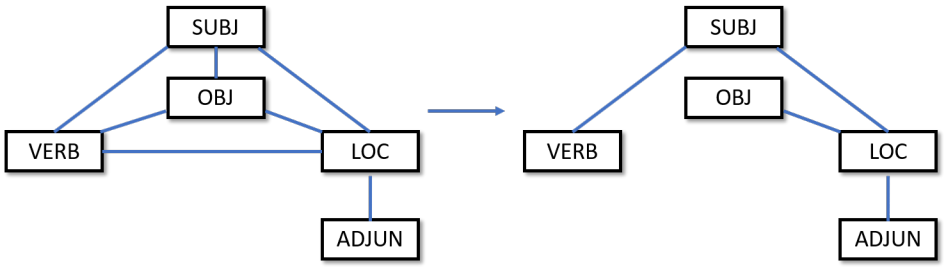

Figure 4.2: An example of reducing full CRF into tree CRF.

Updating and predicting a generic CRF model are difficult, especially when implemented with neural network architecture. We, therefore, should modify the CRF layer into a tree-CRF structure (right side of Figure 4.2) to make the model learnable using dynamic programming. The algorithms for updating and predicting Tree-CRF model, using a node-collapsing method, are presented in the following subsections. They are *exact inference* algorithms, that allow us to calculate the partition function Z (for updating) as well as to find the best y_i (for predicting) without having to iterate over all possible combinations of y. Implementation extending Tensorflow is provided at the author's repository[1].

[1]https://github.com/tuandnvn/ecat_learning/blob/master/crf_tree.py

Update

Updating the model requires us to calculate the partition function Z. The graph collapsing algorithm on LSTMs is as following:

input : Input sequence x_i, output label tuple $y_i = (y_{i1}..y_{iQ})$
Q LSTM models and look up table values for all CRF edges

output: Updated model parameters, including parameters of Q LSTM models, and the look up table L

begin

Calculate log-prob for each node on the graph (for example, $[z_{A_1}, z_{A_2}]$ in Figure 4.3), using a forward pass on Q LSTM models;

Calculate un-normalized log prob for these specific values of y_i (See Equation 4.3);

Set $collapsed\ graph = original\ graph$;

while $collapsed\ graph$ *has edge* **do**

Select an edge AB, where B is a leaf node. We index values of A by u, and B by v;

Follow the update formula at Equation 4.7 to update stored values at A;

$$z_{A_u - collapse - update - B} = z_{A_u} + \sum_v log(exp(L_{A_u B_v} + z_{B_v})) \tag{4.7}$$

Delete B and edge AB from $collapsed\ graph$

end

Set Z = Sum all the values collected from the last node;

Calculate log loss and run back-propagation on all networks (done automatically by Tensorflow mechanism);

end

Algorithm 7: Update step for LSTM-CRF

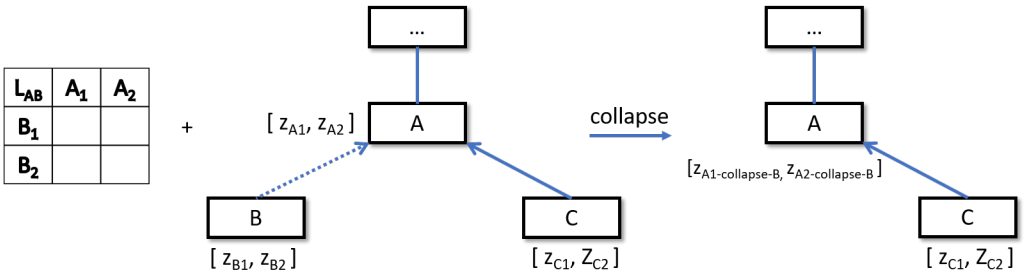

Figure 4.3: Collapsing an edge between nodes A and B into one node when calculating Z for updating. Note that B needs to be a leaf node

Predict

The algorithm for predicting a novel input is very similar to the algorithm for updating the model. The difference lies in another equation for updating the values stored in A (Equation 4.8). We just need to replace the sum operator in updating equation with a max operator.

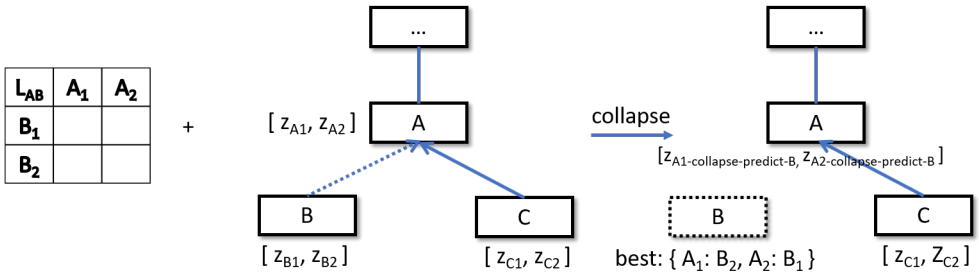

Figure 4.4: Collapsing an edge between nodes A and B into one node when predicting the output for a novel input.

We store a stack of edges that have been collapsed in their collapsing order. We also need to keep a mapping to help to trace the best combination. In Figure 4.4, the *best* dictionary at the collapsed node B maps from any value of A to the value of B that maximizes our log probability for that value of A (Equation 4.9).

When the graph is collapsed to just one node, we can pick its label by selecting one that maximizes its stored z values. Now it is straightforward that by popping from our collapsed edge stack, we can recover the best combination of labels. For example, in Figure 4.4, by picking A_1 as the best label for node A, to recover for the collapsed edge of AB, we pick B_2 as the best label for B.

$$z_{A_u-collapse-predict-B} = z_{A_u} + \max_v log(exp(L_{A_uB_v} + z_{B_v})) \tag{4.8}$$

$$best_B[u] = \arg\max_v log(exp(L_{A_uB_v} + z_{B_v})) \tag{4.9}$$

Complexity: The time complexity of the algorithm is reduced from $\prod_{i \in \overline{1..Q}} |V_i|$ to $\sum_{(s,t)\in\mathcal{E}} |V_s| * |V_t|$ where $|V_i|$ is the number of classes for i-th label.

4.3 Experiment setup

To demonstrate the capability of this model to learn the *spatio-temporal* dynamics of object interactions in actions, we used a data collection of four action types: *push*, *pull*, *slide*, and *roll*, along with three different *spatial* adjuncts used for space configurations between objects, namely *toward* (when the trajectory of a moving object is straightly lined up with a destination static object and makes it closer to that target), *away from* (makes it further from that object) and *past* (moving object getting closer to static object then further again).

For each recorded session, we sliced the events into short segments of 20 frames. Two annotators were assigned to watch and annotate them (segments can be played back).

The set of constraints for output labels are the followings (described on the left side in Figure 4.2).

1. One object (Performer or the other objects) is not allowed to fill two different syntactic slots. Notice that a person can be either a Subject (in *The performer rolls A toward B*) or a Locative (*A rolls toward the performer*). Because an object can take Subject, Object or Locative slots, there are pairwise edges between these slots.

2. When there is no verb, all the other slots should be None. That is why we have the edge from Verb to Subject, Object and Locative.

3. Locative and Adjunct are dependent, because if Locative is None, Adjunct must also be None and vice versa.

Notice that these constraints are *syntactic* constraints, rather than *semantic* constraints. *Semantic* constraints, i.e., to model selection constraints of predicates to its arguments, are not

intended in this experiment, because of the set of objects in this experiment are simple geometrical objects (a cube and a cylinder).

4.4 Evaluation

Captured sessions are split for 5-fold cross-validation, i.e., 24 sessions for training and 6 for testing on each fold. A prediction is correct if all slots are correct. Performances of different models are reported in the following tables:

Model	Precision
Baseline	6%
Quant-LSTM	39%
Quant-LSTM-CRF	48%
Qual-LSTM-CRF	**60%**

Figure 4.5: Evaluation

Label	Precision
Subject	93%
Object	90%
Locative	80%
Verb	83%
Preposition	82%

Figure 4.6: Label precision breakdown for Qual-LSTM-CRF

Firstly, in Figure 4.5 are performance values of 4 different models. **Baseline** model is one in which we predict the value of each slot randomly. **Quant-LSTM** is a model that we predict each slot independently, using raw feature data, and without referring to CRF constraints. **Quant-LSTM-CRF** is an improvement from the previous model after we have constrained the output labels. In **Qual-LSTM-CRF**, we replace the raw feature inputs with discretized feature inputs (see Section 2.2). We can observe a significant improvement of classification using qualitative features. Frame-level quantitative features did improve over the baseline, but the improvement is not as impressive.

Results shown in Figure 4.6 are precision values for different slots in the output tuples. Precision for subjects and objects are high, because to predict their values, we usually just need to decide whether the captured person is the performer who initiates the action (otherwise another person helps move the object, but he is not tracked), and which object is the moving object. Precisions for Locative and Preposition slots are the lowest, because there are ambiguous cases. Ambiguity arises from the difficulty in the *fine-grained* annotation task.

Given these results, it is worth considering possible explanations for our findings. Firstly, as pointed out in Yang and Webb (2009) and Jiang et al. (2017), qualitative representation is a method of discretization, which makes data sparser, therefore easier to learn. Especially when taking the difference between features of two adjacent frames, as a qualitative feature strongly distinguishes between 0 and 1, the effect of a feature change is more pronounced.

The best performance for **Qual-LSTM-CRF** is achieved by configuring two layers of LSTM with 400 nodes on the hidden layers, while for other models, the number of layers does not affect the performance significantly. Different from a feed-forward neural network such as Convolutional Neural Network (CNN), which can learn more abstract and useful features when it gets deeper, LSTM needs some help from the representation of features to reap a benefit from going deeper.

4.5 Conclusions

The overall architecture of this recognizer was presented in (Do and Pustejovsky, 2017a). This chapter could be considered a prolonged version of the paper, with a more detailed explanation of LSTM-CRF and its application. The approach as well as the method used in this recognizer could be of high interest for work in action recognition, and a detailed discussion of the motivation and algorithms used in this recognizer deserve a separate chapter in this dissertation.

The research in this section serves as a preliminary analysis to learning of action representations. Firstly it gives us the semantic treatment of actions which will become foundational to the learning to perform framework in the next chapter. Secondly we found in this chapter the qualitative feature representation of actions benefits classification results. In the next chapter, we will find that the same transformation helps when we learn models to reenact actions.

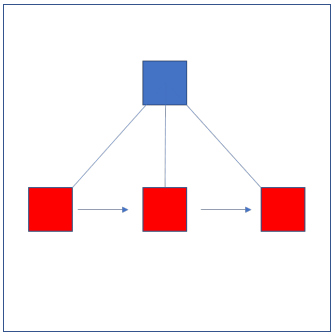

Figure 4.7: The red block moves past the blue block

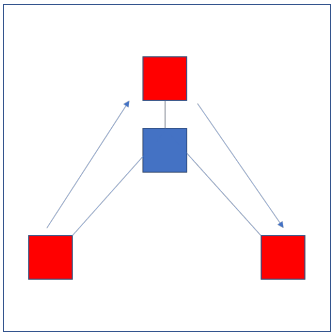

Figure 4.8: The red block moves around the blue block

A final note in this chapter is that action classifiers can be used as an auxiliary component for agents to distinguish their learned actions. We can try to make learning agents learn a new action in isolation, but there are two reasons making distinction to other (already learned) actions might be helpful. The first reason is that we could make reference to the way humans learning a new concept. Humans exhibit a strong *mutual exclusivity bias*, which entails Principle of Contrast (Merriman et al., 1989), i.e., different concepts should have different names and vice versa, different words should be associated with different things. The second reason is from a practical perspective. Let's take an example. A naive learner might erroneously learn both actions "move A past B" and "move A around B" as "A move closer to B, then move further away from B" (Figure 4.7). The learner might not be able to make a distinction between these two actions without referring to a classifier. In this thesis, we will not address the use of action classifiers in action reenactment, but the motivation for its inclusion is compelling if we have many different actions to learn.

Chapter 5

Action reenactment by imitating human demonstration

To facilitate the process of teaching robots new actions and concept, we need an interface to teach robots the mapping between linguistic and visual representations of an action, in composition with participants (agents and objects). The following figure describes the learning flow:

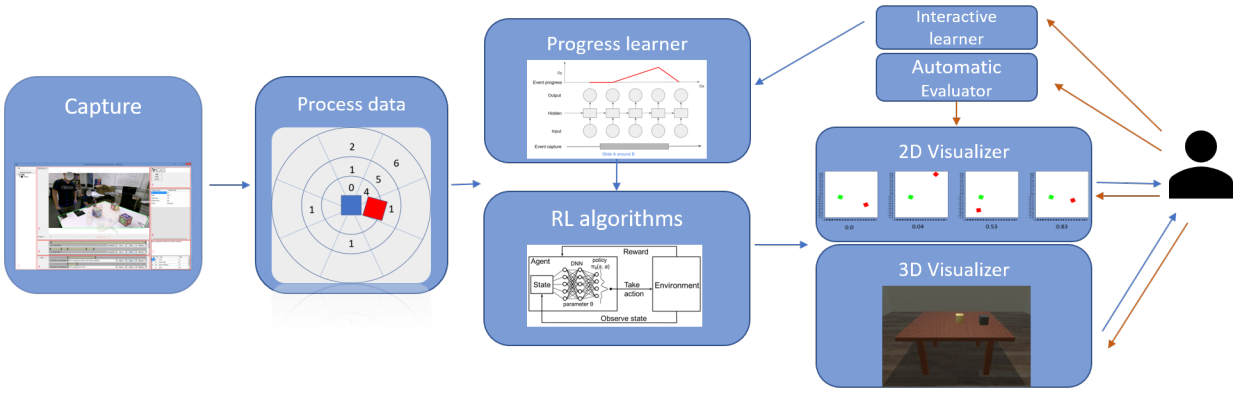

Figure 5.1: Learning workflow; blue arrows are data flows, brown arrows are evaluation flows

This learning process could be mapped to the following pipeline of:

1. **Capturing data using Event Capture and Annotation tool (ECAT)** — ECAT functionality and its usage is already summarized in Chapter 3. Data capture and annotation

guidelines have been addressed in Section 2.1.

2. **Data processing and feature extraction modules** — This actually encompasses various components in ECAT and some other components implemented in Python. Components in ECAT include an algorithm to synchronize data from various capturing streams, such as depth-field and RGB, and one to generate 3-D data from 2-D tracked frame-by-frame object data, an algorithm. Components implemented in Python include an algorithm to recover missing data (when there are 2-D coordinates that could not be mapped to 3-D coordinates), to project data to simulator space, to interpolate coordinates in frames that do not have corresponding tracked data, etc. Feature extraction framework is already addressed in Section 2.2.

3. **RL algorithms using a 2-D simulator** — functionality and implementation of this simulator have been described in Section 2.4.1. Its accompanying search and reinforcement learning algorithms were addressed in Section 2.4.2. The learned progress, described in Section 2.3.2, is used to direct RL algorithms. In the next section, we will only address details implementations of the search and RL algorithms for discrete and continuous cases.

4. **Visualizers** — human evaluation is based on watching demonstrations of actions on 2-D and 3-D visualizers. The 2-D visualizer is a component of the 2-D simulator, and 3-D visualizer is a scene modified from VoxSim, mentioned in Section 2.5. Section 5.3 will elaborate on various experiments carried out on the visualizers.

5. **Automatic evaluators** — machine-based algorithms used to evaluate the set of target actions. Scores from evaluations on 2-D visualizer are used to tune parameters in these automatic evaluators (Section 5.3.3).

6. **Interactive learner** — allows immediate *feedback* to improve the progress learner (5.3.6), therefore improving the search algorithms.

5.1 Models

5.1.1 Search algorithms

Search algorithms have continuous and a discretized versions. For the continuous case, the action space is a Gaussian distribution that has $sigma = diagonal([2.0, 2.0, 0.5])$ and mean located at the center of a playground of size $(2, 2)$. Over the constrained playground, this distribution is close enough to a uniform distribution (The reason we do not use an exact uniform distribution is of implementation details: to have the policy produced in continuous case always follow a Gaussian distribution, so that its API could be unified with RL algorithms)

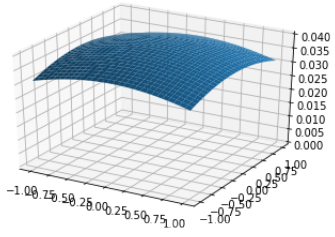

Figure 5.2: Randomize of an action is based on a Gaussian distribution centered at $(0, 0)$

It would be simple enough to derive the discretized version based on our discussion on discretization. One noteworthy point is that when we generate n random actions, we only need to generate one action for each discretized space slot. That reduces the computational expense, while keeping the coverage over the searching space.

5.1.2 Reinforcement learning algorithms

Using Williams Episodic REINFORCE algorithm (drafted in 2.4.2), we will have two different versions, corresponding to the continuous feature space and the discretized feature space as follows:

Continuous space

For the case when the action space is continuous, planning is carried out by selecting the action (coordinates in continuous space) at step k (u_k) based on the current state of the system ($X_{k-1} \in$

R^n) (also continuous values). A stochastic planning step is parameterized by policy parameters $\theta : u_k \sim \pi_\theta(u_k|X_{k-1})$

Problem formulation is as follows:

1. **State**: *transforms* (x- and y- coordinates and rotation) of two blocks in continuous space.
2. **Action**: *transform* of the target location of the moving object.
3. **Reward**: gain of *progress function* over one move.
4. **Policy**: The *Policy estimator* is made by an artificial neural network (ANN), used to produce values μ (mean of the action's transform) and σ^2 (variance of the action's transform). The ANN will be parameterized by a set of weights θ. For simplicity, the dimensions of μ and σ are the same as the degrees of freedom in the simplified simulator (2 dimensions for position and 1 dimension for rotation). An action is generated by a Gaussian distribution $\pi_\theta(u|X) = Gaussian(\mu, \sigma)$.
5. **Baseline function**: A function that estimates the expected value of a state (expected accumulated reward from a state to the end of an episode). The simplest kind of ANN is used here, i.e., a single neuron with *tanh* activation to produce a value from -1 to 1, to predict this value.

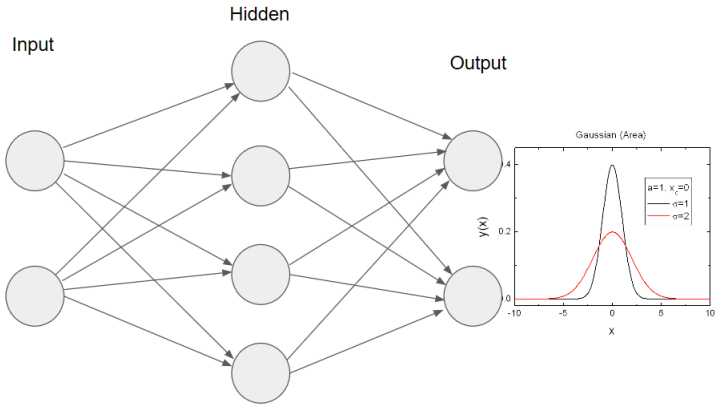

Figure 5.3: An ANN architecture producing Gaussian policy

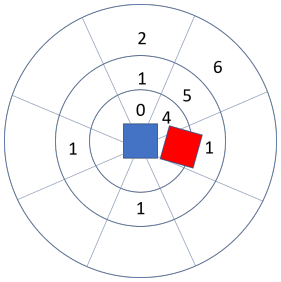

Figure 5.4: Discretizing 2-D searching space around the static object

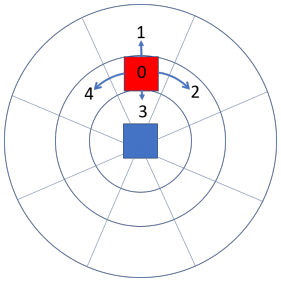

Figure 5.5: Discretizing an action of the moving object

Discretized space

We discretize the searching space using qualitative reasoning method. In specific, the searching space for the *transform* of the target location could be separated into space for (X, Y) coordinates and rotation r. The searching space for (X, Y) could be discretized as in Figure 5.4, the searching space for r could be discretized as in Figure 5.5. Notice the searching space for (X, Y) is so divided that the granularity of discretization is coarser when the moving object gets further away from the static object.

Problem formulation is as follows:

1. **State**: Discretized state of the moving object with regard to the static object (6 values) + discretized previous action (or 0 if the object hasn't moved) (5 values) . This combines into an *one-hot* vector of size 30. Optionally we include the discretized progress of action (5 values), which makes the dimension to increase to 150.

2. **Action**: A discretized action of the moving object can take one of 5 values. Value 0 corresponds to an *early-stopping* of an episode, while values from 1 to 4 correspond to going North, East, South and West (Figure 5.5).

3. **Reward**: gain of *progress function* over one move (same as for continuous case)

4. **Action policy**: An artificial neural network (ANN) will be used to produce a probability distribution of discretized actions for each state. A straightforward implementation uses a fully connected layer for this ANN, with no activation and no bias, i.e., a linear matrix multiplication. A *softmax* layer is put at the end to create a distribution. A (discretized) action is generated from this distribution.

5. **Baseline function**: For baseline function, we can use a linear function over the state vector. Because the input vector is *one-hot*, the corresponding linear coefficient would be the same as the state value.

The reason for the 6-way discretization of relative position is that the four-way symmetry of the static block can be utilized. While internally, we still make a distinction among all the partitions in Figure 5.4, we can use the same action policy for same-numbered slots, such as the slots numbered 1. The previous action is included in the formalized state, because the previous action strongly affects the current action. For example, if the action is *Slide Around* and if the previous action is 4, the next action should also be 4. If the action is *Slide Closer* and if the previous action is 3, the next action should also be 3.

We will optionally include the discretized value of the progress function. The reason is that we want to automatically learn a model that can stop when the progress is high enough. So for example, when the discretized value of progress is 4 (corresponding to when $progress > 0.8$), the appropriate action would be 0. An alternative method would be to exclude discretized progress (which reduces state dimension to only 30), and to apply stopping when $progress > 0.8$. We would show results for both approaches in the following sections.

5.2 Experiment setup

In this experiment, we will use the learning framework drafted above for learning agent to perform the set of following *actions*:

1. An agent moves {object A} **closer to** {object B}
2. An agent moves {object A} **away from** {object B}
3. An agent moves {object A} **past** {object B}
4. An agent moves {object A} **next to** {object B}
5. An agent moves {object A} **around** {object B}

This set of actions, on their linguistic descriptions, differ only in their adjuncts. These adjuncts are prepositions describing different trajectories of motions. For this set, the learning problem is reduced to learning trajectories, or path, of motions.

It is noted that the action types in this set are not homogeneous. Firstly, we would discuss the temporal extent of each action type, whether they are open-ended or close-ended, and whether they have a hard boundary or soft boundary. Secondly, we would discuss the way humans would recognize these action types, whether we base on the trajectory of movement, or we base on the start and ending points of movement. Followings are the differences:

1. **closer to** differ from **next to** that A only gets **closer to** B but does not touch B. **closer to** is a close-ended action, as A can only move closer to B until a certain point. **closer to** has a soft ending, which means that the action is satisfied for a time interval.

2. **away from** is an open-ended action, it also has a soft ending.

3. **past** is an open-ended action and has a soft ending. It combines the effect of **closer to** and **away from**.

4. **next to** has a hard ending and is close-ended.

5. **around** has a soft ending and is open-ended.

From a cognitive point of view, recognition of these action types, excepts possibly for **move next to**, requires consideration of the trajectory as well as the start and ending points of movements. For example, **closer to** conceptually just involves a change of distance between the start and ending positions of the moving object in relative to the static object, but a complex moving trajectory would lead to misinterpretation of the action. **Closer to**, therefore, strongly indicates a trajectory of the moving object toward the static object.

Putting these event types to be learned altogether, we want to examine the capability of a single learning framework that can learn multiple event types. The reason is obvious: we, as humans, can learn all of these actions without prior knowledge of different action types, or without further input from the teachers.

Data preparation

For each action type, we have data recorded with two performers, and each person performed the action 20 times, for a total of 40 demonstrations per action. Annotation took a little

bit longer, about 10 hours. We also hope that the feedback loop could compensate for the small number of demonstrations, as increasing the number of demonstrations might still not be able to give good negative samples to the learner.

5.3 Evaluation

In this section, we will present multiple evaluations. Firstly the performance of the learner progress will be evaluated, comparing between qualitative and quantitative feature sets. Secondly, we will compare between the running time of search algorithms and RL algorithms. We would like to know if the search algorithms are fast enough. If they are fast, and perform equally well to RL algorithms (when evaluated by humans), it might be more reasonable to use search algorithms to avoid the overhead of running RL algorithms.

Thirdly, the performance of RL algorithms against our reward function could be measured by examining the average return for a span of consecutive runs. This figure would be increased over time for a successful RL algorithm. Therefore, we can use this method to avoid running expensive human-driven evaluation for any RL algorithm that could not converge.

There will be one human evaluation based on watching the 2-D simulator, and one human evaluation based on watching simulations from the Unity 3-D visualizer. The human evaluation on 2-D simulator would be carried out on a smaller scale. The purpose of evaluation on 2-D simulator is two-fold: firstly to reduce the number of control algorithms we would finally use for more expensive evaluation on the 3-D visualizer; secondly, that would help to answer if there is any disparity between the way humans judge the same action demonstration on 2-D simulator and 3-D visualizer.

Evaluation with 2-D and 3-D visualizer will be performed by lab members or school students.

In the following sections, we will carry out the following evaluations:

1. Evaluation of the progress learner with quantitative versus qualitative feature sets, addressed in Section 5.3.1.

2. Human evaluation on 2-D demonstrations, addressed in Section 5.3.2.

3. Parameter tuning for automatic evaluators, addressed in Section 5.3.3.

4. Improvement of "Slide Around": Which algorithm works the best, and what is its performance? Addressed at 5.3.4.
5. Can the learner make the distinctions between learned action types? Addressed at 5.3.5.
6. Can we use the feedback from human evaluation to improve the learned model? Addressed at 5.3.6.

5.3.1 Evaluation of the progress learner

The progress learner is a simple LSTM function that processes the feature sequences from captures (or generated demonstrations) and outputs a single value from 0 to 1 corresponding to the progress of an action. The objective of training this LSTM model is to minimize mean squared error (MSE) rate w.r.t annotated target progress values. The following table shows the configuration that achieves the best performance:

Hyper-parameter	Definition	Value
keep_prob	Remaining percentage in dropout (See 2.3.1, 5)	0.6
hidden_size	memory state size	200
num_layers	Number of LSTM layers (See 2.3.1, 3)	2
max_epoch	Number of epoch runs, each epoch run through the whole training data	50
optimizer	Type of optimizer	Adam
learning_rate	Initial learning rate	0.005
lr_decay	Learning rate decay after each epoch	0.03

Table 5.1: Hyper-parameters of LSTM model for progress learner

In the following charts, the performances of the progress learner for different amounts of training data and quantitative versus qualitative features are shown w.r.t the number of training epochs:

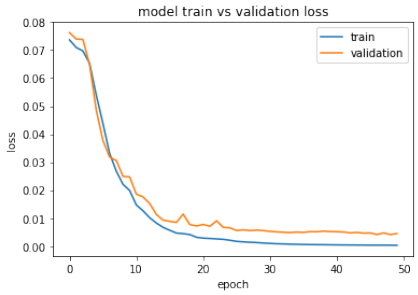

Figure 5.6: MSE with all data and **quantitative** features.

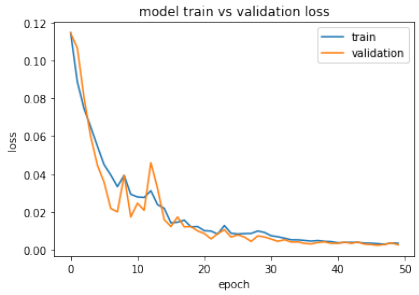

Figure 5.7: MSE with all data and **qualitative** features.

We can observe that with all training data, performance with qualitative features is marginally better than with quantitative features (the With less data (half the data comprises 20 demonstrations, a quarter comprises 10 demonstrations), the model with quantitative features is *overfitting* while model with qualitative features stills presents good fit quality, though the MSE line becomes quite bumpy.

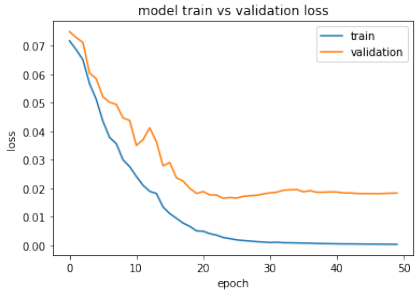

Figure 5.8: MSE with half the data and **quantitative** features.

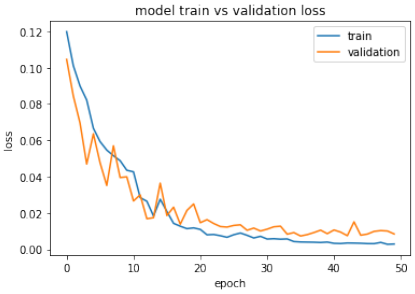

Figure 5.9: MSE with half the data and **qualitative** features.

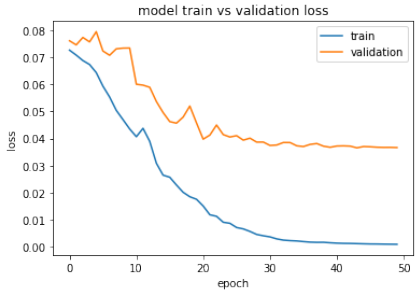

Figure 5.10: MSE with 1/4 the data and **quantitative** features.

Figure 5.11: MSE with 1/4 the data and **qualitative** features.

Mini-conclusion

According to this result, we should use progress learned trained with the qualitative feature set for all downstream evaluations. The reason is that we want to use a model that can be trained with potentially least amount of data. In the following sections, we will still use the progress function learned with all training data (40 demonstrations), leaving one learned with less data (10 demonstrations) for future experiments.

5.3.2 Human evaluation

In this section, we use the progress learner learned in Section 5.3.1, and the beam-search algorithm presented in Section 2.4.2 on continuous space to bootstrap a small-scale human evaluation. Two annotators (college students) are asked to give scores from 0 to 10 (higher scores are considered better) and are also asked to give comments on any video they graded between 3 and 7.

Results of the system with heuristic search show that the progress learner can generate correct demonstrations (Fig. 5.12), but sometimes produces deviations (Fig. 5.13), probably because of the lack of negative training samples. This would be improved by incorporating feedback from evaluators as we will see in 5.3.6.

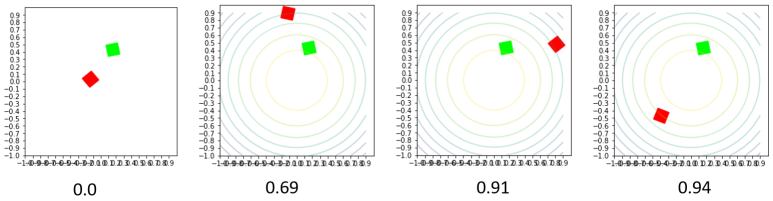

Figure 5.12: A good demonstration of "Move the red block around the green block."

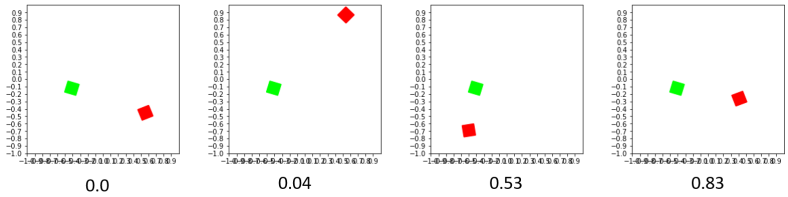

Figure 5.13: A bad demonstration of "Move the red block around the green block." The value beneath each frame is value predicted by the progress learner.

We provide a quantitative breakdown of the results for different actions in Table 5.2. **Evaluator Disparity** is the average of the absolute values of the differences between scores given by two annotators over the demonstrations of a particular action. Based on these scores, we observe that scores given by annotators for all action types, excepts for "Slide Around", are over 5. It suggests that "Slide Around" is the most difficult action skills in this set. Therefore, in the following experiments, the focus will be on methods to improve this result.

Action Type	Average Score	Evaluator Disparity
Slide Closer	5.4	1.57
Slide Away	6.48	2.37
Slide Next To	5.55	1.7
Slide Past	6.38	1.9
Slide Around	2.75	1.03

Table 5.2: Human evaluation for beam search on continuous space

Scores given by the annotators are shown in Table 5.2. Evaluators' comments (in Table 5.3) provide an insight into bad demonstrations. Three types of problems are observed. The first is related to visualization method, e.g., the speed of visualization. We usually visualize the scene in 30 frames, which renders some movements too slow. The second problem is for some action, some generated starting positions are not observed in training data. For example, when demonstrating action of "Slide Closer", performers usually start at a location far from the target. When posed with a starting position that have two blocks close to each other, the learner does not know what action it should take. It might move an object further, then move it back. The third problem is the confusion between different action types.

Action type	Text comments
Slide Next To	Need to be even closer
	Movement is slow
	A gets closer to B, but than bounce back
Slide Closer	A only moves half the way
	A gets closer to B, but not enough
	The starting location of A is too close to B
Slide Away	Need to be even closer
	Get closer to the target before moving away
	Cannot tell if it is Slide Away or Slide Past
Slide Past	A touches B while passing B
	A slides past B than slides back
Slide Around	Lacks one or two more steps
	The last line goes to far from the target
	The last line goes back to the opposite direction

Table 5.3: Samples of some comments given by annotators.

Mini-conclusion

Because it is not economical to run a human evaluation for every experiment, as it would incur a delay between experimental runs, if we want to look for ways to improve models, in the following section (Section 5.3.3), we would discuss methods to generate automatic evaluators, based on results of this section.

As discussed above, there are some issues to be addressed. They are not inherently related to algorithms used, but to the learning methodology. While we will not address the issue of scene

rendering speed, because it is minor, we will consider interactive learning (or incorporation of feedback into learning, in Section 5.3.6) as a way to detect and fix the second problem. For the third problem, we will address possible confusions between different actions by carrying out an experiment in Section 5.3.5, i.e., we will test whether the generated demonstrations can be told apart.

5.3.3 Automatic evaluators

To complement human-driven evaluation, a set of machine-based algorithms to evaluate the set of target actions are created. Each is a tuneable algorithm, called *automatic evaluator*, based on an intuitive interpretation of each action. It is stressed that interpretation of these actions will be varied from person to person, and any effort to encode them in a programmatic way would be just an approximation. These evaluators are used as an oracle to provide quick evaluations of our learning methods.

Outputs of these evaluation algorithms (excepts for *Slide Around*) are binary, which means that we either accept a demonstration as correct or incorrect. Detailed implementations of these evaluation methods are the following:

1. **Slide Closer**: "Slide Closer" means that for all the steps taken in the environment, the moving object needs to get closer and closer to the target object.

   The algorithm is as follows:

   (a) For each action step of the moving object, check the distance toward the static object, it should always getting smaller.

   (b) The distance at the end of the action needs to be small enough (smaller than a threshold parameter).

   (c) If one action step does not satisfy this condition, the whole action sequence is considered wrong (output 0).

2. **Slide Past**: Our interpretation of "Slide Past" is that the distance between two blocks needs to be the widest at the beginning and end states. If the total movement involves multiples action steps, that distance at an intermediate step $<$ max of distance at beginning and distance at the end. Moreover, we also want that the total path that the moving block

has traversed is long enough, so from a certain viewpoint, we can observe some occlusion happens during a period of time. Here it is dictated that the longest edge of the triangle made from the beginning position, the end position and the static object position is the one between beginning and end positions. Also the angles next to this edge need to be smaller than a threshold angle (a parameter).

3. **Slide Away**: Slide away means that for all the steps taken in the environment, the moving object needs to get further and further to the target object.

   The algorithm is as follows:

   (a) For each action step of the moving object, check the distance toward the static object, we should always have each move getting the two objects further.

   (b) The ratio of the distance at the end and at the beginning needs to be higher than a threshold.

   (c) If one action step does not satisfy this condition, the whole action sequence is considered wrong.

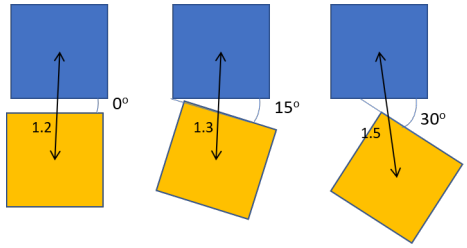

Figure 5.14: Examples of different values for parameters: angle between two blocks, and the distance between two blocks

4. **Slide Next To**: This action is a unique action in this list of actions, because we only care about the final position of the moving block. A perfect position for "slide next to" is when the two blocks are aligned, and exactly next to each other.

   The algorithm is as follows:

   (a) We would set two parameters for this method. One is the threshold for the angle difference between two blocks (two squares). For example, a difference of 0 to 15 degree makes blocks look aligned, but anything larger than that does not do well.

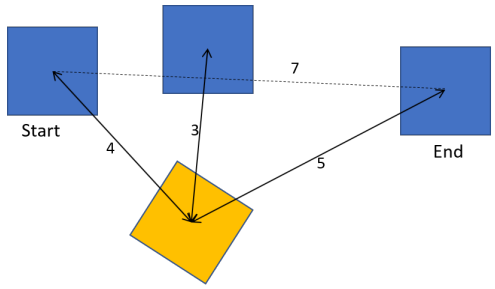

Figure 5.15: A demonstration of evaluation algorithm for Slide Past. We could check the distance between two objects at the beginning, at the end, and one intervening frame.

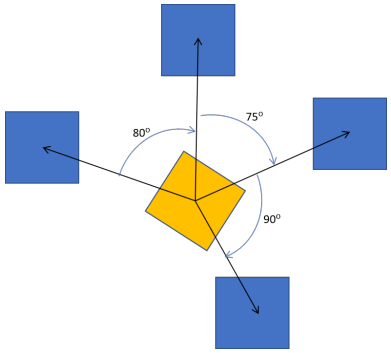

Figure 5.16: A demonstration of evaluation algorithm for Slide Around. We could check the total non-overlapping angle of the movement the moving object makes around the static object. It is 245^o here.

The distance between two square centers is normalized with block size. A threshold of 1.3 seems a reasonable value for this parameter. However, we could tune these parameters accordingly based on human evaluation.

(b) If the values at the end of an action do not satisfy the threshold conditions, the evaluator outputs 0, otherwise 1.

5. **Slide Around**: The interpretation of "Slide Around" is simple: calculate the covering angle of the moving object around the static object from the start point to the endpoint. The angle for each moving step will be positive if the angle is counter-clockwise, negative if the angle is clockwise. The final result is the absolute of the sum of all steps. Note that we do not take into account the change of the distance between two objects over time.

   Two parameters are included in the evaluator, α_1 and α_2. To soften the definition, the output of the evaluator will be either 0, 1 or 0.5. If the calculated covering angle $\alpha < \alpha_1$, output 0, $\alpha_1 <= \alpha <= \alpha_2$, output 0.5, otherwise output 1.

Evaluation of automatic algorithms against human evaluations

Using the human judgment score, it is straightforward to evaluate the automatic evaluators. While the scores given by our machine methods are binary whereas the scores given by anno-

tators range from 0 to 10, these scores are correlated, because we could imagine we can squash the annotators' score to the range from 0 to 1, then apply a binarizer function according to a threshold. Therefore, we can calculate a Pearson correlation coefficient for each parameter value, and select one that maximizes this correlation.

The following are details selections of parameters for each action type:

- **Slide Close**: Based on the values from Table 5.4, it immediately follows that we should choose the value of 3.5, i.e., the distance at the end of an action between two blocks needs to be smaller than 3.5 times the block size.

Threshold	1.5	1.75	2.0	2.25	2.5	2.75	3.0	3.25	3.5	3.75	4.0	4.25	4.5
Correlation	-0.09	0.17	0.29	0.11	0.18	0.22	0.22	0.34	**0.40**	0.39	0.39	0.39	0.34

Table 5.4: Pearson Correlation coefficient (PCC) between automatic and human evaluations of Slide Close for different values of *threshold*

- **Slide Past** The best value combination is when $side\_ratio = 1.1$ and $0.4 * \pi <= angle\_threshold <= 0.5 * \pi$ or $72^o <= angle\_threshold <= 90^o$. Therefore, we can choose $side\_ratio = 1.1$, i.e., the straight path from the beginning to the end of moving object should be comparable to distance from the static object to the moving object, and $angle\_threshold = 90^o$, i.e., the angles adjacent to the moving objects are acute angles. Maximum value on the heatmap is 0.72.

- **Slide Away** Based on the values from Table 5.5, it immediately follows that we should choose the value of the ratio threshold to be 2.3, i.e., the evaluators highly agree with the automatic method when we push one object 2.3 times further to the other object.

Ratio threshold	1.4	1.5	1.6	1.7	1.8	1.9	2.0	2.1	2.2	2.3	2.4	2.5	2.6	2.7	2.8
Correlation	0.04	0.01	0.01	0.15	0.24	0.27	0.11	0.03	0.18	**0.44**	0.41	0.31	0.28	0.28	0.26

Table 5.5: PCC between automatic and human evaluations of Slide Away for different values of *ratio threshold*

- **Slide Next To** Based on the values from Figure 5.19, it immediately follows that we should choose the value for the angle between two blocks to be $0.05 * \pi = 9^o$, and the threshold for the distance between two block centers to be $1.7 * block\_size$. Maximum value on the heatmap is 0.66.

- **Slide Around** Based on the values from Figure 5.18, it immediately follows that we should choose the value for two thresholds to be 1.1 and 1.7. These values are quite close to our original guess of 1 (half a cycle) and 1.5 (three-quarters of a cycle). Maximum value on the heatmap is 0.8.

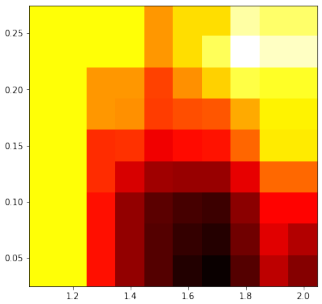

Figure 5.17: The PCC values for different combinations of $angle\_diff$ and $threshold$ for Slide Next To. The best value combination is when $angle\_diff = 0.05$ and $threshold = 1.7$.

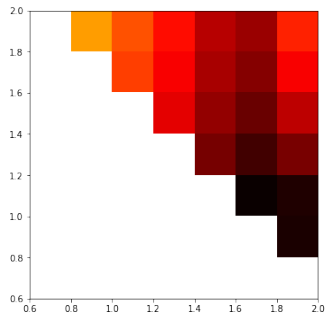

Figure 5.18: The PCC values for different combinations of $alpha_1$ and $alpha_2$ for Slide Around. The best value combination is when $alpha_1 = 1.1$ and $alpha_2 = 1.7$

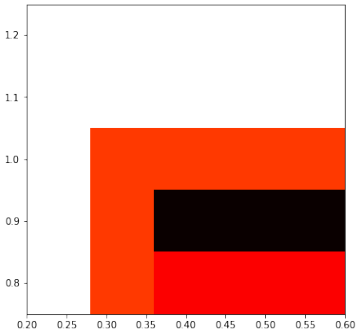

Figure 5.19: Heatmap showing the PCC values for different combination of $side\_ratio$ and $angle\_threshold$ for Slide Past.

Mini-conclusion

In this section, we have used scores given by human experts to create 5 automatic scorers, which we have tuned parameters to achieve highest possible agreement with human evaluations. In the following experiments, if not specified, these automatic scorers are used by default because it

will save some manual evaluation labor cost. In particular, when we want to improve the learned progress function with feedback (Section 5.3.6), we need quick oracle functions to direct our improvement.

Again, it is emphasized that there are probably other ways to parameterize the automatic evaluators that might equally fit with human judgment intuition. For example, one can argue that for good demonstration of **Slide Past**, we should parameterize the shortest distance between two objects (when one past another). However, increasing the number of parameters makes encoding the model more difficult and our target is just to create a simple oracle model that is agreeable to the human judgment scores.

5.3.4 Which algorithm works the best, and what is its performance?

In the first part of this experiment, we collect automatic evaluation scores for each action type and for each search algorithm, and report the average performance of an algorithm. In the second part, we will focus on running different algorithms to improve the performance and finding an interpretable action policy of "Slide Around".

Search algorithm

To measure the performances of search algorithms, we will generate 30 starting configurations. For each configuration, we will run search algorithms (4 variances, *continuous* versus *discrete*, and *greedy* versus *one-step beam-search*)) for 5 different actions. We will evaluate with a few different measurements. The first one is the average progress value of all demonstrations. The second one is the average episode length (number of actions before an episode terminates). The third statistics is the average score calculated with the automatic oracles. The fourth figure is the average time spent on planning the episode.

In the following experiments, hyperparameters are set as follows: the maximum number of steps in one episode $max\_step = 6$, the number of explorations kept at each step in one-step beam-search $l = 36$, the number of random actions tried at each step $n = 9$, the threshold for early-stopping of an episode $progress\_threshold = 0.85$ (See Algorithm 3).

Results:

We can also see that on average, one-step beam search algorithms will lead to higher progress value, and among two variances, the continuous version always performs better than the discrete one (Table 5.6). The search space of a one-step beam-search algorithm inherently

subsumes the search space of a greedy algorithm at the same depth; therefore we usually can find a demonstration that got higher target value with one-step beam-search (There is an exception, which is when the greedy algorithm goes deeper than the one-step beam-search).

Action type	Search algorithm			
	Greedy		One-step beam search	
	Continuous	Discrete	Continuous	Discrete
Slide Closer	0.52	0.4	**0.81**	**0.81**
Slide Away	0.88	0.80	**0.92**	0.88
Slide Next To	0.67	0.56	**0.85**	0.79
Slide Past	0.87	0.85	**0.91**	0.9
Slide Around	0.82	0.75	**0.88**	0.84

Table 5.6: Averaged progress for different action types and search algorithms

Action type	Search algorithm			
	Greedy		One-step beam search	
	Continuous	Discrete	Continuous	Discrete
Slide Closer	1.77	1.27	1.57	2.03
Slide Away	1.60	1.27	1.03	1.8
Slide Next To	1.53	1.1	1.6	1.97
Slide Past	1.67	1.8	1.23	1.6
Slide Around	2.23	1.77	2.33	2.33

Table 5.7: Averaged action lengths for different action types and search algorithms

There is, however, no common pattern could be seen in the performance of different algorithms when automatic evaluation methods are applied. For *Slide Closer*, the greedy version performs much better than the beam-search version when the searching space is discrete (Table 5.8). The reason is that when we run the beam-search algorithm, the learner finds out that it could increase the progress value, by first moving A away from B, then moving A closer to B again (comparing averaged progress value of greedy discrete 0.4 versus beam-search discrete 0.81). This strategy, however, is considered wrong by the automatic evaluation. For *Slide Away*, the result matches our expectation that searching on continuous space gives better results because, in discretized version, all positions of the moving block further than a threshold are considered the same. For *Slide Next To*, it is an advantage of the discrete algorithms that one of the discretized positions is also considered an adjacent position. For *Slide Around*, there is no algorithm showing an advantage. In fact, all four algorithms display low scores.

RL on continuous space

In this section, we will show RL running results when we plan in continuous space, the algorithm is presented in Section 5.1.2. The hyperparameters in these experiments are set at

Action type	Search algorithm			
	Greedy		One-step beam search	
	Continuous	Discrete	Continuous	Discrete
Slide Closer	0.67	**0.8**	0.67	0.13
Slide Away	**0.43**	0.27	0.40	0.3
Slide Next To	0.4	**1.0**	0.3	**1.0**
Slide Past	0.7	0.63	**0.77**	0.6
Slide Around	0.19	0.15	0.15	**0.20**

Table 5.8: Averaged score for different action types and search algorithms

Action type	Search algorithm			
	Greedy		One-step beam search	
	Continuous	Discrete	Continuous	Discrete
Slide Closer	11.25	8.39	97.71	47.06
Slide Away	9.92	7.62	53.67	38.20
Slide Next To	11.62	8.01	95.27	53.14
Slide Past	8.26	7.74	46.41	16.87
Slide Around	8.97	6.57	59.39	29.66

Table 5.9: Averaged time for different action types and search algorithms. Notice that time could not be compared between different actions

$policy\_learning\_rate = 0.1, policy\_decay = 0.92, policy\_decay\_every = 100, value\_learning\_rate = 0.1, value\_decay = 0.92, value\_decay\_every = 100$

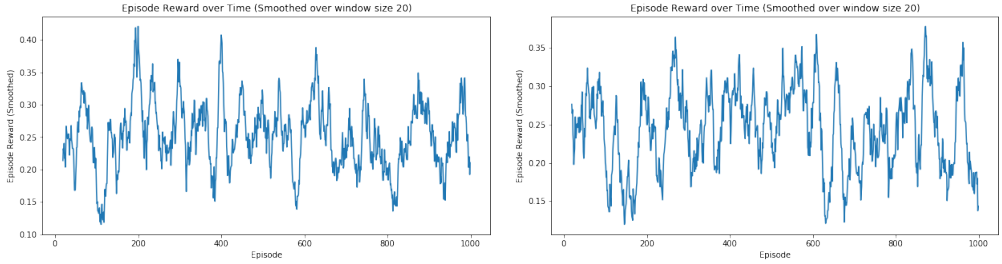

REINFORCE ACTOR-CRITIC

Figure 5.20: Average rewards of REINFORCE versus ACTOR-CRITIC with fixed σ on continuous space for **Slide Around** after 2000 running episodes.

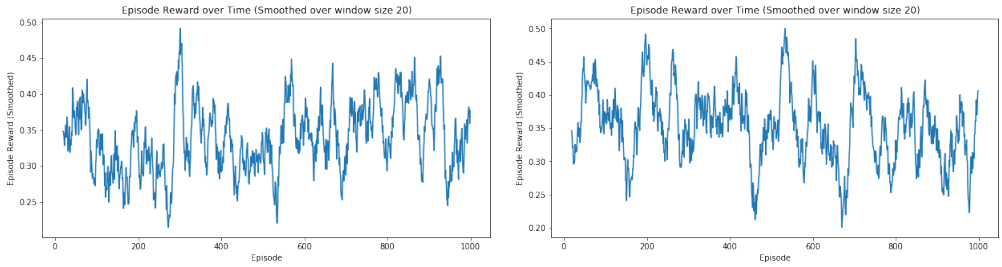

REINFORCE ACTOR-CRITIC

Figure 5.21: Same configuration as in Figure 5.20 but with $3 - action$ hybrid setup.

We can see in Figure 5.20 that both algorithms do not show any improving pattern. It is expected that the searching space is large and continuous, and the number of episodes might not be enough, but we will soon see that discretizing the searching space allows the RL algorithms to pick up learning pattern after a few hundred episodes.

RL on discrete space

States with the quantized progress component: as discussed in Section 5.1.2, for discrete space, we have two versions. In one version, we include the progress value into the discretized state, to find whether an external termination condition is needed. In the other version, we add the termination condition when $progress\ value > 0.8$, and leave the progress value out of each state.

We will start with the first version. We will show RL results for one action **Slide Around** when we plan in discrete space. In the following runs of the experiments, the main hyperparameters are $policy\_learning\_rate = 1$, $policy\_decay = 0.98$, $policy\_decay\_every = 100$, $value\_learning\_rate = 0.1$, $value\_decay = 0.99$, $value\_decay\_every = 100$.

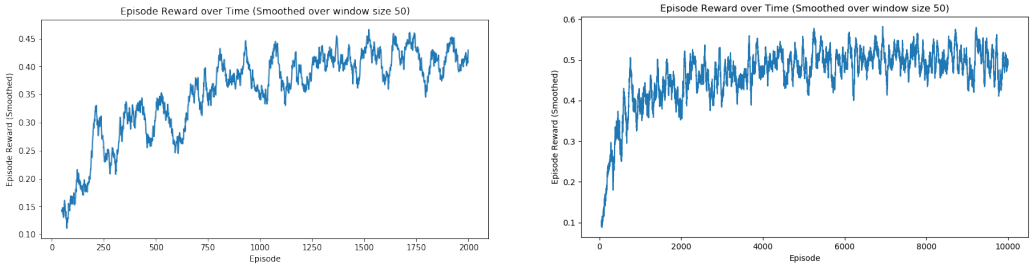

(A) True ACTOR-CRITIC with 2000 episodes (B) True ACTOR-CRITIC with 10000 episodes

Figure 5.22: Average rewards of ACTOR-CRITIC on discrete space for **Slide Around** after 2000 and 10000 running episodes.

In Figure 5.22 (A, B), we report the accumulated reward (or final progress) of running 2000 and 10000 episodes of the ACTOR-CRITIC algorithm. We can see that the algorithm seems to improve from random search in the first 1500 episodes quickly. After running for over 10 hours, the performance of the 10000-episode experiment peaked at around 0.5 and then plateaued.

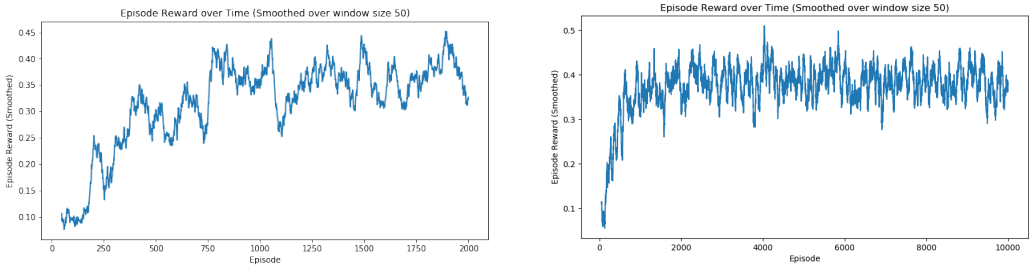

(A) REINFORCE with 2000 episodes

(B) REINFORCE with 10000 episodes

Figure 5.23: Average rewards of REINFORCE on discrete space for **Slide Around** after 2000 and 10000 running episodes.

Results from the REINFORCE algorithm is depicted in Figure 5.23. We can see REINFORCE performed a little bit worse than ACTOR-CRITIC, as the average episode reward peaked at around 0.4, and also reward variation is much more than when we ran with ACTOR-CRITIC.

A side note, not directly related to this learning setup, is that ACTOR-CRITIC algorithm is generally considered to be better than REINFORCE. ACTOR-CRITIC applies instant updates to the state value estimator and the policy learner and therefore ensures faster convergence of the policy. This is confirmed in this experiment, as the run with REINFORCE has much larger variance and worse performance.

One possible shortcoming of this problem formulation is that states corresponding to higher progress values would have much fewer occurrences, and therefore would be much less visited while we are generating episodes. The model, therefore, has not learned much of the action policy when the progress is high. Investigating in the action policy gives us some insights. The following are action probabilities as given by ACTOR-CRITIC learned action policy for a few different states (recorded at 2000 episodes):

Based on observation from Table 5.10, we can observe that the algorithm has learned a reasonable policy at the beginning. When $progress = 0$, which means we are at some beginning

State			Action probabilities	Best action
Position	Previous action	Progress		
0	0	0	[0.007, 0.005, 0.974, 0.005, 0.008]	2
0	2	0	[0.017, 0.004, 0.967, 0.01, 0.002]	2
0	3	0	[0.212, 0.214, 0.194, 0.112, 0.268]	4
0	4	0	[0.173, 0.212, 0.179, 0.111, 0.324]	4
2	0	4	[0.165, 0.192, 0.187, 0.228, 0.227]	3
2	1	4	[0.210, 0.199, 0.247, 0.220, 0.122]	2
2	2	4	[0.192, 0.202, 0.224, 0.257, 0.125]	3
2	4	4	[0.193, 0.195, 0.210, 0.186, 0.216]	4

Table 5.10: Action policies, demonstrated by action probabilities given at different planning states. Recorded using ACTOR-CRITIC after 2000 episodes

State		Action probabilities	Best action
Position	Previous action		
0	0	0.017,0.008,0.956,0.009,0.011	2
0	2	0.051,0.004,0.933,0.007,0.005	2
1	0	0.036,0.003,0.953,0.004,0.004	2
1	2	0.070,0.041,0.882,0.004,0.003	2
2	0	0.023,0.010,0.940,0.010,0.017	2
2	2	0.021,0.007,0.968,0.003,0.001	2
3	0	0.025,0.008,0.939,0.011,0.016	2
3	2	0.034,0.004,0.954,0.005,0.003	2
4	0	0.005,0.002,0.987,0.003,0.003	2
4	2	0.012,0.973,0.013,0.001,0.000	1
5	0	0.008,0.006,0.973,0.005,0.008	2
5	2	0.973,0.011,0.012,0.002,0.002	0

Table 5.11: Action policies, demonstrated by action probabilities given in different planning states (whereas each state does not have the progress component). Recorded using ACTOR-CRITIC after 2000 episodes. Only *legal* states that have action = 0 or action = 2 are included in this table. The full table could be seen in the code repository.

steps, our model strongly prefers actions that move one object so that two objects still keep the same distance. In fact, out of 30 states that have $progress = 0$, 18 states produce 2 as the best option, 5 produces 4 as the best action. Action 2 seems to be strongly preferred over action 4, even though there is no data bias (the number of clockwise captured *Slide Around* demonstrations is the same as counter-clockwise ones). For the first two rows, the activation for action 2 is strong because these states occur many times in generated episodes. We, however, do not see much difference in activation when $progress = 4$, implying that the model failed to generate enough number of demonstrations for effective learning at the end of actions.

States *without* the quantized progress component

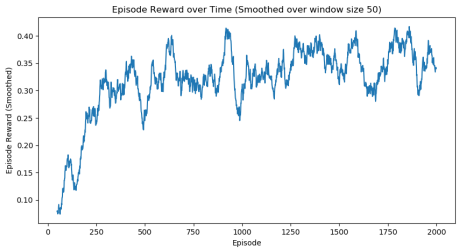

Figure 5.24: Average rewards of ACTOR-CRITIC on discrete space for **Slide Around** after 2000 episodes. Each state does not have quantized progress

Results from running ACTOR-CRITIC algorithm with states without quantized progress is shown in Figure 5.24. For this experiment, we only need 2000 episodes, as the state space is 5 times smaller than when we have quantized progress as a component. The average run result peaks at around 0.40, which is worse than the performance of the same algorithm when incorporating quantized progress. However, interestingly, as seen from Table 5.11, the model has learned a straightforward rule for approximating **Slide Around**. Starting from positions from 0, 1, 3 and 4, the rule is just that you keep choosing action 2 and move the object clockwise while keeping the distance to the static object, stop when progress function does not increase anymore. There are some exceptions that are hard to interpret. At quantized position 5, and the previous action is 2, the learned policy mysteriously decides that it should stop the episode by choosing action 0.

State		Action probabilities	Best action
Position	Previous action		
0	0	0.000,0.000,1.000,0.000,0.000	2
0	2	0.000,0.000,1.000,0.000,0.000	2
1	0	0.000,0.000,1.000,0.000,0.000	2
1	2	0.000,0.000,1.000,0.000,0.000	2
2	0	0.000,0.000,1.000,0.000,0.000	2
2	2	0.000,0.000,1.000,0.000,0.000	2
3	0	0.000,0.000,1.000,0.000,0.000	2
3	2	0.000,0.000,1.000,0.000,0.000	2
4	0	0.000,0.000,1.000,0.000,0.000	2
4	2	0.000,0.000,1.000,0.000,0.000	2
5	0	0.000,0.000,1.000,0.000,0.000	2
5	2	0.000,0.000,1.000,0.000,0.000	2

Table 5.12: Action policies, recorded using 3action *Hybrid ACTOR-CRITIC* after 2000 episodes. Only *legal* states that have action = 0 or action = 2 are included in this table.

Fortunately, running the hybrid version of ACTOR-CRITIC model with 3-action beam search gives us a satisfied action strategy (the selection of value 3 is actually not important, any other value > 1 will behave the same). The following table shows the output of a run with this model. We get a strategy that reads "Always go to the right". That is precisely how we could define *clockwise* **Slide Around**!

However, the artifact that the resulted action policy does not have *counter-clockwise* movement poses an interesting question of which RL algorithm would produce policy with the ability to capture both kinds of action. Moreover, in this setup, we saw an overexposure to actions that provide an immediate reward. RL algorithms quickly reinforce these actions, leading to degenerate action distributions, i.e., for each state, there is only one probable action. If this action is not possible for a certain situation (e.g., it leads to the block falling out of the playground), there is no recoverable strategy, other than randomly pick another action.

Human evaluation

An additional human-evaluation experiment is taken for just the action "Slide Around". Results are shown in the following table (Table 5.13):

Action Type	Average Score	Evaluator Disparity
Beam search continuous	2.75	1.03
Beam search discrete	5.95	0.7
Hybrid ACTOR-CRITIC + beam search	6.7	1.02

Table 5.13: Human evaluation of different algorithms on 30 demonstrations of **Slide Around**

From these results, we can see that beam search on the discrete space is already an improvement over on the continuous space. The action policy learned from Hybrid ACTOR-CRITIC + beam search improves it even more qualitatively, but getting a perfect score is still difficult, for the reason mentioned above.

Mini-conclusion

In this section, we have pitted different algorithms against each other, to find out which algorithm produces the best results. For all actions in our action set, excepts for "Slide Around", beam search on continuous space produces reasonable human-evaluation results. For "Slide Around", beam search on continuous space does not produce a satisfactory result, though on discrete space it produces a higher performance score.

We also ran policy gradient learning methods (ACTOR-CRITIC and REINFORCE) to improve upon search algorithms for performing "Slide Around". On continuous space problem formalization, these algorithms failed to converge, but on discrete space, both algorithms successfully converged to an interpretable policy. Applying the learned policy with greedy action selection produces the best human-evaluation score for this action.

5.3.5 Can the learner make the distinctions between learned action types?

This experiment examines the ability of the learner to distinguish these 5 action types based on human evaluation on 3-D visualizations of generated demonstrations. A set of 150 demonstrations are generated, which is 30 for each action. They are posed to annotators to solicit judgment. After each demonstration, multiple-choice panels are displayed, and the annotator are asked to answer the question: *"Which of these sentences **best** describes the video shown?"*. 6 answers are displayed for choosing, including 5 descriptions of actions, plus " None of these sentences describe the video".

The task requires annotators to predict which description was used to generate the visualization in question. While the experiment in Section 5.3.2 gives us a rough estimation of how well the learning algorithm is, only by juxtaposing different action types for annotators to select, we can measure if learning actions in an isolated manner is enough. Some actions in this set are close enough for confusion, even when demonstrations are made by a human expert.

Because of time limitation, this is the only experiment that we carried out with the 3-D visualizer. With 3-D visualizer, demonstrations would be more realistic and closer to the way we perceive actions, and therefore, we could address some issues that do not occur when evaluation is taken in the 2-D simulator. The first issue is the dependency of spatial perception on the Point of view (POV). Krishnaswamy and Pustejovsky (2017) show that this dependency is not trivial, and changing of POV might lead to different human evaluation. The POV of the 2-D visualizer corresponds to a bird's-eye view, while the POV in 3-D visualizer would be similar to the captured environment, whereas the performers are moving and observing blocks on a table. The second issue is derived from the inherent property of three dimension objects, i.e., they can occlude each other. When that happens, our perception of spatial relationship is distorted, and we resort to prediction, rather than perception, for action recognition.

Results:

(Ongoing.)

5.3.6 Can we use the feedback from human evaluation to improve the learned model?

As mentioned in Section 2, feedback from human evaluation could be used as training data. Generated demonstrations from the first experiment (5.3.4) are complementary to real, captured data, because in learning by demonstration, we do not have any rigorous way to include negative samples. Imagine in real life, you teach your kids how to swing a baseball bat, they observe how you do it, and give a try. Unfortunately, they did it so badly, because they swapped their bottom hand and their top hand. Now you give an instruction to correct that, and they start to hit the ball more often. However, if you are required to give demonstrations of *how to swing the bat really badly* right from the beginning, it might not come straightly to your mind that swapping hands is one bad way[1].

Reflecting on this thought experiment, we can see that learning of action is usually not one-shot learning. It is more of a process, in which we incorporate feedback from teachers to improve gradually. If that applies to humans, it should apply to machines learning from humans as well. In this section, we will investigate the possibility of using interactive methods to improve learned models.

We will focus on two different kinds of feedback, namely *cold feedback* and *hot feedback*. The distinction between cold and hot here refers to the feedback time. *Cold feedback* is given at the end of a demonstration episode to evaluate how well the demonstration is, while *hot feedback* is given in the middle of the demonstration, and giving the clue of not only *whether* the demonstration is bad, but also *where* it is bad, and *how* it should be corrected.

Projecting into the context of the CwC project, *cold feedback* corresponds to positive acknowledgment (pos-ack) and negative acknowledgment (neg-ack) (Krishnaswamy et al., 2017). In that communicating framework, pos-ack could be translated to a head nod or a thumbs up pose with either or both hands, or an utterance of “right” or “yes”, to signal agreement with a choice by the machine. Neg-ack could be mapped to a head shake, thumbs down with either or

[1]This is actually related to my personal experience with baseball. The first time I came to a batting cage, I did not figure out the way to hold the bat, and swing very badly for 10 minutes without any of my friends noticing what is wrong, until some kids standing outside just yelled at me “You hold it wrong, right hand on top”

both hands, or palm-forward stop sign, or "no" utterance, to signal disagreement. In learning framework, this could be used as a binary evaluation signal for machines to update their learned models. [2].

Hot feedback means online corrections in the middle of a demonstration. In the context of CwC project, it might be mapped to a pointing (deixis) including the direction of the hand and/or arm motion. In CwC peer-to-peer setup, in which a person uses multimodal communicative methods to direct an avatar, deixis is used to move attention of the avatar to a target object, or a target location. In LfD framework, we can use this kind of clue to correct an erroneous move of the avatar.

We incorporate *cold feedback* and *hot feedback* into this machine learning framework by the following methods:

- *Cold feedback*: a binary value indicating whether a demonstration is good or bad. Using the grades that we get from annotators (which ranges from 0 to 10), we can pick out the very good and very bad demonstrations, by putting an upper and lower threshold on the grades. We could choose some consistent thresholds for all action types, or choose thresholds depending on how many good or bad samples we received. A reasonable landmark threshold for good and bad could be 6 and 3, i.e., any demonstrations that got higher than 6 are used as additional positive samples, and ones that got lower than 3 as negative samples. The progress learner would be updated with those samples, and new demonstrations would be generated with the same initial configurations as old demonstrations.

  The reason we do not use the demonstration that got some medium score is that they are not obviously bad or good. Many of them start as a good demonstration, but make some mistake at the end, as we have seen in Table 5.3. Technically speaking, they are still "bad demonstrations", but how to use them as negative samples with *cold feedback* method is not obvious.

- *Hot feedback*: The 2-D simulator could be switched to interactive mode (as discussed in Section 2.4.1. In this interface, one can choose to loop from the beginning of a planned demonstration to the end, and choose an action replacement for one that is not appropriate.

[2]The terminology here is just to reflect how much of interactiveness the experiment is, and might not be similar to the terminology in literature in Dialog and Discourse

To test whether the newly learned model performs better than the original model, instead of using human evaluation, we will use the automatic evaluation methods shown in Section 5.3.3. This method will allow us to evaluate effects of updating the original progress learner efficiently.

The reason to look for a way to improve the progress learner, and as a consequence, to improve the search and RL algorithms depending on it, is that when analyzing sample demonstrations planned by one-step beam search algorithm, there are some demonstrations that finally get a high progress score, but fails to capture the meaning of the intended actions. Examples are shown in Fig 5.25. Both demonstrations, planned on discrete planning space, have final progress value in the range of 0.8 to 0.9, but fails to capture "Slide Around". In fact, the moving block only makes it halfway in two opposite rotation directions.

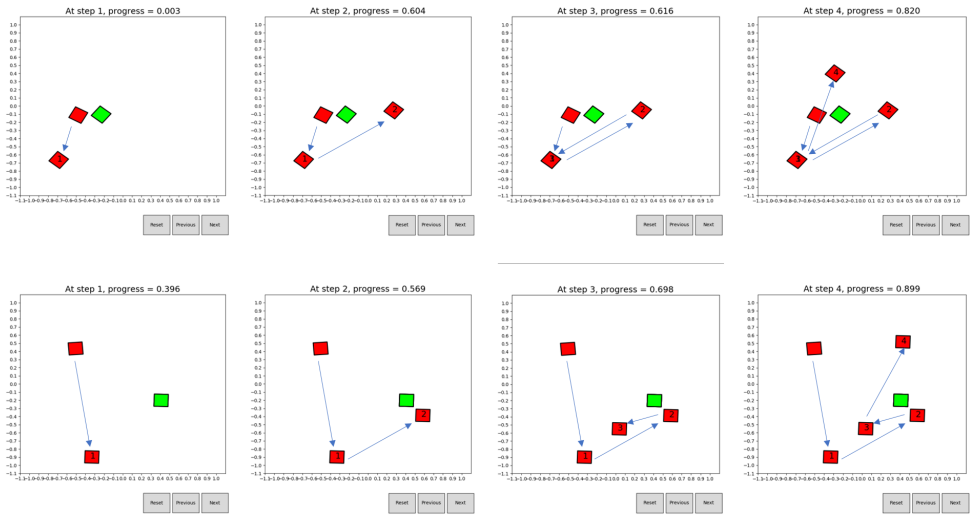

Figure 5.25: Two examples of demonstrations that the red block change the direction from counter-clockwise to clockwise

A simple method to use *cold feedback* is to update the learned model to distinguish between good and bad demonstrations. Bad demonstrations (low scored ones) are treated as negative samples, and therefore are given progress value of 0 at the end. Good demonstrations are given progress value of 1. Feature sequences are extracted from these demonstrations at the final step to be used as updating samples to the progress learner. Algorithm 8 shows our method to incorporate *cold feedback* into the progress learner:

input : A learned progress function f (Section 2.3.2) for one action, an update epoch number n, a learning rate θ
A list of demonstrations l created by the learner, rated as good or bad.
output: An updated (and hopefully) improved learned progress function
for *Epoch* $k \leftarrow 1$ **to** n **do**
  for *Demonstration* $D_i, i \leftarrow 1$ **to** l **do**
    Extract feature from the end of D_i as X;
    if D_i *is good* **then**
      Corresponding label $y = 1$;
    end
    else
      Corresponding label $y = 0$;
    end
    Update f with sample (X, y);
  end
end

Algorithm 8: Algorithm to incorporate cold-feedback

For *hot feedback*, it is more difficult to decide how to update the progress function. There are a few possible ways to guide the direction of updates. The first is based on an intuition that at any step i, if a teacher determines that the learner has made a wrong action a_i, and he selects another action a'_i, the progress value after a'_i (p'_i) must be higher than that after a_i (p_i). Moreover, because the learner has searched through some other candidate actions a_{ik} before arriving at that action a_i, the progress values if those actions are taken should also be smaller than p'_i. The second is that p'_i should always be larger than the corresponding value at the previous step p_{i-1}. The third is that progress values at different steps should be adjusted to fit the linear function, in the same manner as in training. To combine these methods for an update formula is, however, a difficult task and we probably can only find a proper method by trial. Algorithm 9 shows the method used in this experiment, which is based on the first intuition:

input : A learned progress function f (Section 2.3.2) for one action, search breadth n, a learning rate θ, a discount parameter α (e.g., 0.1)
A list of difficult setups l (ones that got low score in a previous demonstration).
output: Same as in Algorithm 8
for *Setup* $S_i, i \leftarrow 1$ **to** l **do**
  for *Time step* $i, i \leftarrow 1$ **to** ∞ **do**
    Run greedy search with S_i in the interactive simulator, i.e., select an action a_i from a set of n candidate actions a_{ik};
    Observe action a_i the learner makes (a_i can be None if the the learner cannot find an action leading to better progress value);
    Optionally the teacher selects another action a'_i that is considered a better candidate action. If he does, the learner's action is replaced by the teacher's action;
    Record progress value p'_i for a'_i;
    Extract feature sequence f'_i for a'_i;
    for $k \leftarrow 1$ **to** n **do**
      Record progress value p_{ik} ;
      Extract feature sequence X_{ik} ;
    end
    if *The teacher clicks* ***Update*** **then**
      Break;
      Record the number of steps h;
    end
  end
  for *Time step* $i, i \leftarrow 1$ **to** h **do**
    for $k \leftarrow 1$ **to** n **do**
      if $p_{ik} > p'_i$ **then**
        Set target value $t = p'_i * (1 - \alpha)$;
        Update f with sample $(X = X_{ik}, y = t)$;
      end
    end
  end
end
if *The teacher clicks* ***Save*** **then**
  Save the updated model to a new file;
end

Algorithm 9: Interactive algorithm to use hot feedback

Results

Cold feedback

Because of time limitation, in this section, we will only present results from an experiment with Slide Around. This action, which has on average more number of steps than other actions, is of more interest in reinforcement learning framework. In this experiment, we will see the effect of updating the learned progress function with two sources of *cold feedback*: from human evaluation score and from automatic scorer (Section 5.3.3).

In particular, among 30 demonstrations of "Slide Around" generated and sent to annotators to evaluate, 19 demonstrations got good scores, indexed with 0, 2, 3, 4, 6, 8, 9, 11, 12, 16, 17, 20, 21, 23, 24, 25, 27, 28 and 29, 4 demonstration got bad score, indexed with 10, 13, 18, 19. They are divided into two sets, one that has index smaller than 15, and the remaining. The *cold feedback* Algorithm 8 is used to update the original progress function to create one updated functions. The original one and the updated ones are all used to generate new demonstrations for another set of 30 setups (The first 30 demonstrations are given to annotators for human evaluation, reported in Section 5.3.2. The second 30 setups are different initial setups, created in Section 5.3.4, and used only for machine evaluation. Here, again, *setup* means the starting position of a demonstration).

We can also use the automatic scorer to select the good and bad demonstrations from the original set of 30 setups, update the model, and apply the learned model on the second 30 setups. The result is given in Table 5.14. Because continuous sampling has a higher variance, for this algorithm, the experiment ran twice and the scores are averaged.

Progress function	Search algorithm			
	Greedy		One-step beam search	
	Continuous	Discrete	Continuous	Discrete
Original model	0.19	0.15	0.16	0.20
Human-Feedback Updated	**0.40**	**0.20**	0.58	0.42
Auto-Feedback Updated	0.38	**0.20**	**0.60**	**0.65**

Table 5.14: Averaged score of 30 setups for action type = *Slide Around* with 4 different search algorithms. 3 different models of progress functions are compared: Original model, Update model with human feedback (Human-Feedback Updated), Update model with automatic feedback (Auto-Feedback Updated)

As reflected in Figure 5.14, there is not much difference between the results from two variances. The result for the method using automatic feedback performs a little bit worse with greedy algorithms but performs better with beam-search algorithms. This just reflects different

selections of bad and good demonstrations to update the model. It only proves that the automatic scorer can also be used to improve the learned progress function. If we use them in a bootstrapping loop, we can improve the learned progress function to generate a policy performing as well as the expectation from the automatic scorer. We will not investigate further in that direction.

Hot feedback

We will investigate whether the use of *hot feedback* could improve performance, but not for the original model, but the model that has been improved with *cold feedback* (for a stronger baseline). Again we will start with selecting bad demonstrations from the first 30 setups, and apply the updated model to the second 30 setups. In particular, using Human-Updated model, we ran the greedy search algorithm on continuous space twice, and picked out 5 setups that generate lowest demonstrations scores. We reloaded them on interactive mode, making corrections, updating the model following Algorithm 9, then saving it into a new model file. Using that updated model and run search algorithms over the second set of setups give the results as reported in Figure 5.15.

Progress function	Search algorithm			
	Greedy		One-step beam search	
	Continuous	Discrete	Continuous	Discrete
Human-Feedback Updated	0.40	0.20	**0.58**	0.42
Hot-Feedback Updated	**0.5**	**0.37**	0.44	0.30

Table 5.15: Averaged score of 30 setups for action type = *Slide Around* with 4 different search algorithms. Comparison between the updated model with human feedback (Human-Feedback Updated) and the model updated with *hot feedback* (Hot-Feedback Updated)

Surprisingly, the updated model performs worse when paired with beam search algorithm. This is somewhat counter-intuitive but could be explained as follows: the way we inspect and update the model step-by-step has made the model strongly favors the greedy algorithms. This might not be very undesirable, as we always want the faster and simpler algorithm (greedy) to perform well.

Mini-conclusion

In this subsection, we have gone through a few different techniques to improve learned models interactively. Two techniques, *cold-feedback* and *hot-feedback*, and their relevance to the

CwC project, are addressed. While the methods are currently executed in a 2-D simulation environment, they could be extended to work with a real-time interactive environment as well.

We have seen these methods could be used to improve the baseline model, with different advantages. *Cold-feedback* methods, which focus only on whether the final step of a demonstration is good or bad, has an advantage when running with beam-search algorithms, while *Hot-feedback* methods, improving the progress function on each demonstration step-by-step, favor the greedy algorithms.

We also have seen that we do not need a large amount of data to update the model. For *cold-feedback*, we have used about 20 feedback scores, while for *hot-feedback*, we have made corrections to 5 setups. While this is still not one-shot learning, the number of demonstrations is small enough for interactive learning.

5.4 Conclusions

As we have included a mini-conclusion after each experiment, in this section, we will only summarize the lessons that we have learned over the course of setting up and solving this problem.

The first lesson is that for the problem at hand, true RL methods, i.e., our policy gradient methods, are not necessarily better than simpler search algorithms. Even though we have successfully run policy gradient methods, producing a satisfying action policy, it incurs a few issues. The most problematic issue is the formalization of states and actions: firstly, we need domain knowledge to carry out space discretization in the manner as we have described; secondly, the way we represent states cannot capture action trajectory from the beginning of the demonstration. The second issue is computational overhead. Running RL methods is often time-consuming. Probably for this problem, search algorithms are more appropriate than RL algorithms.

The second lesson is that we can improve learned models by interactively guiding the learning agents. This direction of research might be of high interest for machine learning community. More research needs to be done so that we can use this learning framework in a generic machine learning setup.

Last but not least, one issue with the capturing setup described in this chapter is that we do not have natural language inputs. All of our actions are constrained in a frame-based manner. Therefore, as we move forward to the next chapter, we will flip the learning problem on its

head and considering it from another perspective, that taking natural language instructions into consideration.

Chapter 6

Performing actions by observing synthetic demonstrations

In this chapter, we will flip the problem on its head, by considering a different learning setup. In Chapter 5, we generate real observations of actions by first giving descriptions of the actions, then capturing demonstrators performing the actions. In this chapter, we will generate synthetic demonstrations of actions in a search space, which is termed *maze traversal space*, and record observations into video snippets. These videos are posed to annotators to solicit textual description of the trajectory in the visual scene.

The learning objectives in both setups are the same: given textual inputs describing actions (*instructions*), plan actions (sequence of action steps) on a grounded visual environment. In this setup, which is termed *synthetic demonstration* to contrast with the previous *real demonstration* setup, we will generate demonstrations on the 2-D simulator. This approach usually allows quicker data collections, and also allows us to solicit instructions of natural language utterances (c.f. the previous approach, where we predefined a set of action types with binding arguments).

In training phase, we will learn a machine learning model by feeding into it a parallel corpus of instructions and corresponding sequences of actions as video captures. In evaluating phase, we will pose to the machine learning model a textual instruction, and the starting configuration of visual environment (*maze puzzle*). The task would be for the learned model to direct a selected block to traverse the maze toward some final target. The evaluation objective would be for the planned trajectory follows as close as possible to the intended trajectory.

6.1 Models

Firstly, in this setup, we could not directly use a progress function like in Chapter 5, because the textual instructions are in natural language form, preventing us from creating different progress functions for different action types. Therefore, we will use a model that generates sequences of actions directly from the sequence of instructional utterances. Not surprisingly, this model is called Sequence-to-Sequence (or Seq2Seq) model. The input sequence is the stream of words in the input instruction, and the output sequence will be a sequence of the following actions: *left, right, up, down, STOP*.

In this section, we will first discuss Seq2Seq models used for generation of actions from textual instructions. The focus will be an advanced form of Seq2Seq models, called Attention RNN, described in Section 6.1.2. These models are recently developed for neural machine translation (Wu et al., 2016) and image caption generation (Xu et al., 2015), achieving state-of-the-art results for both tasks. It is noted that Image-to-caption model is not truly Seq2Seq, but instead maps 2-D convolutional features to sequence, but these two models can all be classified as Attention RNN, because their decoder components are identical, i.e., an attention RNN decoder.

6.1.1 Seq2Seq RNN for controlling

So far, in this dissertation, we have met with a simple form of RNNs, which is a function from a sequence of features to a single numerical data, i.e., the action progress value. This form of RNNs is the typical setup for classification and regression. A more advanced form of RNNs allows ones to produce a sequence from a sequential input. These models are commonly called sequence to sequence (Seq2Seq) models (actually the multi-layer LSTM implicitly uses Seq2Seq on the lower layers).

The simplest form of Seq2Seq models has *temporal alignment* between the input and output sequences, e.g., one output for one input at each time step, or the sampling rates of input and output are resonant. This setup can be used for *classical* controlling problems, e.g., there is a controlling signal recorded every second, and observations (e.g., of a drone) are recorded at 30 times per second. Translation from a textual instruction to controlling actions is usually not temporal aligned, though both the instruction and output actions follow a left to right narrative

order.

A more appropriate form of Seq2Seq models for non-aligned sequence translations is called **Encoder-decoder**. In the simplest form, Encoder-decoder models are two RNNs stacking on top of each other (Figure 6.1).

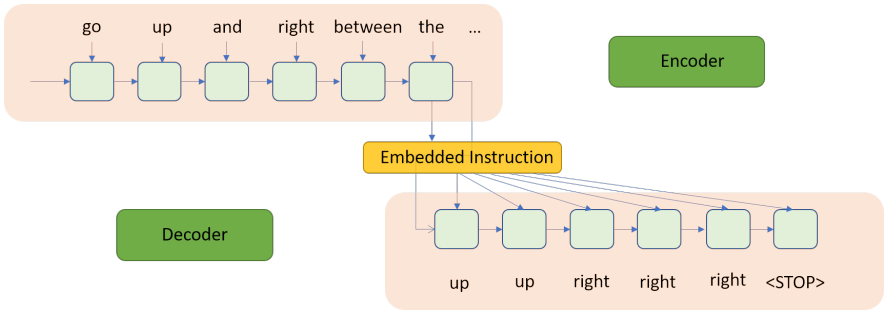

Figure 6.1: Encoder-decoder model

The encoder is a sequence-to-one RNN that takes a sequential input and produces an embedded representation of the input instruction. The decoder is a one-to-sequence RNN that digests the embedded representation as inputs for all time steps, while the final state from the encoder is (optionally) passed on to be the initial state for the decoder.

6.1.2 Attention RNN

Attention RNN is developed, in the first place, as an extension to the encoder-decoder framework in neural machine translation (Bahdanau et al., 2015). What is called *attention* is a trick applied to the embedded representation. Instead of having only one embedding as the information mediator between the encoder and decoder (shown in Figure 6.1), we will have multiple embedded representations (called *annotations*), one for each input time step, as shown in Figure 6.2. Prediction at each output time step is conditioned on a function over all annotations. In this dissertation, we will use condition of Bahdanau attention style with a **weighted sum** of input annotations (shown in Figure 6.2 as $\bigoplus$ operator). Weights are usually calculated as functions of current decoder state and each annotation (higher weight is depicted with more intense color in Figure 6.2). Intuitively, this method allows alignment between words (or phrases) in the input and the output so that words in input sentence that are more predictive for the current output step have more contribution to the prediction.

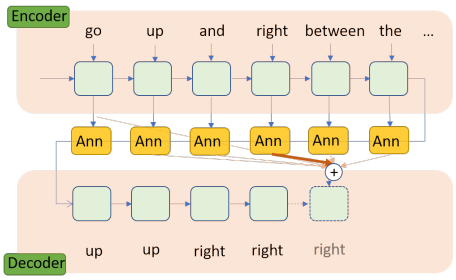

Figure 6.2: Attention RNN model (Bahdanau additive attention style)

Attention RNN is also a flavor of attention methods, which have garnered tremendous interest in machine learning community in recent years. Attention methods have been hailed as the "holy grail" to improve all deep learning networks, including Convolutional neural networks (CNNs) and Recurrent neural networks (RNNs) (See (Vaswani et al., 2017)). The attention trick has also been related to Neural Turing machines (Olah and Carter, 2016; Graves et al., 2014) and Neural Programmer (Neelakantan et al., 2016), two powerful frameworks for learning of execution (programs). In this dissertation, we would not dive deep into the working mechanism of attention (please refer to (Bahdanau et al., 2015) for mathematical formulas) as well as the recent discussion of attention methods.

Instead, we will focus on how to adapt this method to the task at hand. While the previously described tasks have one input and one output, our task has two different inputs, one textual and one being the visual grounding. Applying the neural translation method directly (text sequence to text sequence) is tantamount to ignoring visual grounding. We, however, can still use it as a baseline method.

To incorporate visual grounding into this Seq2Seq method, we can condition action prediction at each time step of the decoder with the current environment state (cf. (Tanti et al., 2018) for the use of image input for caption generation). For this method, we can feed the current environment state as a visual image at each time step, concatenated with the input to the decoder (the weighted annotation). The output of the prediction, i.e., the selected action, is sent to the controller component, moving the purple block accordingly; we again feed the new environment state to the decoder to infer for the next step. This loop is presented in Figure 6.3.

Notice that in training phase, we ignore the controller loop, and directly use the frames from the visual input to feed into the inputs of the decoder. We will only address this issue in the conclusion part, under the term of *exposure bias*.

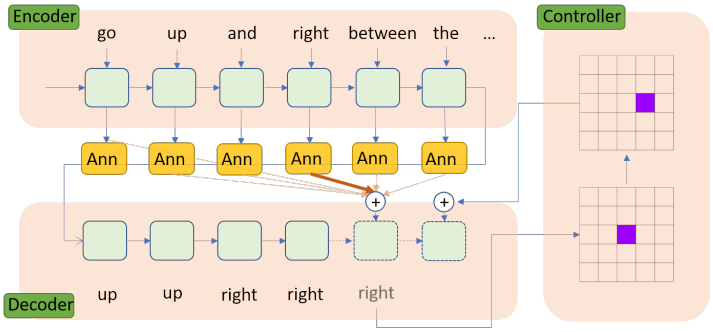

Figure 6.3: Seq2Seq model with controlling loop from the visual state to the input of the decoder)

Common practices

Some common practices used in training Seq2Seq attention models are as follows:

- Beam search and greedy search in Seq2Seq models: analogous to beam search and greedy search in RL framework. The difference lies in the objective to optimize in searching. While search algorithms, as discussed in Section 2.4.2, aim to maximize the objective of the progress function, beam and greedy search in Seq2Seq models aim to maximize the probability of the output sequence. We need to search over the output space because, in RNNs, there is no method to run efficient sequence inference, such as Viterbi method, to find the sequence with global maximum probability. The reason is that cell states are propagated over time, and therefore, the probability distribution of actions is not the same for different inference time (or the sequential model is not *stationary*). It is also noted that the sequence probability objective is related but not the same as the training objective (i.e., perplexity), as well as the external evaluation objective, that we will discuss shortly.

  All of our experimental models would use greedy search for simplicity.

- Word embedding: we need to turn from words into feature vectors before feeding into neural networks, by a method called word embedding. Because the size of our vocabulary is small, we will train our own word embedding. Even though we can use the same word embedding for input and output (shared word embedding), it usually does not hurt model's performance by training separate embeddings for source and target vocabularies. In fact, using shared word embedding might even hurt model's performance, because an instruction phrase like "move to the left of the green rectangle" might actually mean

going to the right direction, if the green rectangle lies further to the right. Using the same embedding for the word "left" at the input and the word "left" at the output will be incorrect in this case.

- Internal evaluation: is a measure of objective that is used in gradient optimization method. In typical Seq2Seq models, we usually use **perplexity** as the internal evaluation. The formula of **perplexity** is 2^H where H is the averaged number of bits needed to code the next symbol in the output sequence. At each time step, this value is calculated by the cross-entropy between the predicted symbol probabilities and the target probabilities. A smaller value of perplexity means a higher predictive power of the model, and a model has absolute confidence in prediction when its perplexity (over some evaluation corpus) equals 1.

- External evaluation: is a measure of objective that usually reflects a better qualitative comparison between an output candidate and a reference. For machine translation problem, BLEU score (Papineni et al., 2002) is an appropriate external evaluation, as it accounts for phrase matching between candidate and references outputs. For the problem at hand, an appropriate external evaluation will be one that reflects whether two trajectories are convergent or divergent. In Figure 6.4, we see an example of this qualitative distinction that we are not able to capture in internal evaluation method. In both figures, the orange trajectory corresponds to the reference path (one used to generate the textual instruction), and the gray one is to the inferred (candidate) trajectory. In Figure 6.4 A, the reference actions are *down, down, right, right, down, down, right, right*, the candidate (inferred) actions are *right, right, down, down, right, right, down, down*, i.e., the prediction is wrong at every time step. Same applies to the situation in Figure 6.4 B, but we can qualitatively judge that the candidate trajectory in A matches its corresponding reference better than in B.

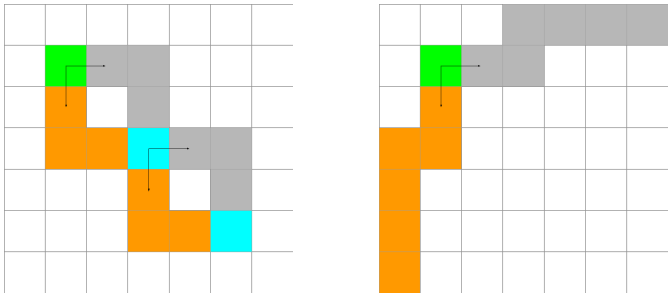

(A) These two paths are convergent (B) These two paths are divergent

Figure 6.4: While the internal evaluation is agnostic to *convergent* versus *divergent* paths, external evaluation measure accounts for this distinction. Starting position is color *green*, intercepting positions are *blue*, candidate path follows the gray cells, and reference path follows orange cells

A good external evaluation score between two trajectories is the averaged distance from each cell of any trajectory to its closest neighbor on the other trajectory. Let's call that a NEIGHBOR score. A smaller evaluation score means more similar trajectories. If the reference trajectory is identical to the candidate trajectory, the evaluation score will be 0. Detailed calculation of a few sample pairs of trajectories is presented in Figure 6.5.

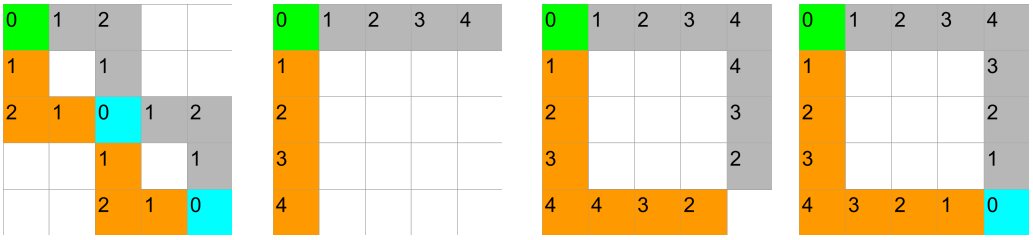

(A) Score = 16/15 = 1.07 (B) Score = 20 / 9 = 2.2 (C) Score = 38/15 = 2.53 (D) Score = 32/16 = 2

Figure 6.5: NEIGHBOR scores of some sample trajectories. The value of each cell is the distance to the closest cell on the other trajectory. Shared cells have the value of 0.

This evaluation method provides an opportune measurement for the problem at hand, mainly to make the distinction between convergent and divergent trajectories, as we see in the scores of Fig. 6.5 A versus Fig. 6.5 B. Between B and D, it is apparent that two trajectories in D are convergent, while they are divergent in B, and therefore D's score should be lower than B's score. C score is higher than B score, which is unexpected

(we might expect the score to be somewhere between scores of B and D). However, an evaluation method that is justifiable in every case is difficult to find.

6.2 Data preparation

Generating demonstrations:

Demonstrations were generated merely by creating a grid of size 15x15, then scattering 3 rectangles, 3 triangle and 2 L shapes on top. To make the maze puzzle a little bit more interesting, we colored the shapes with a few different simple colors like yellow, red, green, blue and purple. The moving block is always a purple cell.

The source and target locations of a purple block are so generated that they are of at least 15 moving step distance to each other. A path from the source to the target location is generated. For the trajectory to be less monotonous, we will not use the shortest path from the source to the target (indeed, the shortest path is first generated, then a blocking wall is generated to block this path, then the chosen path is generated to avoid the blocking wall). Details of demonstration generation are provided in the code.

Soliciting instructions:

There are 3 folders, named [0,1,2], each with 100 puzzles. Annotators were asked to choose one folder to give instructions by speaking to an audio recorder. They were asked to tell the name of the maze puzzle first, then give their instruction. Annotators are mostly master students in Brandeis' Computational Linguistic program.

In total, 15 annotators submitted their recorded audios. 8 annotators submitted for the first 100 puzzles, 8 other submitted for the second 100 puzzles, while only 1 annotator submitted for the third 100 puzzles. These were transcribed by an annotator into text. Because of time limitation, for each puzzle indexed from 0 to 199, 4 annotations were transcribed, for one indexed from 200 to 299, the only one was transcribed.

The following snapshots are taken from a puzzle indexed 0. 4 transcribed instructions given for this specific maze puzzle are also provided.

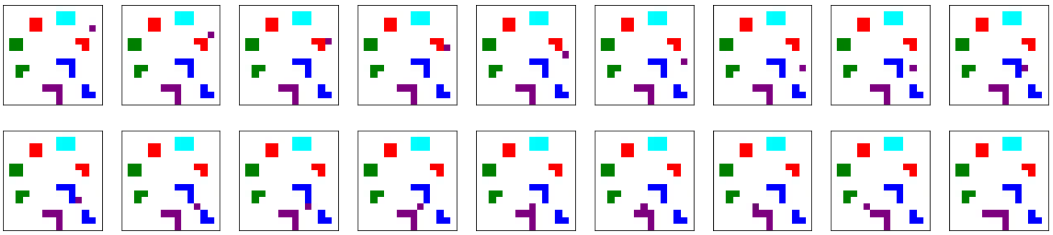

Figure 6.6: Frames of a recorded video snippet

move the purple square down on the right side of the blue L and red L then move the purple square left between red L and purple L and it ends at the left side of the purple L
move the purple block down then left so that is directly between the blue L shape and the red L shape then move it down again until it reaches the top of the red L shape then move it straight left until it reaches 1 cell beyond the purple L shape
move the purple block down until it is in position between the 2 red L shapes and move it to the left until it is in front of purple L shape then move it down 1 block space
move the purple block down on the right of the blue L left and between the 2 red Ls to the left of the purple L

We use all textual instructions of the first 200 puzzles for training and validation data so that one instruction is used for validation, and the remaining are used for training. Therefore, training and validation share the same set of puzzles. For testing, instructions of the last 100 puzzles are used (puzzles that are not seen in training).

6.3 Evaluation

In this section, we will evaluate two different methods: the baseline method of attention RNN *without* visual grounding and the improved model *with* visual grounding. Three evaluation measures will be provided: perplexity on the training and evaluation dataset, NEIGHBOR score on the evaluation and testing dataset and effective output length. Notice that effective output length is the number of output actions that are *legal* in the visual environment, i.e., it does not move the target block outside of the playground, or toward a cell occupied by an obstacle object.

The following chart and table shows results of running the baseline method with $num\_units = 128$, $optimizer = StochasticGradientDescent$, $learning\_rate = 0.2$, $num\_train\_steps =$

2000. Based on perplexity scores and NEIGHBOR scores in this running, early-stopping is a good strategy, as it shows that after step 1400, both evaluation perplexity and NEIGHBOR score increases. Output effective length is much shorter than the average reference length because, without *visual grounding*, the moving block *blindly* crashes into obstacles or walls.

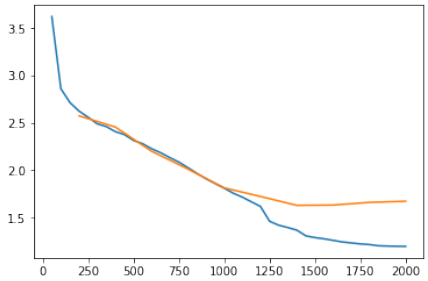

Figure 6.7: Perplexity of training (blue line) and evaluating (orange line) over 2000 steps (each step is one mini-batch update)

Step	NEIGHBOR		Avg. length	
	Eval	Test	Eval	Test
1400	4.04	4.10	10.4	8.84
1600	4.18	4.12	10.33	8.6
1800	4.15	4.00	10.06	8.94
2000	4.13	4.01	10.62	8.94
Ref.			18.24	17.89

Figure 6.8: External evaluation scores for model *without* visual grounding, at different values of steps

The following table shows the same evaluation for the model with visual grounding.

Step	NEIGHBOR		Avg. length	
	Eval	Test	Eval	Test
1400	3.27	3.88	11.32	8.98
1600	3.36	3.75	11.87	9.21
1800	3.21	3.77	11.56	9.33
2000	3.17	3.65	11.33	9.30
Ref.			18.24	17.89

Table 6.1: External evaluation scores for model *with* visual grounding, at different values of steps

We can see a small improvement of the model with visual grounding. Improvement is made w.r.t both external evaluation scores as well as the averaged length of output sequences. Improvement is higher for Evaluation dataset, probably because the same puzzles fed into training are used for Evaluation dataset. The improvement is, however, not very satisfactory. It is very likely that data sparseness is the culprit. Collecting more data is expensive, but there is a possible method to handle this issue. We could augment the training data by shifting the cells in each

puzzle while keeping the instruction and commands intact. We will leave it for future work.

6.4 Conclusions

In this chapter, we have given a brief discussion on a newer framework for learning of execution, namely sequence to sequence model for controlling. A technically challenging controlling problem is proposed, and we have applied Seq2Seq method with different levels of complexity to solve it. Contrasting the methods used in Chapter 5 and this chapter allows us to reflect on the similarity and difference between them. Even though we do not apply them to the same problem, we will shortly see that they are appropriate for different kinds of planning problems.

To a certain extent, Seq2Seq for execution is analogous to reinforcement learning algorithms. The progress value is intrinsically coded into the probability of the *STOP* signal at each time step, i.e., when this (progress) value is high, we decide to complete the action. The function that the decoder of Seq2Seq models calculates has precisely the same signature with a learned policy in RL. This function takes in a state that combines the encoded information of the instruction and current planning state (hidden state of decoder cell in Seq2Seq versus formalized location/orientation environment states in RL) and outputs a probability distribution of actions.

Regarding formalization of states in these methods, we have seen that we formalize reinforcement learning states using domain knowledge, i.e., we know beforehand that the actions we want to learn only involve relative positions between objects. In contrast, states in Seq2Seq methods are of "black box" nature, i.e., we do not know the meaning of different features in hidden states of Seq2Seq's decoder. Moreover, an interesting difference is that in RL methods, we found that mapping from continuous states to discrete states through feature extraction methods (e.g, qualitative spatial reasoning) allows RL algorithms to work more efficiently. In Seq2Seq methods, we actually transform the discrete states of output (chains of discrete actions) into continuous multi-dimensional hidden states.

Even though we have discussed the strength of RL methods in Section 5.4, in this section, we will reiterate some advantages of reinforcement learning methods (e.g., REINFORCE) over Seq2Seq methods:

- Adaptation to novel environment setups: we can see that in Chapter 5, the original envi-

ronment for capturing demonstrations is largely different from the environment for generating demonstrations. Moreover, even if we add other constraints to environment setup, the RL and search methods will still work. For example, if we change size or shape of the playground (See Section 5.1.1) or add more objects to it, algorithms belonging to RL types can accommodate easily.

- Ability to learn skills with limited training dataset: by formalizing states and action space with domain knowledge, we can make reinforcement learning to work with a limited amount of training data.

- Can be trained to optimize a *global* sequence objective, rather than *local* step objectives: we have seen in Section 6.1.2 that for Seq2Seq models, we usually use two different evaluation methods, cross-entropy is used for training because it is differentiable, and external evaluation is better for qualitative judgment but is not differentiable. In contrast, the optimization target in reinforcement learning is a global objective, such as the progress function in Section 5.3.1, which is not differentiable for each action step.

- Avoidance of *exposure bias*: *exposure bias* is a problem of Seq2Seq models that reinforcement learning model does not have, regarding the difference between inputs of the decoder in training versus inference phase. Even though Figure 6.2 shows that output of the decoder at the current time step is fed as input to the next step, this only applies for inference phase. In training phase, we disregard the output from the previous time step and use the correct label to feed into the next step. In other words, the model is only exposed to correct data in training but has to make prediction sequentially in inference. While it can be mitigated by a smart learning schedule alternating between feeding correct labels and passing previous predictions, this is inherently not an issue of reinforcement learning framework, where the model generates, then learns from its own samples.

Advantages of the Seq2Seq methods are the followings:

- Ability to learn skills with very large state spaces: given enough amount of data, Seq2Seq can be used for very large searching space. For problems such as Neural Machine Translation, the searching space for output has the size of V^T where V is the size of vocabulary (10^4), and T is output's average length (30), which makes it larger than the number of

particles in the universe (estimated at 10^{86}). For RL methods, this space would be too large to search over, if the policy is started at random.

- Ability to learn skills without domain knowledge to formalize states and actions, therefore it can be applied to a wide spectrum of problems. This is probably the most critical aspect of Seq2Seq model that makes it so popular and successful.

Now we can see why the problem in Chapter 5 needs a different solution from the one in Chapter 6. The first problem calls for a solution even if we have a limited amount of training data, whereas to sufficiently solve the second problem, we probably need more data than a thousand samples. We can try to add domain knowledge to solve the second problem (i.e., to define what is a rectangle, or an L-shape), but finding presentations for arbitrary shapes is harder than simple one-cell blocks. That is why we feed visual states as plain flatten vectors to the algorithm in this chapter. Another reason RL would be challenging to apply to the second problem is that defining a proper reward function is hard. Yet we could use the *external* evaluation score as reward function in a training sample, but how to calculate it in a generated demonstration?

Recently, there are novel machine learning methods that can take advantages of both Seq2Seq and Reinforcement learning. One is called MIXER (Mixed Incremental Cross-Entropy Reinforce) (Ranzato et al., 2016). It is an optimization method that combines both cross-entropy and REINFORCE. In particular, it first learns a baseline policy with Seq2Seq loss function, then starts optimizing this policy with external evaluation objective using REINFORCE. This approach has been shown to work for three classical Seq2Seq tasks: machine translation, text summarization and image captioning. Another notable model is called Seq2Seq Learning as Beam-Search Optimization (Wiseman and Rush, 2016), adopting beam search method to rank output sequences according to external evaluation scores.

This mixing between reinforcement learning methods and Seq2Seq methods is intellectually exciting and technically challenging. To the best of our knowledge, there is not yet a conclusive answer to the question of which method works better for the problem of execution from natural language instructions. We will leave further investigation for future work.

The problem of turning natural language instructions into commands with visual grounding is relatively new and potentially of interest for the research community in AI and Computational Linguistics alike. One of the barriers to research in this direction is the lack of an interesting dataset. Interactive games that require cooperative behaviors between users to control characters

might be an excellent source. We would also leave that direction for future work.

We have not yet addressed in this chapter what will happen if an instruction is incorrect, i.e., there is no chain of actions that could satisfy the input instruction. There are a few ways to handle this issue. An approach that uses domain knowledge and does not use machine learning can find mentions of objects in the instruction, then locate them in the visual environment; one can then find rules regarding relative positions between starting position of the moving block and the obstacles to decide if an instruction is executable or not. A machine learning approach could generate unlikely configurations semi-automatically from a given instruction. In training, it can pair an instruction with an unlikely configuration as a negative sample. In inference, it can produce a "NOT EXECUTABLE" to signal that it could not move forward given an incorrect instruction.

This chapter is brief, and there are issues not addressed at length, but hopefully, it has shed light on our problem from another perspective. We also hope that this conclusion has included useful discussion for future considerations.

Chapter 7

Conclusions and Future directions

7.1 Conclusions

As a conclusion is a place for us to reflect on the dissertation as a whole, I think it is opportune for me herein to tell you my journey to this intellectual culmination. As all worthwhile journeys bring us to unusual corners of the world, my journey has brought me to meet with many ideas, some are marvelous, some are intriguing, and some are pretty esoteric. The ideas most influential to this work are ideas from Communicative with Computer (CwC) initiative, e.g., the idea that human-machine interaction is facilitated by multimodal communicative means on visually grounded environments, and that mutual understanding between humans and machines on the high level of complexity are built upon machine knowledge of simple concepts. That leads me to propose the use of learning from demonstration as a modality for human-machine communication and collaboration, and this methodology can be utilized to teach machines primitive action skills as a potential foundation for machine learning of more complex actions.

I borrow much of my sequential modeling framework from my undergraduate thesis, which has an English title "Building of resources and methods for Vietnamese Sign Language Recognizer". In that thesis, I collected a parallel corpus of sign language sentences and text captions, then used a simple blob detection method to detect hand and face regions of signers, translating to sign feature vectors through embedding methods, producing a language model with Hidden Markov Model (HMM). This capturing, annotating and learning framework inspires me to develop ECAT, funneling my attention toward usage of multimodal resource for machine

learning.

During my study at Brandeis, the first research that is formative to this dissertation is my work on TimeML corpus. It introduced me to the theoretical foundation of Dynamic Event Structure (Pustejovsky, 2013) and linguistic treatment of temporal and spatial expressions. The idea about frame-based structure as the language of actions (as I have used in Chapter 4 and Chapter 5) are brought to me when I was doing a project on disambiguation of verbs using Corpus Pattern Analysis (CPA) approach (Hanks, 2004).

To summarize, this dissertation contributes a feasibility study for a methodology to teach AI agents action skills through multimodal communicative interfaces. Through this line of research, it can be demonstrated that machine learning methods, such as reinforcement learning and sequence to sequence learning alike can be used to teach skills to robotic agents by demonstrating actions to them. Moreover, learning can be aided by interactive communication between machine learners and human teachers. These conclusions flow from analysis of three experimental setups. The first experimental setup, described in Chapter 4, provides a learning method for fined-grain action recognition. The second experimental setup, detailed in Chapter 5, gives us a playground to test the usefulness of reinforcement learning methods in action reenactment. The third one, drafted in Chapter 6, is contrasting to other setups in data collection and representation methods, but complementary in the shared purpose of mapping from instructions to actions on a grounded visual environment, giving us a complete landscape of learning methodology.

Besides, this dissertation has the following contributions:

It investigates the use of temporal-sequential modeling, in particular, recurrent neural networks for controlling problems. Controlling agents on a visually grounded environment through textual instructions is a new problem that is potentially interesting for AI, Machine Learning (ML) and Computational Linguistic (CL) communities alike. For AI, controlling is a fundamental application. For ML, it is both intriguing and revealing to compare between analogous methods such as policy gradient and Seq2Seq. For CL, generating simulations of motion events from linguistic descriptions is of recent interest (Pustejovsky and Krishnaswamy, 2014), and controlling from linguistic instructions is the same problem in disguise.

This dissertation proves that we can leverage on both advantages of classical structural machine learning theory and modern deep learning methods. Qualitative reasoning, and in particular, qualitative spatial reasoning, is considered a classical structural approach to problem

formalization, thereby can be employed to enforce human bias on machine learning models. While in recent times, it is more common to see that data compensate for domain knowledge and structural bias in ML models, this problem at hand presents an opportunity of using both methods.

The findings in this dissertation work also have the following additional implications:

On learning from demonstrations Learning from a limited number of training samples (or one-shot learning) is a (very) difficult problem. Learning from Demonstrations in reality usually needs as few samples as possible. Encoding human bias into machine learning models is one potential approach. In this work, we have discussed mostly bias in relative positioning of objects in space (under the name of QSR). Usually the more bias we add to the models, the less number of training samples we would need to train them. However, for some human biases, it is not straightforward that we can employ them in machine learning models. Instead, we would still need to integrate them in action formal representations. For example, human bias for actions that are composed of "repetition" of other sub-actions, is not easy to be learned directly from data or to be imposed on machine learning models.

On human-machine interaction We have learned that communicative means, such as positive and negative acknowledgments and deixis, are suitable for interactive learning. Even though the setup in this dissertation only uses a 2-D simulator for interaction interface, the same learning principles apply for the real-time 3-D interface between machines and humans used in CwC project.

On formal semantics of actions One of our original thoughts about potential applications of this work is to automatically mine formal semantic representation of actions from data (as discussed in Section 1.1.9). So far this is still an open question to be addressed: action representations collected from data are heterogeneous, while their formal semantic representations are prototypical. This problem can hardly be framed as a machine learning problem because the formal structural semantic representation is not friendly to machine learning methods.

On reinforcement learning methods We have used algorithms on RL framework to learn trajectory-based action skills. To recapitulate lessons learned in Chapter 5, greedy search is a cheap and flexible method, while policy gradient has computational overhead. However, policy gradient could produce expected action policy using discretization on searching space.

On Seq2Seq for controlling We have used Seq2Seq for a controlling problem, framed as a neural machine translation task. The results are not yet very satisfactory, probably because

of data sparseness. A possible method to handle this issue is generating augmented data for training. We will explore that direction in future work.

7.2 Future directions

Throughout the previous chapters, several areas that call for future research have been discussed. We will herein focus on three lines of research that can be considered extensible from this dissertation. For each direction, a few extensions will be listed in order of relevancy. Items listed first are either more relevant to the problem at hand, are aimed to be an improvement over a current weakness, or are more readily realizable by extending this dissertation work. Items listed last are either an open-ended direction or a difficult question spawn from this dissertation work that needs a broader or holistic approach to solve.

7.2.1 Extensions to the methodology

Real-time LfD So far the discussions have been about an *offline* framework. To make it work in an online manner, we need continuous capturing and annotation of actions. Two approaches can be employed to aid real-time capturing and annotation. The first approach is to keep the current real demonstration setup but change the capturing and annotation platform. ECAT is offline and independent to the CwC human-machine communication interface. Therefore, we have to create a bridging module between these two applications. To replace offline annotation phase, we can record actions potentially by having users giving signal words (like "START" and "STOP") as well as spoken descriptions of performed actions. This extension requires integration of a speech recognizer into this module.

The second approach is to forfeit the real demonstration capturing, and instead using deixis (pointing) inputs to create synthetic demonstrations for actions in virtual space. This setup is, in fact, readily available with current development stage of CwC interface (Krishnaswamy et al., 2017), in which users, to give direction for a trajectory action, can communicate to the virtual agent a sequence of exact locations. This approach is also suitable for the use of feedback loop, as we have discussed in Section 5.3.6.

Virtual reality LfD Virtual reality (VR) could be used as a shared collaborative environment between humans and machines. During the past years, the VR community has been focus-

ing more on applications on embroidering human experience, whether in game, in education, or in telecommunication. In the meantime, it can also be used as a platform for teaching human skills to AI. Imagine in a VR environment, we can set up a teaching classroom, and the lesson is the usage of a cutting tool, e.g., a knife, on some objects. In this environment, human teachers are posed with a *puzzle*, e.g., a knife is put at some locations (on a table, on the floor, etc.), an object is of different kinds (a fruit, a piece of meat, etc.). We can, thereby, teach machines the way we hold a knife (by the handle of course), and the way we use it for a vast number of tasks. Even though this would require more realistic physical simulation in the virtual environment, it is not far-fetched from the current development stage of VR.

7.2.2 Things to learn

We will look into other types of actions (or in a broader sense, types of things) that we can learn from demonstrations. A diagram of potential extensions is given in Figure 7.1. We can summarize that in this thesis we learn *path*-only *action* skills by matching *trajectories* of experts' demonstrations, using *feature-based* ML. That leads to a few future directions as the followings:

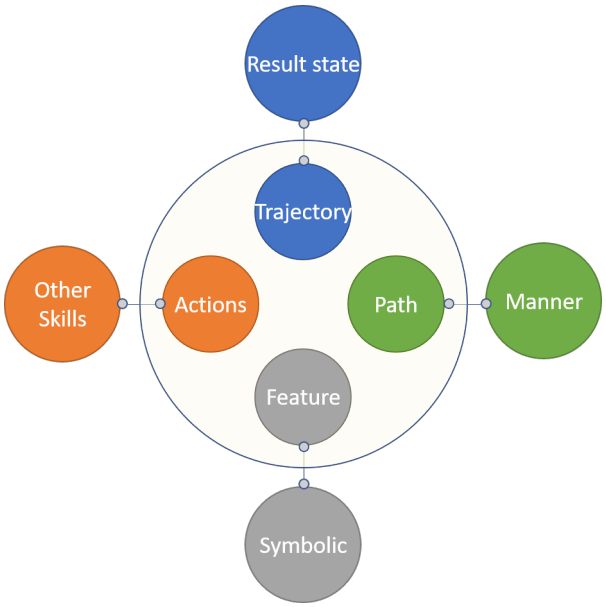

Figure 7.1: Some extension dimensions

Path- versus manner- aspect of actions Learning manner aspect of actions requires fine-

grained treatment of object affordances. For example, for learners to make the distinction in performing "rolling a bottle" and "sliding a bottle", we need to equip it with reasoning mechanism related to how an object's pose and position dictating its affordances. These questions, hopefully, can be answered by referring to a developing language for objects and events in our lab named VoxML (Pustejovsky and Krishnaswamy, 2016).

Symbolic- versus feature- based learning Learning complex actions from simple actions requires an additional semantic layer for objects and actions. For example, to learn "make a row from given objects", the learner needs to be equipped with multiple concepts. It needs to know the concept of composite objects to realize that a "row" is composed of "blocks". Assuming that the learner observes rows of length 2 and length 3, it also needs to be equipped with the concept of *repetition* to infer that structures made from more blocks are also rows. It also needs even more complicated abstract concepts, such as object axis, to infer that building a longer row is to extend it on the longest axis.

This dissertation is, by no mean, call for exclusive use of learning from demonstration method. Demonstrations alone are not enough for robots to pick up complex concepts. We should only consider it as one modality for teaching action skills to AI agents. That leads to the question that for what kind of action skills, LfD is appropriate. Probably a generic and suitable approach would be a holistic one, where we teach trajectory action skills from demonstration and reinforcement learning, and teach complex skills by communicative means. The reason is that trajectory-based action skills readily lend themselves to LfD feature-based methods.

An example of teaching complex actions structurally composed of sub-actions using human-machine communication is Scheutz's work in translating natural language directives to action execution (Dzifcak et al., 2009; Williams et al., 2015).

Other skills The discussions about LfD in this thesis are not only limited to real physical actions but also apply to more abstract skills, such as game playing, e.g., "Go", "Catan" or any other games. Research in this direction has built up a head of steam in recent years and has achieved significant and recognized milestones, such as the success of Google's *AlphaGo* and *AlphaGo Zero* programs, that have beaten human masters in the ancient Chinese Game of Go (Silver et al., 2016, 2017). While the more recent version of AlphaGo does not use any human data to guide its strategy evolution, graphical computer games with even larger searching space (e.g, *Montezuma's Revenge* or *Super Mario*) could benefit from the use of human knowledge to add priors to the learning models. Moreover, not all problems can use an exclusively self-play

RL framework, e.g., if they incur costly simulations.

Trajectory versus Result state As discussed in Section 1.1.11, for humans to distinguish between the mean of actions versus the goal of actions, we possess a powerful reasoning cognitive process, equipped with a complex set of cognitive biases. When we teach new skills to machines, we can let them learn this distinction from data, which is challenging. To the best of our knowledge, there is not yet any research on how to apply this mechanism from human learning to machine learning. Another more straightforward method is that we can communicate to them this intention.

7.2.3 Machine learning

In this section, we will, lastly, turn into further considerations of machine learning methods for execution. We will take a tour through a few recently developed ML methods that have relevance to the learning framework in this thesis.

Other ways to find reward functions In Reinforcement learning, there is nothing more important than having a correct reward function. Recently there are many algorithms developed to find reward functions more sensibly. For example, algorithms belonging to Inverse Reinforcement Learning (IRL) family (mentioned in Section 2.3.2) look for optimal reward functions automatically. An explanation for this approach is that our intuition is not adequate to create proper reward functions, i.e., the learning agents can be trained to optimize a secondary objective, while the learned policy still produces good rewards based on our intended high-level objective.

In this thesis, we have seen the use of an RNN-trained progress function as a reward function. Our function is designed with the intention of guiding the learners progressively over the course of an action. Therefore, we design the function to produce a linear value from 0 to 1. It might be better to relax this design constraint and look for a more adaptive way to create progress function.

Neural Programmer As mentioned in Section 6.4, related frameworks to learning of execution are Neural Programmer (Neelakantan et al., 2016), and Neural Enquirer (Yin et al., 2016) for program execution (which we will use a common term of Neural Programmers). The nature of the problems in this thesis is a little bit different to the ones in these work, to the extent that the solutions to the problems in this thesis can be fuzzy, while Neural Programmers solve

for exact solutions. For example, Neural Programmers are used to solve the task of question answering on tables, e.g., to answer *What is the sum of numbers in column A whose field in column B is greater than 10*. Neelakantan et al. (2016) show that neural networks, like the ones used in this thesis (LSTM and LSTM with Attention), could be used for this problem, but fail to produce correct results reliably, whereas Neural Programmers can be applied to achieve close to 100% accuracy.

One interesting idea from the work of Yin et al. (2016) is a breakdown of complex queries into multiple steps of simpler queries, and learning of simpler executors lead to a combined model that can answer complex queries. This sounds almost like what we want to achieve when we combine multiple models of primitive actions for a model of more complex actions.

Bibliography

Eren Erdal Aksoy, Minija Tamosiunaite, and Florentin Wörgötter. Model-free incremental learning of the semantics of manipulation actions. *Robotics and Autonomous Systems*, 71: 118–133, 2015.

Muhannad Alomari, Paul Duckworth, Nils Bore, Majd Hawasly, David C Hogg, and Anthony G Cohn. Grounding of human environments and activities for autonomous robots. In *International Joint Conferences on Artificial Intelligence (IJCAI)*, 2017.

UF Andrew, D Mark, and D White. Qualitative spatial reasoning about cardinal directions. In *Proc. of the 7th Austrian Conf. on Artificial Intelligence. Baltimore: Morgan Kaufmann*, pages 157–167, 1991.

Katharina Antognini and Moritz M Daum. Toddlers show sensorimotor activity during auditory verb processing. *Neuropsychologia*, 2017.

Brenna D Argall, Sonia Chernova, Manuela Veloso, and Brett Browning. A survey of robot learning from demonstration. *Robotics and autonomous systems*, 57(5):469–483, 2009.

Minoru Asada, Eiji Uchibe, and Koh Hosoda. Cooperative behavior acquisition for mobile robots in dynamically changing real worlds via vision-based reinforcement learning and development. *Artificial Intelligence*, 110(2):275–292, 1999.

Dzmitry Bahdanau, Kyunghyun Cho, and Yoshua Bengio. Neural machine translation by jointly learning to align and translate. *Proceedings of the 3rd International Conference on Learning Representations (ICLR)*, 2015.

Michael Bain and Claude Sommut. A framework for behavioural cloning. *Machine Intelligence 15*, 15:103, 1999.

Collin F Baker, Charles J Fillmore, and John B Lowe. The berkeley framenet project. In *Proceedings of the 36th Annual Meeting of the Association for Computational Linguistics and 17th International Conference on Computational Linguistics-Volume 1*, pages 86–90. Association for Computational Linguistics, 1998.

Mikhail Belkin, Siyuan Ma, and Soumik Mandal. To understand deep learning we need to understand kernel learning. *arXiv preprint arXiv:1802.01396*, 2018.

Mehul Bhatt, Hans Guesgen, Stefan Wölfl, and Shyamanta Hazarika. Qualitative spatial and temporal reasoning: Emerging applications, trends, and directions. *Spatial Cognition & Computation*, 11(1):1–14, 2011.

Aude Billard, Sylvain Calinon, Ruediger Dillmann, and Stefan Schaal. Robot programming by demonstration. In *Springer handbook of robotics*, pages 1371–1394. Springer, 2008.

Gary Bishop, Greg Welch, et al. An introduction to the kalman filter. *Proc of SIGGRAPH, Course*, 8(27599-23175):41, 2001.

Daniel G Bobrow. *Qualitative reasoning about physical systems*, volume 1. Elsevier, 2012.

Robert Bogue. Domestic robots: Has their time finally come? *Industrial Robot: An International Journal*, 44(2):129–136, 2017.

Greg Brockman, Vicki Cheung, Ludwig Pettersson, Jonas Schneider, John Schulman, Jie Tang, and Wojciech Zaremba. Openai gym, 2016.

Sylvain Calinon and Aude Billard. Teaching a humanoid robot to recognize and reproduce social cues. In *Robot and Human Interactive Communication, 2006. ROMAN 2006. The 15th IEEE International Symposium on*, pages 346–351. IEEE, 2006.

Sylvain Calinon, Florent Guenter, and Aude Billard. On learning, representing, and generalizing a task in a humanoid robot. *IEEE Transactions on Systems, Man, and Cybernetics, Part B (Cybernetics)*, 37(2):286–298, 2007.

Anthony G Cohn and Jochen Renz. Qualitative spatial representation and reasoning. *Foundations of Artificial Intelligence*, 3:551–596, 2008.

Matthias Delafontaine, Anthony G Cohn, and Nico Van de Weghe. Implementing a qualitative calculus to analyse moving point objects. *Expert Systems with Applications*, 38(5):5187–5196, 2011.

Tuan Do. Event-driven movie annotation using mpii movie dataset. 2016.

Tuan Do and James Pustejovsky. Fine-grained event learning of human-object interaction with lstm-crf. *Proceedings of the European Symposium on Artificial Neural Networks, Computational Intelligence and Machine Learning (ESANN)*, 2017a.

Tuan Do and James Pustejovsky. Learning event representation: As sparse as possible, but not sparser. *International Workshop on Qualitative Reasoning (QR)), at IJCAI-17*, 2017b.

Tuan Do, Nikhil Krishnaswamy, and James Pustejovsky. Ecat: Event capture annotation tool. *Proceedings of ISA-12: International Workshop on Semantic Annotation*, 2016.

James Dougherty, Ron Kohavi, Mehran Sahami, et al. Supervised and unsupervised discretization of continuous features. In *Machine learning: proceedings of the twelfth international conference*, volume 12, pages 194–202, 1995.

Krishna SR Dubba, Anthony G Cohn, David C Hogg, Mehul Bhatt, and Frank Dylla. Learning relational event models from video. *Journal of Artificial Intelligence Research*, 53:41–90, 2015.

Juraj Dzifcak, Matthias Scheutz, Chitta Baral, and Paul Schermerhorn. What to do and how to do it: Translating natural language directives into temporal and dynamic logic representation for goal management and action execution. In *Robotics and Automation, 2009. ICRA'09. IEEE International Conference on*, pages 4163–4168. IEEE, 2009.

Michael Firman. Rgbd datasets: Past, present and future. In *Proceedings of the IEEE Conference on Computer Vision and Pattern Recognition Workshops*, pages 19–31, 2016.

Christian Freksa. Qualitative spatial reasoning. *Cognitive and Linguistic aspects of Geographic space*, 63:361–372, 1991.

Christian Freksa. *Using orientation information for qualitative spatial reasoning*. Springer, 1992.

Yarin Gal and Zoubin Ghahramani. A theoretically grounded application of dropout in recurrent neural networks. In *Advances in Neural Information Processing Systems*, pages 1019–1027, 2016.

Anja Gampe, Jens Brauer, and Moritz M Daum. Imitation is beneficial for verb learning in toddlers. *European Journal of Developmental Psychology*, 13(5):594–613, 2016.

Barbara P Garner and Doris Bergen. Play development from birth to age four. *Play from birth to twelve: contexts perspectives, and meanings*, 2006.

Sergio Garrido-Jurado, Rafael Muñoz-Salinas, Francisco José Madrid-Cuevas, and Manuel Jesús Marín-Jiménez. Automatic generation and detection of highly reliable fiducial markers under occlusion. *Pattern Recognition*, 47(6):2280–2292, 2014.

Y Gatsoulis, M Alomari, C Burbridge, C Dondrup, P Duckworth, P Lightbody, M Hanheide, N Hawes, and AG Cohn. Qsrlib: a software library for online acquisition of qualitative spatial relations from video. In *Workshop on Qualitative Reasoning (QR16), at IJCAI-16*, 2016.

György Gergely, Harold Bekkering, and Ildikó Király. Developmental psychology: Rational imitation in preverbal infants. *Nature*, 415(6873):755, 2002.

Alex Graves, Greg Wayne, and Ivo Danihelka. Neural turing machines. *arXiv preprint arXiv:1410.5401*, 2014.

David Gunning. Explainable artificial intelligence (xai). *Defense Advanced Research Projects Agency (DARPA), nd Web*, 2017.

Patrick Hanks. Corpus pattern analysis. In *Euralex Proceedings*, volume 1, pages 87–98, 2004.

Nick Hawes, Christopher Burbridge, Ferdian Jovan, Lars Kunze, Bruno Lacerda, Lenka Mudrová, Jay Young, Jeremy Wyatt, Denise Hebesberger, Tobias Kortner, et al. The strands project: Long-term autonomy in everyday environments. *IEEE Robotics & Automation Magazine*, 24(3):146–156, 2017.

Junhu He. *Robotic In-hand Manipulation with Push and Support Method*. PhD thesis, University of Hamburg, 2017.

Lisa Anne Hendricks, Zeynep Akata, Marcus Rohrbach, Jeff Donahue, Bernt Schiele, and Trevor Darrell. Generating visual explanations. In *European Conference on Computer Vision (ECCV)*, pages 3–19. Springer, 2016.

Sepp Hochreiter and Jürgen Schmidhuber. Long short-term memory. *Neural computation*, 9 (8):1735–1780, 1997.

Anthony Hoogs and AG Amitha Perera. Video activity recognition in the real world. In *AAAI*, pages 1551–1554, 2008.

Zhiheng Huang, Wei Xu, and Kai Yu. Bidirectional lstm-crf models for sequence tagging. In *Conference on Empirical Methods in Natural Language Processing (EMNLP)*, 2015.

Ray Jackendoff. *Semantics and Cognition*. MIT Press, 1983.

Xiang Jiang, Erico N de Souza, Xuan Liu, Behrouz Haji Soleimani, Xiaoguang Wang, Daniel L. Silver, and Stan Matwin. Partition-wise recurrent neural networks for point-based ais trajectory classification. In *25th European Symposium on Artificial Neural Networks, Computtional Intelligence and Machine Learning*, pages 529–534. ESANN, 2017.

Rafal Jozefowicz, Wojciech Zaremba, and Ilya Sutskever. An empirical exploration of recurrent network architectures. In *International Conference on Machine Learning (ICML)*, pages 2342–2350, 2015.

Diederik P Kingma and Jimmy Ba. Adam: A method for stochastic optimization. *arXiv preprint arXiv:1412.6980*, 2014.

Hema S Koppula and Ashutosh Saxena. Anticipating human activities using object affordances for reactive robotic response. *IEEE transactions on pattern analysis and machine intelligence*, 38(1):14–29, 2016.

Hema Swetha Koppula, Rudhir Gupta, and Ashutosh Saxena. Learning human activities and object affordances from rgb-d videos. *The International Journal of Robotics Research*, 32 (8):951–970, 2013.

Nikhil Krishnaswamy. *Monte Carlo Simulation Generation Through Operationalization of Spatial Primitives*. PhD thesis, Brandeis University, 2017.

Nikhil Krishnaswamy and James Pustejovsky. Voxsim: A visual platform for modeling motion language. In *Proceedings the 26th International Conference on Computational Linguistics: System Demonstrations*, 2016.

Nikhil Krishnaswamy and James Pustejovsky. Do you see what i see? effects of pov on spatial relation specifications. In *Proc. 30th International Workshop on Qualitative Reasoning*, 2017.

Nikhil Krishnaswamy, Pradyumna Narayana, Isaac Wang, Kyeongmin Rim, Rahul Bangar, Dhruva Patil, Gururaj Mulay, Ross Beveridge, Jaime Ruiz, Bruce Draper, et al. Communicating and acting: Understanding gesture in simulation semantics. In *12th International Conference on Computational Semantics (IWCS), Short papers*, 2017.

Benjamin Kuipers. How shall we learn how to learn how to grasp? *ICRA Workshop on Representations for Object Grasping and Manipulation*, 2010.

Quoc V Le, Will Y Zou, Serena Y Yeung, and Andrew Y Ng. Learning hierarchical invariant spatio-temporal features for action recognition with independent subspace analysis. In *IEEE Conference on Computer Vision and Pattern Recognition (CVPR)*, pages 3361–3368. IEEE, 2011.

Ian Lenz, Honglak Lee, and Ashutosh Saxena. Deep learning for detecting robotic grasps. *The International Journal of Robotics Research*, 34(4-5):705–724, 2015.

Wenbin Li and Mario Fritz. Recognition of ongoing complex activities by sequence prediction over a hierarchical label space. In *Applications of Computer Vision (WACV), 2016 IEEE Winter Conference on*, pages 1–9. IEEE, 2016.

Wei Liang, Yibiao Zhao, Yixin Zhu, and Song-Chun Zhu. Evaluating human cognition of containing relations with physical simulation. In *CogSci*, 2015.

Tomas Lozano-Perez. Robot programming. *Proceedings of the IEEE*, 71(7):821–841, 1983.

John H Maunsell and David C Van Essen. Functional properties of neurons in middle temporal visual area of the macaque monkey. ii. binocular interactions and sensitivity to binocular disparity. *Journal of Neurophysiology*, 49(5):1148–1167, 1983.

William E Merriman, Laura L Bowman, and Brian MacWhinney. The mutual exclusivity bias in children's word learning. *Monographs of the society for research in child development*, pages i–129, 1989.

Arvind Neelakantan, Quoc V Le, and Ilya Sutskever. Neural programmer: Inducing latent programs with gradient descent. *Proceedings of the 4th International Conference on Learning Representations (ICLR)*, 2016.

Chris Olah and Shan Carter. Attention and augmented recurrent neural networks. *Distill*, 2016. doi: 10.23915/distill.00001. URL `http://distill.pub/2016/augmented-rnns`.

Nicolas Papernot, Patrick McDaniel, Somesh Jha, Matt Fredrikson, Z Berkay Celik, and Ananthram Swami. The limitations of deep learning in adversarial settings. In *Security and Privacy (EuroS&P), 2016 IEEE European Symposium on*, pages 372–387. IEEE, 2016.

Kishore Papineni, Salim Roukos, Todd Ward, and Wei-Jing Zhu. Bleu: a method for automatic evaluation of machine translation. In *Proceedings of the 40th annual meeting on association for computational linguistics*, pages 311–318. Association for Computational Linguistics (ACL), 2002.

James Pustejovsky. Dynamic event structure and habitat theory. In *Proceedings of the 6th International Conference on Generative Approaches to the Lexicon (GL2013)*, pages 1–10. ACL, 2013.

James Pustejovsky and Nikhil Krishnaswamy. Generating simulations of motion events from verbal descriptions. *Lexical and Computational Semantics (* SEM 2014)*, page 99, 2014.

James Pustejovsky and Nikhil Krishnaswamy. Voxml: A visual object modeling language. *Proceedings of LREC*, 2016.

James Pustejovsky, Nikhil Krishnaswamy, and Tuan Do. Object embodiment in a multimodal simulation. *AAAI Spring Symposium: Interactive Multisensory Object Perception for Embodied Agents*, 2017.

Hossein Rahmani and Ajmal Mian. 3d action recognition from novel viewpoints. In *IEEE Conference on Computer Vision and Pattern Recognition (CVPR)*, pages 1506–1515, 2016.

Marc'Aurelio Ranzato, Sumit Chopra, Michael Auli, and Wojciech Zaremba. Sequence level training with recurrent neural networks. *Proceedings of the 4th International Conference on Learning Representations (ICLR)*, 2016.

Shaoqing Ren, Kaiming He, Ross Girshick, and Jian Sun. Faster r-cnn: Towards real-time object detection with region proposal networks. In *Advances in Neural Information Processing Systems*, pages 91–99, 2015.

Anna Rohrbach, Marcus Rohrbach, Niket Tandon, and Bernt Schiele. A dataset for movie description. In *IEEE Conference on Computer Vision and Pattern Recognition (CVPR)*, 2015.

Marcus Rohrbach, Sikandar Amin, Mykhaylo Andriluka, and Bernt Schiele. A database for fine grained activity detection of cooking activities. In *IEEE Conference on Computer Vision and Pattern Recognition (CVPR)*, pages 1194–1201, 2012.

Amitava Roy and Sankar K Pal. Fuzzy discretization of feature space for a rough set classifier. *Pattern Recognition Letters*, 24(6):895–902, 2003.

Michael S Ryoo and JK Aggarwal. Ut-interaction dataset, icpr contest on semantic description of human activities (sdha). In *IEEE International Conference on Pattern Recognition Workshops*, volume 2, page 4, 2010.

Christiane Schwier, Catharine Van Maanen, Malinda Carpenter, and Michael Tomasello. Rational imitation in 12-month-old infants. *Infancy*, 10(3):303–311, 2006.

Iulian Vlad Serban, Tim Klinger, Gerald Tesauro, Kartik Talamadupula, Bowen Zhou, Yoshua Bengio, and Aaron C Courville. Multiresolution recurrent neural networks: An application to dialogue response generation. In *AAAI*, pages 3288–3294, 2017.

Amir Shahroudy, Jun Liu, Tian-Tsong Ng, and Gang Wang. Ntu rgb+ d: A large scale dataset for 3d human activity analysis. In *IEEE Conference on Computer Vision and Pattern Recognition (CVPR)*, pages 1010–1019. IEEE, 2016.

Zhangzhang Si and Song-Chun Zhu. Learning and-or templates for object recognition and detection. *IEEE Transactions on Pattern Analysis and Machine Intelligence*, 35(9):2189–2205, 2013.

David Silver, Aja Huang, Chris J Maddison, Arthur Guez, Laurent Sifre, George Van Den Driessche, Julian Schrittwieser, Ioannis Antonoglou, Veda Panneershelvam, Marc Lanctot, et al. Mastering the game of go with deep neural networks and tree search. *nature*, 529 (7587):484–489, 2016.

David Silver, Julian Schrittwieser, Karen Simonyan, Ioannis Antonoglou, Aja Huang, Arthur Guez, Thomas Hubert, Lucas Baker, Matthew Lai, Adrian Bolton, et al. Mastering the game of go without human knowledge. *Nature*, 550(7676):354, 2017.

William D Smart and L Pack Kaelbling. Effective reinforcement learning for mobile robots. In *IEEE International Conference on Robotics and Automation (ICRA)*, volume 4, pages 3404–3410. IEEE, 2002.

Nitish Srivastava, Geoffrey Hinton, Alex Krizhevsky, Ilya Sutskever, and Ruslan Salakhutdinov. Dropout: A simple way to prevent neural networks from overfitting. *The Journal of Machine Learning Research*, 15(1):1929–1958, 2014.

Jakob Suchan, Mehul Bhatt, and Paulo E Santos. Perceptual narratives of space and motion for activity interpretation. In *27th International Workshop on Qualitative Reasoning*, page 32, 2013.

Richard S Sutton and Andrew G Barto. *Reinforcement learning: An introduction*. Draft version, 2 edition, 2018.

Amir Tamrakar. Cwc blocks world (bw) apparatus, api reference manual. Technical report, 2015.

Marc Tanti, Albert Gatt, and Kenneth P Camilleri. Where to put the image in an image caption generator. *Natural Language Engineering*, 24(3):467–489, 2018.

Hamid R Tizhoosh. Reinforcement learning based on actions and opposite actions. In *International conference on artificial intelligence and machine learning*, volume 414, 2005.

Michael Tomasello and Ann Cale Kruger. Joint attention on actions: acquiring verbs in ostensive and non-ostensive contexts. *Journal of Child Language*, 19(2):311333, 1992. doi: 10.1017/S0305000900011430.

Ashish Vaswani, Noam Shazeer, Niki Parmar, Jakob Uszkoreit, Llion Jones, Aidan N Gomez, Łukasz Kaiser, and Illia Polosukhin. Attention is all you need. In *Advances in Neural Information Processing Systems*, pages 6000–6010, 2017.

Harini Veeraraghavan, Nikolaos Papanikolopoulos, and Paul Schrater. Learning dynamic event descriptions in image sequences. In *IEEE Conference on Computer Vision and Pattern Recognition (CVPR)*, pages 1–6. IEEE, 2007.

Ronald J Williams. Simple statistical gradient-following algorithms for connectionist reinforcement learning. *Machine learning*, 8(3-4):229–256, 1992.

Tom Williams, Gordon Briggs, Bradley Oosterveld, and Matthias Scheutz. Going beyond literal command-based instructions: Extending robotic natural language interaction capabilities. In *AAAI*, pages 1387–1393, 2015.

Sam Wiseman and Alexander M Rush. Sequence-to-sequence learning as beam-search optimization. In *Conference on Empirical Methods in Natural Language Processing (EMNLP)*, 2016.

Chenxia Wu, Jiemi Zhang, Silvio Savarese, and Ashutosh Saxena. Watch-n-patch: Unsupervised understanding of actions and relations. In *IEEE Conference on Computer Vision and Pattern Recognition (CVPR)*, pages 4362–4370. IEEE, 2015.

Yonghui Wu, Mike Schuster, Zhifeng Chen, Quoc V Le, Mohammad Norouzi, Wolfgang Macherey, Maxim Krikun, Yuan Cao, Qin Gao, Klaus Macherey, et al. Google's neural machine translation system: Bridging the gap between human and machine translation. *arXiv preprint arXiv:1609.08144*, 2016.

Kelvin Xu, Jimmy Ba, Ryan Kiros, Kyunghyun Cho, Aaron Courville, Ruslan Salakhudinov, Rich Zemel, and Yoshua Bengio. Show, attend and tell: Neural image caption generation with visual attention. In *International Conference on Machine learning (ICML)*, pages 2048–2057, 2015.

Guangzheng Yang and Thomas S Huang. Human face detection in a complex background. *Pattern recognition*, 27(1):53–63, 1994.

Ying Yang and Geoffrey I Webb. Discretization for naive-bayes learning: managing discretization bias and variance. *Machine learning*, 74(1):39–74, 2009.

Pengcheng Yin, Zhengdong Lu, Hang Li, and Ben Kao. Neural enquirer: Learning to query tables with natural language. *International Joint Conferences on Artificial Intelligence*, 2016.

Jay Young and Nick Hawes. Learning by observation using qualitative spatial relations. In *Proceedings of the 2015 International Conference on Autonomous Agents and Multiagent Systems*, pages 745–751. International Foundation for Autonomous Agents and Multiagent Systems, 2015.

Wojciech Zaremba, Ilya Sutskever, and Oriol Vinyals. Recurrent neural network regularization. *arXiv preprint arXiv:1409.2329*, 2014.

Xu-Yao Zhang, Fei Yin, Yan-Ming Zhang, Cheng-Lin Liu, and Yoshua Bengio. Drawing and recognizing chinese characters with recurrent neural network. *IEEE transactions on pattern analysis and machine intelligence*, 40(4):849–862, 2018.